2SM

Emissions Trends and Drivers Supplementary Material

Coordinating Lead Authors:

Shobhakar Dhakal (Nepal/Thailand), Jan Christoph Minx (Germany), Ferenc L. Toth (Austria/Hungary)

Authors:

Andy Reisinger (New Zealand), William F. Lamb (Germany/United Kingdom), Niklas Döbbeling (Germany), Thomas Wiedmann (Australia/Germany), Klaus Hubacek (the Netherlands/the United States of America), Robbie M Andrew (Norway), Monica Crippa (Italy), Piers M. Forster (United Kingdom), Jos Olivier (the Netherlands), Glen P.Peters (Norway), Julia Pongratz (Germany), Matt Rigby (United Kingdom), Marielle Saunois (France), Steven J. Smith (the United States of America), Efisio Solazzo (Italy), Hanqin Tian (the United States of America), Kornelis Blok (the Netherlands), Harry Clark (New Zealand), Annette Cowie (Australia), Jan Sigurd Fuglestvedt (Norway), Oliver Geden (Germany), Veronika Ginzburg (the Russian Federation), Céline Guivarch (France), Joanna I. House (United Kingdom), Rachid Mrabet (Morocco), Gert-Jan Nabuurs (the Netherlands), Keywan Riahi (Austria), Anders Hammer Strømman (Norway), Roberto Schaeffer (Brazil), Detlef P. van Vuuren (the Netherlands), Alaa Al Khourdajie (United Kingdom/Syria), Raphael Slade (United Kingdom)

Review Editors:

Barbara Amon (Germany), David I. Stern (Australia)

Chapter Scientists:

Lazarus Chapungu (Zimbabwe), William F. Lamb (Germany/United Kingdom)

This chapter should be cited as:

Dhakal, S., J.C. Minx, F.L. Toth, Reisinger, W. F. Lamb, N. Döbbeling, T. Wiedmann, K. Hubacek, R. M. Andrew, M. Crippa, P. M. Forster, J. Olivier, G. P. Peters, J. Pongratz, M.Rigby, M. Saunois, S. J. Smith, E. Solazzo, H. Tian, K. Blok, H. Clark, A. Cowie, J.S Fuglestvedt, O. Geden, V. Ginzburg, C. Guivarch, J. I. House, R. Mrabet, G. J. Nabuurs, K. Riahi, A. H. Strømman, R. Schaeffer, D. P. van Vuuren, A. Al Khourdajie, R Slade, 2022: Emissions Trends and Drivers Supplementary Material. In *IPCC, 2022: Climate Change 2022: Mitigation of Climate Change. Contribution of Working Group III to the Sixth Assessment Report of the Intergovernmental Panel on Climate Change* [P.R. Shukla, J. Skea, R. Slade, A. Al Khourdajie, R. van Diemen, D. McCollum, M. Pathak, S. Some, P. Vyas, R. Fradera, M. Belkacemi, A. Hasija, G. Lisboa, S. Luz, J. Malley, (eds.)]. Available from https://www.ipcc.ch/report/ar6/wg3/.

Table of Contents

2.SM.1 Historic Greenhouse Gas Emissions 1990–2019: Dataset Description

This section provides a brief description of the dataset on historic greenhouse gas (GHG) emissions compiled for AR6 WGIII (the contribution of Working Group III to the IPCC Sixth Assessment Report) on climate change mitigation. The dataset is publicly available (https://zenodo.org/record/5566761) and has undergone additional peer review (Minx et al. 2021). Sections 2.SM.1 and 2.SM.2 included in this Supplementary Material are taken (in most parts) directly from Minx et al. (2021). It is included here solely to provide full transparency over the data used in this report and enable easy access to all information.

2.SM.1.1 Overview

The historic emissions dataset used in Chapter 2 provides a comprehensive, synthetic set of estimates for global GHG emissions disaggregated by 27 economic sectors and 228 countries and territories. Its focus is on anthropogenic GHG emissions: natural sources and sinks are not included. Five groups of gases are distinguished: (i) CO_2 emissions from fossil fuel combustion and industry (CO_2-FFI); (ii) CO_2 emissions from land use, land-use change and forestry (CO_2-LULUCF); (iii) methane emissions (CH_4); (iv) nitrous oxide emissions (N_2O); (v) fluorinated gases (F-gases) comprising hydrofluorocarbons (HFCs), perfluorocarbons (PFCs), sulphur hexafluoride (SF_6) as well as nitrogen trifluoride (NF_3). Other F-gases that are internationally regulated as ozone-depleting substances under the Montreal Protocol such as chlorofluorocarbons (CFCs) and hydrochlorofluorocarbons (HCFCs) are not included. GHG emissions data are analysed both in native units (except F-gases) as well as in CO_2-equivalents (CO_2-eq) as commonly done in wide parts of the climate change mitigation community using global warming potential with a 100-year time horizon (GWP100) from AR6 (Forster et al. 2021). The impact of using alternative metric choices in tracking aggregated GHG emissions is discussed in Section 2.SM.3 of this Supplementary Material.

The dataset is compiled from four sources: (i) the full EDGARv6.0 release for CO_2-FFI as well as non-CO_2 GHGs covering the time period 1970–2018 (Crippa et al. 2021); (ii) EDGARv6.0 fast-track data for CO_2-FFI providing preliminary estimates for 2019 and 2020 (Crippa et al. 2021); (iii) CO_2-LULUCF as the average of three bookkeeping models, consistent with the approach of the global carbon project (Friedlingstein et al. 2020); and (iv) 2019 non-CO_2 emissions based on Olivier and Peters (2018). The resulting synthetic dataset as presented here has undergone additional peer review (Minx et al. 2021).

As shown in Table 2.SM.1, sectoral detail is organised along five major economic sectors harmonised with the sector chapters used in this report: energy supply (Chapter 6); building (Chapter 9); transport (Chapter 10); Industry (Chapter 11); and Agriculture, Forestry and Other Land Use (AFOLU) (Chapter 7). A further classification for assigning our 228 countries and territories to regions is used, combining the standard Annex I/non-Annex I distinction with geographical location, as documented in Annex II of this report. The dataset including the sector and region classification, and GWP100 by gas can be found at https://zenodo.org/record/5566761.

While there is a growing number of global emissions inventories, only a few of them provide a wide coverage of gases, sectors, activities, and countries or regions that are sufficiently up to date to comprehensively track progress and thereby aid discussions in science and policy. Table 2.SM.2 provides an overview of global emission inventories. Many inventories focus on individual gases and subsets of activities. Few provide sectoral detail and, particularly for non-CO_2 GHG emissions, there is often a considerable time-lag in reporting. GHG emissions reporting under the United Nations Framework Convention on Climate Change (UNFCCC) provides reliable, comprehensive and up-to-date statistics for Annex I countries across all major GHGs. Non-Annex I countries – except least-developed countries and small island states for which this is not mandatory – provide GHG emissions inventory information through biennial update reports (BURs), but with much less stringent reporting requirements in terms of sector, gas and time coverage (Gütschow et al. 2016; Deng et al. 2021). As a result, many still lack a well-developed statistical infrastructure to provide detailed and timely reports (Janssens-Maenhout et al. 2019).

Table 2.SM.1 | Overview of the two-level sector aggregation with reference to assigned source/sink categories conforming to the IPCC reporting guidelines (IPCC 2006, 2019) as well as relevant GHGs.

Sector	Sub-sector	IPCC (2006)	Gases
AFOLU (Agriculture, Forestry and Other Land Use)	Biomass burning (agricultural waste burning on fields)	3.C.1.b (bio)	CH_4, N_2O
	Enteric fermentation	3.A.1.a.i (fossil), 3.A.1.a.ii (fossil), 3.A.1.b (fossil), 3.A.1.c (fossil), 3.A.1.d (fossil), 3.A.1.e (fossil), 3.A.1.f (fossil), 3.A.1.g (fossil), 3.A.1.h (fossil)	CH_4
	Managed soils and pasture	3.C.4 (fossil), 3.C.5 (fossil), 3.C.6 (fossil), 3.C.3 (fossil), 3.C.2 (fossil)	CO_2, N_2O
	Manure management	3.A.2.a.i (fossil), 3.A.2.a.ii (fossil), 3.A.2.b (fossil), 3.A.2.c (fossil), 3.A.2.i (fossil), 3.A.2.d (fossil), 3.A.2.e (fossil), 3.A.2.f (fossil), 3.A.2.g (fossil), 3.A.2.h (fossil)	CH_4, N_2O
	Rice cultivation	3.C.7 (fossil)	CH_4
	Synthetic fertiliser application	3.C.4 (fossil)	N_2O
	Land use, land-use change, and forestry		CO_2
Buildings	Non-CO_2 (all buildings)	2.F.3 (fossil), 2.F.4 (fossil), 2.G.2.c (fossil)	c-C4F8, C4F10, CF4, HFC-125, HFC-227ea, HFC-23, HFC-236fa, HFC-134a, HFC-152a, SF_6
	Non-residential	1.A.4.a (bio), 1.A.4.a (fossil)	CO_2, CH_4, N_2O
	Residential	1.A.4.b (bio), 1.A.4.b (fossil)	CO_2, CH_4, N_2O
Energy systems	Coal-mining fugitive emissions	1.B.1.a (fossil), 1.B.1.c (fossil)	CO_2, CH_4
	Electricity and heat	1.A.1.a.i (bio), 1.A.1.a.i (fossil), 1.A.1.a.ii (bio), 1.A.1.a.ii (fossil), 1.A.1.a.iii (bio), 1.A.1.a.iii (fossil)	CO_2, CH_4, N_2O
	Oil and gas fugitive emissions	1.B.2.a.iii.2 (bio), 1.B.2.a.iii.2 (fossil), 1.B.2.a.iii.3 (fossil), 1.B.2.a.iii.4 (fossil), 1.B.2.b.iii.2 (fossil), 1.B.2.b.iii.4 (fossil), 1.B.2.b.iii.5 (fossil), 1.B.2.b.iii.3 (fossil), 1.B.2.b.ii (fossil), 1.B.2.a.ii (fossil)	CO_2, CH_4, N_2O
	Other (energy systems)	1.A.1.c.ii (bio), 1.A.1.c.ii (fossil), 1.A.1.c.i (bio), 1.A.1.c.i (fossil), 1.A.4.c.i (bio), 1.A.4.c.i (fossil), 1.A.5.a (bio), 1.A.5.a (fossil), 1.B.1.c (bio), 2.G.1.b (fossil), 5.B (fossil), 5.A (fossil)	CO_2, CH_4, N_2O, SF_6
	Petroleum refining	1.A.1.b (bio), 1.A.1.b (fossil)	CO_2, CH_4, N_2O
Industry	Cement	2.A.1 (fossil)	CO_2
	Chemicals	1.A.2.c (bio), 1.A.2.c (fossil), 2.A.2 (fossil), 2.A.4.d (fossil), 2.A.4.b (fossil), 2.A.3 (fossil), 2.B.1 (fossil), 2.B.2 (fossil), 2.B.3 (fossil), 2.B.5 (fossil), 2.B.8.f (fossil), 2.B.8.b (fossil), 2.B.8.c (fossil), 2.B.8.a (fossil), 2.B.4 (fossil), 2.B.6 (fossil), 2.B.9.b (fossil), 2.D.3 (fossil), 2.G.3.a (fossil), 2.G.3.b (fossil)	CO_2, CH_4, N_2O, c-C4F8, C2F6, C3F8, C4F10, C5F12, C6F14, CF4, HFC-125, HFC-134a, HFC-143a, HFC-152a, HFC-227ea, HFC-32, HFC-365mfc, NF3, SF_6, HFC-23
	Metals	1.A.1.c.i (fossil), 1.A.1.c.ii (fossil), 1.A.2.a (bio), 1.A.2.a (fossil), 1.A.2.b (bio), 1.A.2.b (fossil), 1.B.1.c (fossil), 2.C.1 (fossil), 2.C.2 (fossil), 2.C.3 (fossil), 2.C.4 (fossil), 2.C.5 (fossil), 2.C.6 (fossil)	CO_2, CH_4, N_2O, C2F6, CF4, SF_6
	Other industry	1.A.2.d (bio), 1.A.2.d (fossil), 1.A.2.e (bio), 1.A.2.e (fossil), 1.A.2.f (bio), 1.A.2.f (fossil), 1.A.2.k (fossil), 1.A.2.i (fossil), 1.A.5.b.iii (fossil), 2.F.1.a (fossil), 2.F.2 (fossil), 2.F.5 (fossil), 2.E.1 (fossil), 2.E.2 (fossil), 2.E.3 (fossil), 2.G.1.a (fossil), 2.G.2.c (fossil), 2.G.2.b (fossil), 2.G.2.a (fossil), 2.D.1 (fossil), 5.A (fossil)	CO_2, CH_4, N_2O, HFC-125, HFC-134a, HFC-143a, HFC-152a, HFC-227ea, HFC-236fa, HFC-245fa, HFC-32, HFC-365mfc, C3F8, C6F14, CF4, HFC-43-10-mee, HFC-134, HFC-143, HFC-23, HFC-41, c-C4F8, C2F6, NF3, SF_6, HCFC-141b*, HCFC-142b*, C4F10
	Waste	4.A.1 (fossil), 4.D.2 (fossil), 4.D.1 (fossil), 4.C.1 (fossil), 4.C.2 (bio), 4.C.2 (fossil), 4.B (fossil)	CO_2, CH_4, N_2O
Transport	Domestic aviation	1.A.3.a.ii (fossil)	CO_2, CH_4, N_2O
	Inland shipping	1.A.3.d.ii (bio), 1.A.3.d.ii (fossil)	CO_2, CH_4, N_2O
	International Aviation	1.A.3.a.i (fossil)	CO_2, CH_4, N_2O
	International Shipping	1.A.3.d.i (bio), 1.A.3.d.i (fossil)	CO_2, CH_4, N_2O
	Other (transport)	1.A.3.e.i (bio), 1.A.3.e.i (fossil), 1.A.4.c.ii (fossil), 1.A.4.c.iii (bio), 1.A.4.c.iii (fossil)	CO_2, CH_4, N_2O
	Rail	1.A.3.c (bio), 1.A.3.c (fossil)	CO_2, CH_4, N_2O
	Road	1.A.3.b (bio), 1.A.3.b (fossil)	CO_2, CH_4, N_2O

Note that EDGARv6.0 distinguishes biogenic CO_2 and CH_4 sources with a ‘bio’ label, with all other sectors ‘fossil’ by default, even if that source is not related to fossil fuel activities. The fossil/bio label is hence not descriptive in nature. Two HCFC gases (denoted with *) are included in the dataset, despite being neither PFCs nor HFCs (and hence regulated under Montreal). This is to preserve consistency with current and previous versions of EDGAR, which include these gases. Their total warming effect is low (about 10 $MtCO_2$-eq in 2019) and the major HCFC sources are not included. Source: Minx et al. (2021).

Table 2.SM.2 | Overview of global inventories of GHG emissions. Source: Minx et al. (2021).

Dataset name	Short name	Version	Gases	Geographic coverage	Activity split	Time period	Reference	Link
Emissions Database for Global Atmospheric Research	EDGAR	6.0	CO_2-FFI, CH_4, N_2O, F-gases: HFCs, PFCs, SF_6, NF_3	228 countries; global	4 main sectors, 24 subsectors	1970–2018	Crippa et al. (2021)	https://edgar.jrc.ec.europa.eu/report_2021
Potsdam Real-time Integrated Model for probabilistic Assessment of emissions Paths	PRIMAP-hist	2.3.1	CO_2-FFI, CH_4, N_2O, F-gases: HFCs, PFCs, SF_6, NF_3	All UNFCCC member states, most non-UNFCCC territories	4 sectors	1750–2019	Gütschow et al. (2021b)	https://www.pik-potsdam.de/paris-reality-check/primap-hist/
Community Emissions Data System	CEDS	v_2021_02_05	SO_2, NO_x, BC, OC, NH_3, NMVOC, CO, CO_2, CH_4, N_2O	221 countries	60 sectors	1750–2019 (1970–2019 for CH_4 and N_2O)	Hoesly et al. (2018); McDuffie et al. (2020); O'Rourke et al. (2021)	http://www.globalchange.umd.edu/ceds/
UNFCCC: Annex I Party GHG Inventory Submissions		2021	CO_2, CH_4, N_2O, NO_x, CO, NMVOC, SO_2, F-gases: HFCs, PFCs, SF_6, NF_3	Parties included in Annex I to the Convention	Energy, industry, agriculture, LULUCF, waste	1990–2019		https://unfccc.int/ghg-inventories-annex-i-parties/2021
GCP: Global Carbon Budget	GCP-GCB	2020	CO_2-FFI, CO_2-LULUCF	Global, 259 countries for FFI	5 main sectors, 14 subsectors	CO_2-LULUCF: 1850–2019 CO_2-FFI: 1750–2019	Friedlingstein et al. (2020)	https://doi.org/10.18160/GCP-2020
Global, Regional, and National Fossil-Fuel CO_2 Emissions	CDIAC-FF	V2017	CO_2-FFI	259 countries, global	5 main categories	1751–2017	Gilfillan et al. (2020)	https://energy.appstate.edu/research/work-areas/cdiac-appstate
Energy Information Administration International Energy Statistics	EIA	2021	CO_2-FFI	230 countries, global	3 fuel types	1980–2018; 1949–2018 (global)	EIA (2019)	https://www.eia.gov/international/data/world
BP Statistical Review of World Energy	BP	2021 70th edition	CO_2-FFI	108 countries, 7 regions	8 activities, 3 fossil and 3 other fuel types	1965–2019	BP (2021)	https://www.bp.com/en/global/corporate/energy-economics/statistical-review-of-world-energy.html
International Energy Agency CO_2 Emissions from Fuel Combustion	IEA	2021	CO_2-FFI	190 countries	3 fossil fuels, 6 sectors	1971–2020; OECD: 1960–2020	IEA (2021a,b)	https://www.iea.org/data-and-statistics/data-product/greenhouse-gas-emissions-from-energy-highlights
PKU-FUEL			CO_2, CO, $PM_{2.5}$, PM_{10}, TSP, BC, OC, SO_2, NO_x, NH_3, PAHs	Global (0.1 degree grid cells)	6 sectors, 5 fuel types	1960–2014		http://inventory.pku.edu.cn/
Carbon Monitor			CO_2-FFI	11 countries, global	6 sectors	2019–very recent	Liu et al. (2020)	https://carbonmonitor.org/
Bookkeeping of land-use emissions	BLUE	2020	CO_2-LULUCF	Global (0.25 degree grid cells)	no split	1700–2019	Hansis et al. (2015); updated simulations described by Friedlingstein et al. (2020)	https://doi.org/10.18160/GCP-2020
OSCAR – an Earth system compact model	OSCAR	2020	CO_2-LULUCF	Global (10 regions)	no split	1701–2019	Gasser et al. (2020); Friedlingstein et al. (2020)	https://doi.org/10.18160/GCP-2020
Houghton and Nassikas Bookkeeping Model	H&N	2020	CO_2-LULUCF	Global (187 countries)	no split	1850–2019	Houghton and Nassikas (2017); Friedlingstein et al. (2020)	https://doi.org/10.18160/GCP-2020

Dataset name	Short name	Version	Gases	Geographic coverage	Activity split	Time period	Reference	Link
The Greenhouse gas – Air pollution INteractions and Synergies Model	GAINS	2020	CO_2, CH_4, N_2O, F-gases	Global (172 regions)	3 main sectors, 16 subsectors	1990–2015	Höglund-Isaksson (2012; 2020); Winiwarter et al. (2018)	https://gains.iiasa.ac.at/models/index.html
EPA-Global Non-CO_2 Greenhouse Gas Emissions	US-EPA	2019	CH_4, N_2O, F-gases: HFCs, PFCs, SF_6	Global (195 countries)	4 major sectors	1990–2015	EPA (2021)	https://www.epa.gov/global-mitigation-non-co2-greenhouse-gases
GCP – global nitrous oxide budget	GCP/INI	2020	N_2O	10 land regions and 3 oceanic regions	21 natural and human sectors	1980–2016	Tian et al. (2020)	https://www.globalcarbonproject.org/nitrousoxidebudget/
FAOSTAT – Emissions Totals	FAOSTAT	2021	CO_2, CH_4, N_2O	Global (191 countries)	15 activities in AFOLU	1961–2019	Tubiello et al. (2013, 2021); Federici et al. (2015); Tubiello (2019)	http://www.fao.org/faostat/en/#data/GT
Fire Inventory from NCAR	FINN		CO_2, CH_4, N_2O	Global			Wiedinmyer et al. (2011)	
Global fire assimilation system	GFAS		CO_2, CH_4, N_2O	Global			Kaiser et al. (2012)	
Global fire emissions database	GFED		CO_2, CH_4, N_2O	Global			Van der Werf et al. (2017)	https://www.geo.vu.nl/~gwerf/GFED/GFED4/
Quick fire emissions dataset	QFED		CO_2-LULUCF, CH_4, N_2O	Global			Darmenov and da Silva (2013)	

2.SM.1.2 The Emissions Database for Global Atmospheric Research (EDGAR)

EDGAR emission estimates included in Chapter 2 emissions dataset are derived from the full version 6 release (Crippa et al. 2021). This includes CO_2 and non-CO_2 GHG emission estimates from 1970 to 2018 computed from stable international statistics, and fast-track estimates of fossil CO_2 emissions up to the year 2020. The following general EDGAR methodological description is largely taken from Janssens-Maenhout et al. (2019). EDGAR bottom-up emission inventory estimates are calculated from international activity data and emission factors following the 2006 IPCC Guidelines for National Greenhouse Gas Inventories (IPCC 2006) – updated according to the latest scientific knowledge. Emissions (*EM*s) from a given sector *i* in a country *C* accumulated during a year *t* for a chemical compound *x* are calculated with the country-specific activity data (*AD*), quantifying the activity in sector *i*, with the mix of *j* technologies (*TECH*) and with the mix of *k* (end-of-pipe) abatement measures (*EOP*) installed with the share *k* for each technology *j*, the emission rate with an uncontrolled emission factor (*EF*) for each sector *i* and technology *j* and relative reduction (*RED*) by abatement measure *k*, as summarised in the following formula:

Equation 2.SM.1

$$EM_i(C,t,x) = \sum_{j,k} \left[AD_i(C,t) \cdot TECH_{i,j}(C,t) \cdot EOP_{i,j,k}(C,t) \cdot EF_{i,j}(C,t,x) \cdot \left(1 - RED_{i,j,k}(C,t,x)\right)\right]$$

The activity data are sector dependent and vary from fuel combustion in energy units of a particular fuel type, to the amount of products manufactured, or to the number of animals or the area or yield of cultivated crops. The technology mixes, (uncontrolled) emission factors and end-of-pipe measures are determined at different levels: country-specific, regional, country group (e.g., Annex I/non-Annex I), or global. Technology-specific emission factors are used to enable an IPCC Tier-2 approach (see Box 2.SM.1), taking into account the different management and technology processes or infrastructures (e.g., different distribution networks) under specific 'technologies', and modelling explicitly abatements/ emission reductions – for example, the CH_4 recovery from coal mine gas at country level under the 'end-of-pipe measures'. As with national inventories, emissions are accounted over a period of one calendar year in the country or territory in which they took place (i.e., a territorial accounting principle) (IPCC 2006, 2019). A more complete description of the data sources and methodology for EDGARv6 is provided in Crippa et al. (2021).

To compute emissions up to the most recent years, a fast-track methodology is applied, as described in Oreggioni et al. (2021). The underlying principle is to extrapolate trends based on observed activity patterns in representative sectors. For CO_2-FFI emissions, the fast track estimates were based on the latest BP coal, oil and natural gas consumption data (BP 2021). Emission updates for cement, lime, ammonia and ferroalloys production beyond 2018 are based on stable statistics. In particular these include US Geological Survey statistics, urea production and consumption statistics from the International Fertilizer Association, gas flaring statistics from the Global Gas Flaring Reduction Partnership, steel production statistics from the World Steel Association, and cement clinker production statistics from UNFCCC data. Fast-track extensions for non-CO_2 GHG emissions are based on Olivier and Peters (2018). For CH_4 and N_2O these are based on agricultural statistics from the UN's Food and Agricultural Organization (FAO) (CH_4 and N_2O), fuel production and transmission statistics from the International Energy Agency (IEA) and BP (CH_4) as well as data from national GHG inventory reports on coal production (CH_4 recovery) and the production of chemicals (N_2O abatement) submitted by Annex-I countries to the UNFCCC following a common reporting format (CRF) (e.g., UNFCCC 2021). For F-gases the fast-track extension was based on the most recent national emission inventories, submitted under the UNFCCC (up to 2018). Given the absence of international statistics, for all remaining countries and years, a simple extrapolation was used, with fast-track data by Olivier and Peters (2020). Here the procedure was to calculate the country- and sector-specific emissions growth between 2018 and 2019 in Olivier and Peters (2020), then multiply each growth rate with the 2018 values in the Chapter 2 emissions data.

2.SM.1.3 Accounting for CO_2 Emissions Land Use, Land-use Change and Forestry (CO_2-LULUCF)

All fluxes of CO_2-LULUCF are considered. This includes CO_2 fluxes from the clearing of forests and other natural vegetation (by anthropogenic fire and/or clear-cut), afforestation, harvest activities, land-use related forest degradation, shifting cultivation (cycles of

Box 2.SM.1 | Methodological Standards for Compiling Greenhouse Gas Inventories According to IPCC Guidelines

The 2006 Guidelines for National Greenhouse Gas Inventories and their 2019 refinements by the Intergovernmental Panel on Climate Change (IPCC) provide methodological guidance for compiling greenhouse gas (GHG) emissions inventories at different levels of sophistication (IPCC 2006, 2019). The levels of methodological complexity for estimating GHG emissions and removals are organised according to different *tiers*. *Tier 1* is the most basic method. It applies a simple default methodology as well as default emission factors and other parameters defined in the IPCC Guidelines. *Tier 2* methods replace those default values by country-specific data and can use more detailed calculations and activity data. *Tier 3* refers to methods that may apply country-specific equations for calculating emissions along with more details regarding activity data, technologies and practices, providing the most granular approach to estimation. *Tier 2* and *Tier 3* are also referred to as *higher tier methods* and are generally considered to be more accurate than a *Tier 1* method, especially when it comes to reporting changes in emissions over time (IPCC 2006).

forest clearing for agriculture, then abandonment), and regrowth of forests and other natural vegetation following wood harvest or abandonment of agriculture, and emissions from peat burning and drainage. Some of these activities lead to emissions of CO_2 to the atmosphere, while others lead to CO_2 sinks. CO_2-LULUCF therefore is the net sum of emissions and removals from all human-induced land-use changes and land management. Note that CO_2-LULUCF is referred to as (net) land-use change emissions, E_{LUC}, in the context of the global carbon budget (Friedlingstein et al. 2020). Agriculture per se, apart from conversions between different agricultural types, does not lead to substantial CO_2 emissions as compared to land-use changes such as clearing or regrowth of natural vegetation. Therefore, CO_2 fluxes in the AFOLU sector refer almost exclusively to forestry and other land use (changes), while the agricultural part of the sector is mainly characterised by CH_4 and N_2O fluxes.

Since in reality anthropogenic CO_2-LULUCF emissions co-occur with natural CO_2 fluxes in the terrestrial biosphere, models have to be used to distinguish anthropogenic and natural fluxes (Friedlingstein et al. 2020). CO_2-LULUCF as reported here is calculated via a bookkeeping approach, as originally proposed by Houghton et al. (2003), tracking carbon stored in vegetation and soils before and after land-use change. Response curves are derived from the literature and observations to describe the temporal evolution of the decay and regrowth of vegetation and soil carbon pools for different ecosystems and land-use transitions, including product pools of different lifetimes. These dynamics distinguish bookkeeping models from the common approach of estimating 'committed emissions' (assigning all present and future emissions to the time of the land-use change event), which is frequently derived from remotely-sensed land-use area or biomass observations (Ramankutty et al. 2007). Most bookkeeping models also represent the long-term degradation of primary forest as the reduction of standing vegetation and soil carbon stocks in secondary forests, and include forest management practices such as wood harvesting. Since the effects of environmental changes are excluded by the bookkeeping approach, bookkeeping CO_2-LULUCF emissions estimates isolate the effects of anthropogenic (land-use-related) drivers.

The definition of CO_2-LULUCF emissions by global carbon cycle models, as used here and in Canadell et al. (2021), differs from IPCC definitions (IPCC 2006) applied in national greenhouse gas inventories (NGHGI) for reporting under the climate convention (Grassi et al. 2018) and, similarly, from FAO estimates of carbon fluxes on forest land (Tubiello et al. 2021). This means that NGHGI data include natural terrestrial fluxes caused by changes in environmental conditions, such as the effects of rising atmospheric CO_2 (CO_2-fertilisation), climate change, and nitrogen deposition – sometimes called 'indirect effects' as opposed to the direct anthropogenic effects of land-use change and management (Houghton et al. 2012) (Section 2.2.2.1 and Chapter 7) – through adoption of the IPCC so-called land-use proxy approach when they occur on areas that countries declare as managed. Since environmental changes turned the terrestrial biosphere into a massive sink, removing about one-third of annual anthropogenic emissions in the last decade (Friedlingstein et al. 2020), it is unsurprising that global emission estimates are smaller based on NGHGI than for global models' definitions (Figure 2.SM.1). About 3.2 $GtCO_2\ yr^{-1}$ (for the period 2005–2014) was found to be explicable by these conceptual differences in anthropogenic forest sink estimation related to the representation of environmental change impacts and the areas considered as managed (Grassi et al. 2018).

These two conceptually different approaches have different aims: the global models' approach separates natural from anthropogenic drivers – that is, the effects of changes in environmental conditions from effects of land-use change and land management. By contrast, the NGHGI approach separates fluxes based on areas, with all those occurring on managed land being declared anthropogenic. Given that observational data of carbon stocks or fluxes cannot distinguish the co-occurring effects of environmental changes and land-use activities, an area-based approach that does not require this distinction can more consistently be implemented across countries. These conceptual differences between global models and NGHGI approaches have been acknowledged (Petrescu et al. 2020a; Canadell et al. 2021) and approaches have been developed to map the two definitions to each other (Grassi et al. 2018, 2021). For non-CO_2 GHGs, drivers and areas coincide, such that FAOSTAT data for CH_4 and N_2O is complementary to bookkeeping CO_2-LULUCF emissions.

Following the approach taken by the global carbon budget (Friedlingstein et al. 2020), the approach taken here is to use the average of estimates from three bookkeeping models: Bookkeeping of land-use emissions (BLUE) (Hansis et al. 2015), H&N (Houghton and Nassikas, 2017), and an earth system compact model (OSCAR) (Gasser et al. 2020). Key differences across these estimates, including land-use forcing, are summarised in Table 2.SM.4. Since bookkeeping models do not include emissions from organic soils, emissions from peat fires and peat drainage are added from external datasets: Peat burning is based on the Global Fire Emissions Database (GFEDv4) (van der Werf et al. 2017) and introduces large interannual variability to the CO_2-LULUCF emissions due to synergies of land-use and climate variability, particularly in Southeast Asia, strongly noticeable during El Niño events such as in 1997. Peat drainage is based on estimates by Hooijer et al. (2010) for Indonesia and Malaysia in H&N, and added to BLUE and OSCAR from the global FAO data on organic soils emissions from croplands and grasslands (Conchedda and Tubiello 2020).

2.SM.2 Uncertainties in GHG Emissions Estimates

Estimates of historic GHG emissions – CO_2, CH_4, N_2O and F-gases (HFCs, PFCs, SF_6, NF_3) – are uncertain to different degrees. Assessing and reporting uncertainties is crucial in order to understand whether available estimates are sufficiently accurate to answer – for example, whether GHG emissions are still rising, or if a country has achieved an emissions-reduction goal (Marland 2008). These uncertainties can be of a scientific nature, such as when a process is not sufficiently understood. They also arise from incomplete or unknown parameter information (activity data, emission factors, and so on), as well as estimation uncertainties from imperfect modelling techniques. There are at least three major ways to examine uncertainties in emission estimates (Marland et al. 2009): (i) by comparing estimates made

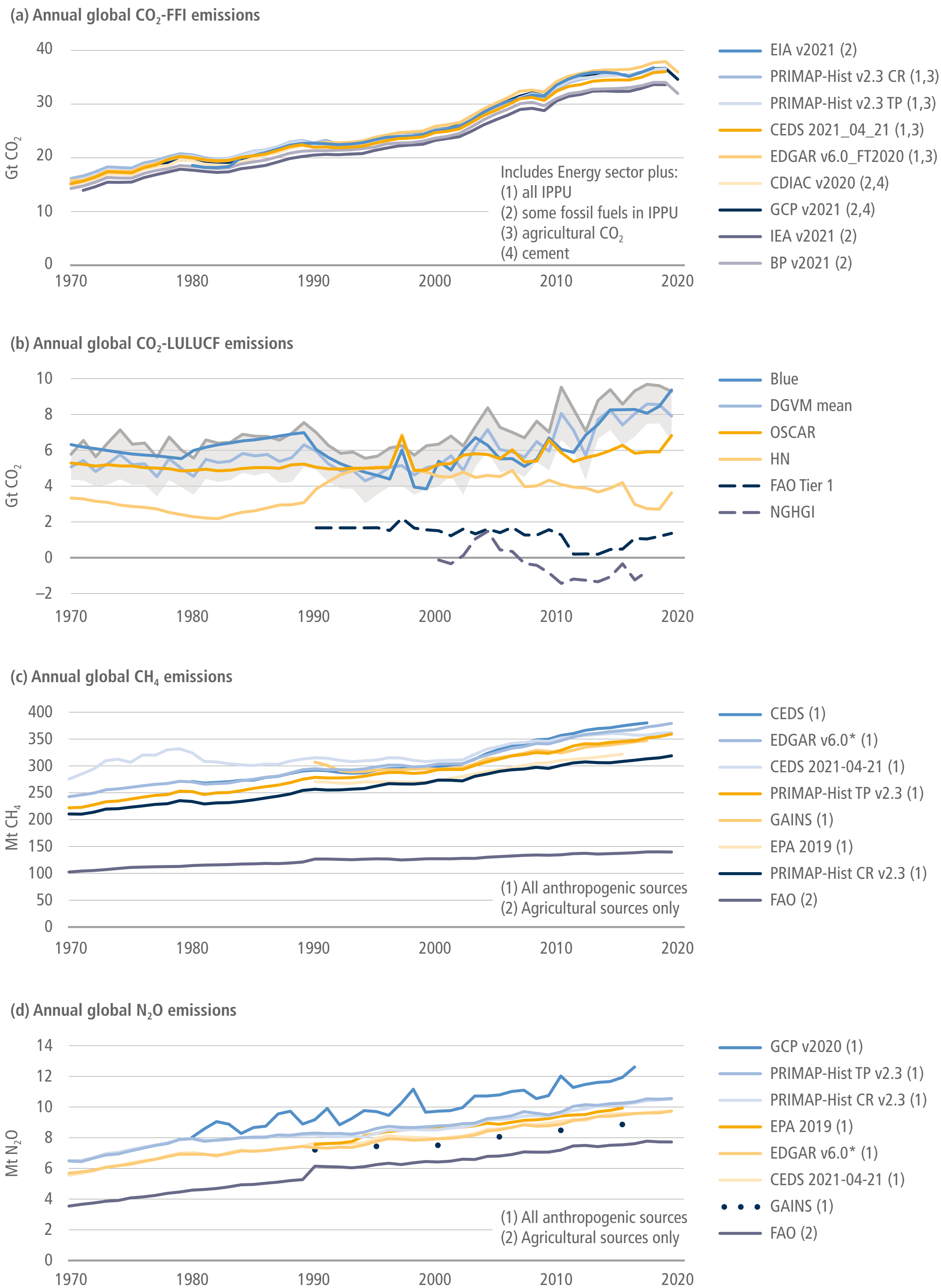

Figure 2.SM.1 | Estimates of global anthropogenic greenhouse gas emissions from different data sources 1970–2019.

Figure 2.SM.1 (continued): Estimates of global anthropogenic greenhouse gas emissions from different data sources 1970–2019. Top-left panel: CO_2-FFI emissions from: EDGAR – Emissions Database for Global Atmospheric Research (this dataset) (Crippa et al. 2021); GCP – Global Carbon Project (Friedlingstein et al. 2020; Andrew and Peters 2021); CEDS – Community Emissions Data System (Hoesly et al. 2018; O'Rourke et al. 2021); CDIAC Global, Regional, and National Fossil-Fuel CO_2 Emissions (Gilfillan et al. 2020); PRIMAP-hist – Potsdam Real-time Integrated Model for probabilistic Assessment of emissions Paths (Gütschow et al. 2016, 2021b); EIA – Energy Information Administration International Energy Statistics (EIA 2019); BP – BP Statistical Review of World Energy (BP 2021); IEA – International Energy Agency (IEA 2021b; (a); IPPU refers to emissions from industrial processes and product use. **Top-right panel:** Net anthropogenic CO_2-LULUCF emissions from: BLUE – Bookkeeping of land-use emissions (Hansis et al. 2015; Friedlingstein et al. 2020); DGVM-mean – Multi-model mean of CO_2-LULUCF emissions from dynamic global vegetation models (Friedlingstein et al. 2020); OSCAR – an earth system compact model (Friedlingstein et al. 2020; Gasser et al. 2020); H&N – Houghton and Nassikas Bookkeeping Model (Houghton and Nassikas 2017; Friedlingstein et al. 2020); for comparison, the net CO_2 flux from FAOSTAT (FAO Tier 1) is plotted, which comprises net emissions and removals on forest land and from net forest conversion (FAOSTAT 2021; Tubiello et al. 2021), emissions from drained organic soils under cropland/grassland (Conchedda and Tubiello 2020), and fires in organic soils (Conchedda and Tubiello 2020; Prosperi et al. 2020), as well as a net CO_2 flux estimate from National Greenhouse Gas Inventories (NGHGI) based on country reports to the UNFCCC, which include land-use change, and fluxes in managed lands (Grassi et al. 2021). **Bottom-left panel:** Anthropogenic CH_4 emissions from: EDGAR (above); CEDS (above); PRIMAP-hist (above); GAINS – The Greenhouse gas – Air pollution Interactions and Synergies Model (Höglund-Isaksson et al. 2020); EPA-2019: Greenhouse gas emission inventory (US-EPA 2019); FAO –FAOSTAT inventory emissions (Tubiello et al. 2013; Tubiello 2018; FAOSTAT 2021); **Bottom-right panel:** Anthropogenic N_2O emissions from: GCP – global nitrous oxide budget (Tian et al. 2020); CEDS (above); EDGAR (above); PRIMAP-hist (above); GAINS (Winiwarter et al. 2018); EPA-2019 (above); FAO (above). Differences in emissions across different versions of the EDGAR dataset are shown in the Supplementary Material (Figure 2.SM.2). Source: Minx et al. (2021).

by independent methods and observations (e.g., comparing top-down vs bottom-up estimates; modelling against remote sensing data) (Li et al. 2020; Saunois et al. 2020; Petrescu et al. 2020a, 2021); (ii) by comparing estimates from multiple sources and understanding sources of variation (Macknick, 2011; Andres et al. 2012; Andrew 2020; Ciais et al. 2021); (iii) by evaluating multiple estimates from a single source (Hoesly and Smith 2018) including approaches such as uncertainty ranges estimated through statistical sampling across parameter values applied, for example, at the country or sectoral level (Monni et al. 2007; Andres et al. 2014; Solazzo et al. 2021), or to spatially distributed emissions (Tian et al. 2019).

Uncertainty estimates can be rather different depending on the method chosen. For example, the range of estimates from multiple sources is bounded by their interdependency; they can be lower than true structural plus parameter uncertainty estimates or than estimates made by independent methods. In particular, it is important to account for potential bias in estimates, which can result from using common methodological or parameter assumptions across estimates, or from missing sources, which can result in a systemic bias in emission estimates (see N_2O discussion below). Independent top-down observational constraints are, therefore, particularly useful to bound total emission estimates (Petrescu et al. 2021).

Solazzo et al. (2021) evaluated the uncertainty of EDGAR's source categories and totals for the main GHGs (CO_2-FFI, CH_4, N_2O). This study is based on the propagation of the uncertainty associated with input parameters (activity data and emission factors) as estimated by expert judgement (Tier-1) and compiled by the IPCC (2019, 2006). A key methodological challenge is determining how well uncertain parameters are correlated between sectors, countries, and regions. The more highly correlated parameters (e.g., emission factors) are across scales, the higher the resulting overall uncertainty estimate. Solazzo et al. (2021) assume full covariance between the same source categories where similar assumptions are being used, and independence otherwise. For example, they assume full covariance where the same emission factor is used between countries or sectors, while assuming independence where country-specific emission factors are used. This strikes a balance between extreme assumptions (full independence or full covariance in all cases) that are likely unrealistic, but still leans towards higher uncertainty estimates. When aggregating emission sources, assuming full covariance increases the resulting uncertainty estimate. Uncertainties calculated with this methodology tend to be higher than the range of values from ensemble of dependent inventories (Saunois et al. 2016, 2020). The uncertainty of emission estimates derived from ensembles of gridded results from bio-physical models (Tian et al. 2018) adds an additional dimension of spatial variability, and is therefore not directly comparable with aggregate country or regional uncertainty, estimated with the methods discussed above.

This section provides an assessment of uncertainties in GHG emissions data at the global level. The uncertainties reported here combine statistical analysis, comparisons of global emissions inventories and expert judgement of the likelihood of results lying outside a defined confidence interval, rooted in an understanding gained from the relevant literature. At times, we also use a qualitative assessment of confidence levels to characterise the annual estimates from each term, based on the type, amount, quality, and consistency of the evidence as defined by the IPCC (IPCC 2014).

Such a comprehensive uncertainty assessment covering all major groups of GHGs and considering multiple lines of evidence has been missing in the literature. The absence has provided a serious challenge for a transparent, scientific reporting of GHG emissions in climate change assessments such as those by IPCC's Working Group III or the UN Emissions Gap Report, which have only more recently started to deal with the issue (Blanco et al. 2014; UNEP 2020). Most of the available studies in the peer-reviewed literature using multiple lines of evidence for their assessment have focused on individual gases as in the Global Carbon Budget (Friedlingstein et al. 2020), the Global Methane Budget (Saunois et al. 2020) or the Global Nitrous Oxide Budget (Tian et al. 2020) or covered multiple gases, but mainly considered individual lines of evidence (Janssens-Maenhout et al. 2019; Solazzo et al. 2021).

We adopt a 90% confidence interval (5th–95th percentile) to report the uncertainties in our GHG emissions estimates – that is, there is a 90% likelihood that the true value will be within the provided range if the errors have a Gaussian distribution, and no bias is assumed. This is in line with previous reporting in IPCC AR5 (Blanco et al. 2014; Ciais et al. 2014). Note that national emissions inventories submitted to the UNFCCC are requested to report uncertainty using a 95% or 2σ confidence interval. The use of this broader uncertainty

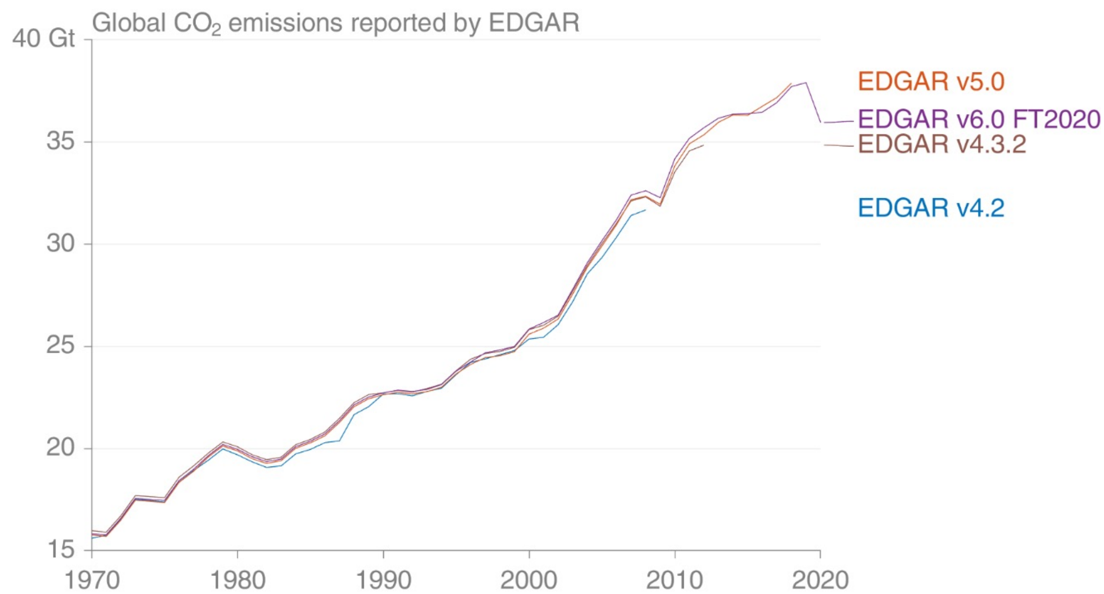

Figure 2.SM.2 | Comparison of estimates from different versions of the EDGAR database for CO_2 from fossil fuel combustion and industry. EDGAR v6.0 FT2020 refers to the Chapter 2 emissions dataset, as documented in this supplementary material and in Minx et al. (2021).

interval implies, however, a relatively high degree of knowledge about the uncertainty structure of the associated data, particularly regarding the distribution of uncertainty in the tails of the probability distributions. Such a high degree of knowledge is not present across all regions, emission sectors, and species considered here. Note that, in some cases below, we convert 1σ uncertainty results from the literature to a 90% confidence interval by implicitly assuming a normal distribution. While we do this as a necessary assumption to obtain a consistent estimate across all GHGs, we note that this itself is an assumption that may not be valid. We have made use of the best available information in the literature, but note that much more work on uncertainty quantification remains to be done. Using IPCC uncertainty language, we cannot assign *high confidence* to the robustness of most existing uncertainty estimates.

2.SM.2.1 CO_2 Emissions from Fossil Fuels and Industrial Processes (CO_2-FFI)

Several studies have compared estimates of annual CO_2-FFI emissions from different global inventories (Macknick 2011; Andres et al. 2012; Gütschow et al. 2016; Janssens-Maenhout et al. 2019; Andrew, 2020; Petrescu et al. 2020b). However, estimates are not fully independent as they all ultimately rely on many of the same data sources. For example, all global inventories use one of four global energy datasets to estimate CO_2 emissions from energy use, and these energy datasets themselves all rely on the same national energy statistics, with few exceptions (Andrew 2020). Some divergence between these estimates (Figure 2.SM.2) are related to differences in the estimation methodology, conversion factors, emission coefficients, assumptions about combustion efficiency, and calculation errors (Marland et al. 2009; Andrew 2020). Key differences for nine global datasets are highlighted in Table 2.SM.3 (see also Table 2.SM.2 for further information on the inventories).

Another important source of divergence between datasets is differences in their respective system boundaries (Macknick 2011; Andres et al. 2012; Andrew 2020). Hence, differences across CO_2-FFI emissions estimates do not reflect full uncertainty due to source data dependencies. At the same time, the observed range across estimates from different databases exaggerates uncertainty, to the extent that they largely originate in system boundary differences (Macknick 2011; Andrew 2020).

Across global inventories, mean global annual CO_2-FFI emissions track at 34 ± 2 $GtCO_2$ in 2014, reflecting a variability of about ±5.4% (Figure 2.SM.1). However, this variability is almost halved when system boundaries are harmonised (Andrew 2020). EDGAR CO_2-FFI emissions, as used there, track at the top of the range as shown in Figure 2.SM.1. This is partly due to the comprehensive system boundaries of EDGAR, but also due to the assumption of 100% oxidation of combusted fuels as per IPCC default assumptions. Once system boundaries are harmonised, EDGAR continues to track at the upper end of the range, but no longer at the top. EDGAR CO_2-FFI estimates are further well-aligned with emission inventories submitted by Annex I countries to the UNFCCC – even though some variation can occur for individual countries (Andrew 2020; Minx et al. 2021). Differences in FFI-CO_2 emissions across different versions of the EDGAR dataset are shown in Figure 2.SM.2.

Uncertainties in CO_2-FFI emissions arise from the combination of uncertainty in activity data and uncertainties in emission factors including assumptions for combustion completeness and non-combustion uses. CO_2-FFI emissions estimates are largely derived from energy consumption activity data, where data uncertainties are comparatively small due to well-established statistical monitoring systems, although there are larger uncertainties in some countries and time periods (Macknick 2011; Andres et al. 2012; Ballantyne et al. 2015; Janssens-Maenhout et al. 2019; Andrew, 2020). Most

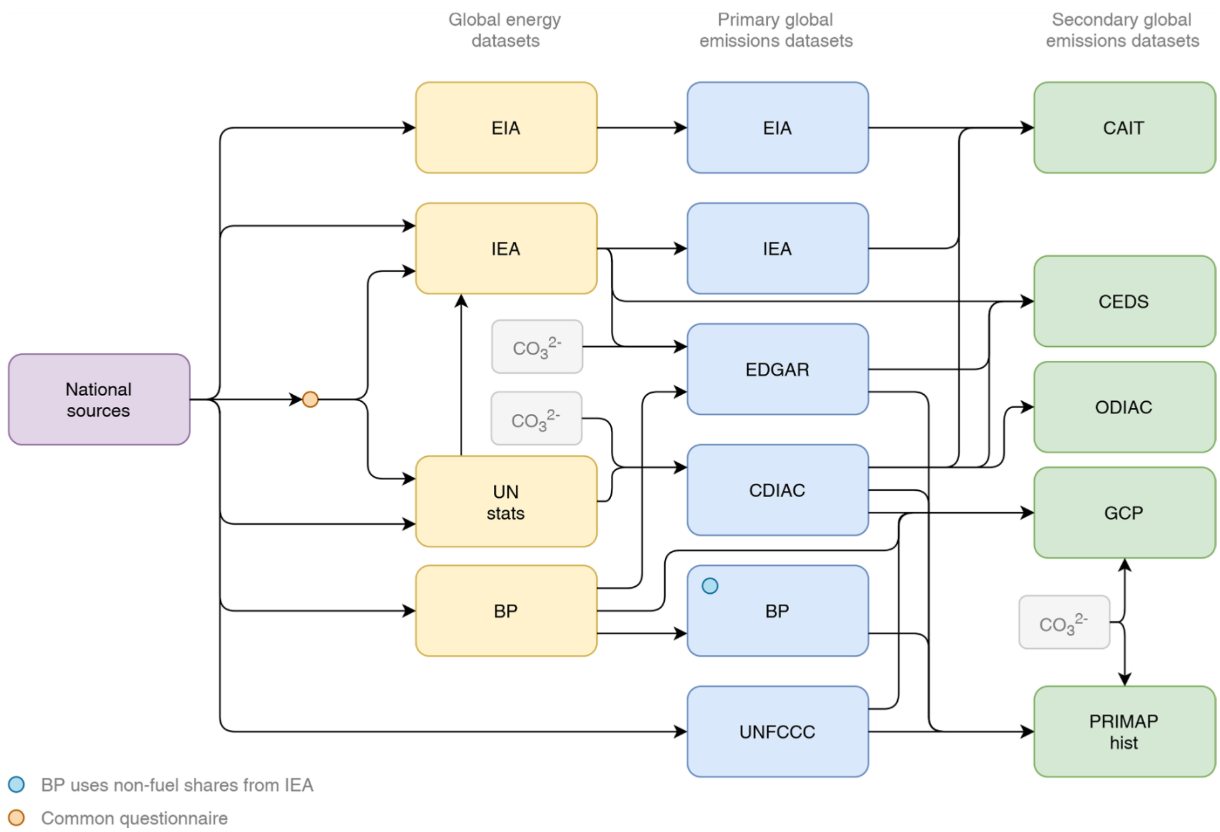

Figure 2.SM.3 | Dependencies of selected global energy and CO_2 emissions datasets. Here a 'primary' emissions dataset is one that calculated emissions directly from energy data, rather than collating emissions estimates from other sources. In addition to energy data sources, some emissions datasets include emissions from carbonates, which rely on other data sources. Some national data are first collated by regional organisations. 'UN stats' is the United Nations Statistics Office (not UNFCCC). Source: Andrew (2020).

of the underlying uncertainties are systematic and related to underlying biases in the energy statistics and accounting methods used (Friedlingstein et al. 2020). Uncertainties are lower for fuels with relatively uniform properties such as natural gas, oil or gasoline, and higher for fuels with more diverse properties, such as coal (IPCC 2006; Blanco et al. 2014). Uncertainties in CO_2 emissions estimates from industrial processes – that is, non-combustive oxidation of fossil fuels and decomposition of carbonates – are higher than for fossil fuel combustion. At the same time, products such as cement also take up carbon over their life cycle, which are often not fully considered in carbon balances (Xi et al. 2016; Sanjuán et al. 2020; Guo et al. 2021). However, recent versions of the global carbon budget include specific estimates for the cement carbonation sink and estimate average annual CO_2 uptake at 0.70 $GtCO_2$ for 2010–2019 (Friedlingstein et al. 2020).

Uncertainties for energy consumption data (and, therefore, CO_2-FFI emissions) are generally higher for the first year of their publication when less data is available to constrain estimates. In the BP energy statistics, 70% of data points are adjusted by an average of 1.3% of a country's total fossil fuel use in the subsequent year, with further more modest revisions later on (Hoesly and Smith 2018). Uncertainties are also higher for developing countries, where statistical reporting systems do not have the same level of maturity as in many industrialised countries (Gregg et al. 2008; Marland, 2008; Andres et al. 2012; Guan et al. 2012; Korsbakken et al. 2016; Janssens-Maenhout et al. 2019; Friedlingstein et al. 2019, 2020; Andrew, 2020). However, these customary country groupings do not always predict the extent to which a country's energy data has undergone historical revisions (Hoesly and Smith 2018). Uncertainties in CO_2-FFI emissions before the 1970s are higher than for more recent estimates. Over the last two to three decades uncertainties have increased again because of increased fuel production and consumption in some developing countries with less rigorous statistics and more uncertain fuel properties (Marland et al. 2009; Ballantyne et al. 2015; Friedlingstein et al. 2020).

The global carbon project (Le Quéré et al. 2018; Friedlingstein et al. 2019, 2020) assesses uncertainties in global anthropogenic CO_2-FFI emissions estimates within one standard deviation (1σ) as ±5% (±10% at 2σ). This is broadly consistent with the ±8.4% uncertainty estimate for CDIAC (Andres et al. 2014) as well as the ±7 to ±9% uncertainty estimate for EDGARv4.3.2 and v5 (Janssens-Maenhout et al. 2019; Solazzo et al. 2021) at 2σ. It remains at the higher end of the ±5% to ±10% range provided by Ballantyne et al. (2015). Consistent with the above uncertainty assessments, we present

Table 2.SM.3 | System boundaries and other key features of global FFI-CO_2 emissions datasets. Comparison of some important general characteristics of nine emissions datasets, with green indicating a characteristic that might be considered a strength. Columns four to six refer to CO_2 emission estimates for industrial processes and product use. Since all datasets are under development, these details are subject to change. Based on Andrew (2020). Source: Minx et al. (2021).

	Primary source	Uses IPCC emission factors	Includes venting & flaring	Includes cement	Includes other carbonates	Non-fuel use based on:	Reports bunkers separately	By fuel type	By sector	Includes official estimates
CDIAC	yes	no	yes	yes	no	national data	yes	yes	no	no
BP	yes	yes	no	no	no	national data	no	no	no	no
IEA	yes	yes	no	no	no	national data	yes	yes	yes	no
EDGAR	yes	yes	yes	yes	yes	national data	yes	no	yes	no
EIA	yes	no	yes	no	no	US data	no	yes	No	no
GCP	partial	no	yes	yes	partial	national data	yes	yes	no	yes
CEDS	mostly	no	yes	yes	yes	national data	yes	yes	yes	yes
PRIMAP-hist	no	no	yes	yes	yes	national data	yes	no	yes	yes
UNFCCC CRFs	yes	partial	yes	yes	yes	national data	yes	yes	yes	yes

uncertainties for global anthropogenic CO_2 emissions at ±8% for a 90% confidence interval in line with IPCC AR5 (Blanco et al. 2014).

2.SM.2.2 Anthropogenic CO_2 Emissions from Land use, Land-use Change and Forestry (CO_2-LULUCF)

CO_2-LULUCF emissions are drawn from three global bookkeeping models. For 1990–2019, average net CO_2-LULUCF emissions are estimated at 6.1, 4.3, and 5.6 $GtCO_2\ yr^{-1}$ for Bookkeeping of land-use emissions (BLUE), Houghton and Nassikas Bookkeeping Model (H&N), and an earth system compact model (OSCAR) (Friedlingstein et al. 2020). Gross emissions 1990–2019 for BLUE, H&N, OSCAR are 17, 9.6 and 19 $GtCO_2\ yr^{-1}$, while gross removals are 11, 5.3, 13 $GtCO_2\ yr^{-1}$, respectively. For 1990–2019 maximum average differences are 9.1 and 7.8 $GtCO_2\ yr^{-1}$ for gross emissions and removals, respectively (Friedlingstein et al. 2020). Note that 2016–2019 is extrapolated in H&N and 2019 in OSCAR based on the anomalies of the net flux for the gross fluxes. Differences in the models underlying this observed variability are reported in Table 2.SM.4. In the longer term, a consistent general upward trend since 1850 across models is reversed during the second part of the 20th century. Since the 1980s, however, differing trends across models are related to, among other things, different land-use forcings (Gasser et al. 2020). Further differences between BLUE and H&N can be traced in particular to: (i) differences in carbon densities between natural and managed vegetation, or between primary and secondary vegetation; (ii) a higher allocation of cleared and harvested material to fast turnover pools in BLUE compared to H&N; and (iii) to the inclusion sub-grid scale transitions (Bastos et al. 2021).

Uncertainties in CO_2-LULUCF emissions can be more comprehensively assessed through comparisons across a suite of dynamic global vegetation models (DGVM) (Friedlingstein et al. 2020). DGVM models are not included in the CO_2-LULUCF mean estimate provided here, because the typical DGVM setup includes the loss of additional sink capacity. The loss of additional sink capacity arises because DGVMs isolate LULUCF emissions from natural fluxes caused by historical environmental changes by subtracting a counterfactual simulation without land-use change from one with land-use change (Pongratz et al. 2014). In particular, forests have increased their carbon density over time due to CO_2 and other environmental effects beneficial for plant growth. The 'additional sink capacity' forests would have created at the unaltered pre-industrial extent is 'lost' through land-use change and included in the DGVM estimates of CO_2-LULUCF, but excluded in bookkeeping estimates that disregard changes in carbon densities in response to environmental changes. The loss of additional sink capacity makes up about 40% of the DGVM estimate in recent years (Obermeier et al. 2021).

Nonetheless, a CO_2-LULUCF estimate from the DGVM multi-model mean remains consistent with the average estimate from the bookkeeping models, as shown in Figure 2.SM.1. Variation across DGVMs is large with a standard deviation at around 1.8 $GtCO_2\ yr^{-1}$, but is still smaller than the average difference between bookkeeping models at 2.6 $GtCO_2\ yr^{-1}$ as well as the current estimate of H&N (Houghton and Nassikas 2017) and its previous model versions (Houghton et al. 2012). DGVMs differ in methodology, input data and how comprehensively they represent land-use-related processes. In particular land management, such as crop harvesting, tillage, or grazing (all implicitly included in observation-based carbon densities of bookkeeping models) can alter CO_2 flux estimates substantially, but are included to varying extents in DGVMs, thus increasing model

Table 2.SM.4 | Key differences between global bookkeeping estimates for CO_2-LULUCF emissions.

	Bookkeeping model		
	BLUE[a]	**H&N**[b]	**OSCAR**[c]
Geographical scale of computation	0.25 degree gridscale	Country	10 regions and 5 biomes
Carbon densities of soil and vegetation	Literature-based	Based on country reporting	calibrated to DGVMs
Land-use forcing	LUH2[d,e]	FAO[f]	LUH2 and FAO[d,e,f]
Representation of processes (indicative effect on AFOLU CO_2 emissions)			
Sub-grid scale ('gross') land-use transitions	yes (↑)	no (↓)	yes (↑)
Pasture conversion	From all natural vegetation types proportionally (↑)	From grasslands first (↓)	From all natural vegetation types proportionally (↑)
Distinction rangeland vs pasture	yes (↓)	no (↑)	no (↑)
Coverage peat drainage (as in Global Carbon Budget 2020)	World (↑)[g]	South East Asia (↓)[h]	World (↑)[g]

Notes: DGVM – dynamic global vegetation model; LUH2 and FAO refer to land-use forcing datasets; arrows indicate tendency of process to increase or decrease emissions compared to the other estimates' choice. Source: Minx et al. (2021).

Literature: [a] Hansis et al. (2015); [b] Houghton and Nassikas (2017); [c] Gasser et al. (2020); [d] Hurtt et al. (2020); [e] Chini et al. (2021); [f] FAO (2015); [g] based on rangeland-pasture distinction of the HYDE dataset (Goldewijk et al. 2017) and forest cover map of Hurtt et al. (2020); see Friedlingstein et al. (2020) for details; [h] Conchedda and Tubiello, (2020); [i] Hooijer et al. (2010).

spread (Arneth et al. 2017). For all types of models, land-use forcing is a major determinant of emissions and removals, and its high uncertainty impacts CO_2-LULUCF estimates (Bastos et al. 2021). The reconstruction of land-use change of the historical past, which has to cover decades to centuries of legacy LULUCF fluxes, is based on sparse data or proxies (Goldewijk et al. 2017; Hurtt et al. 2020), while satellite-based products suffer from complications in distinguishing natural from anthropogenic drivers (Hansen et al. 2013; Li et al. 2018) or accounting for small-scale disturbances and degradation (Matricardi et al. 2020). Lastly, regional carbon budgets can be substantially over- or under-estimated when the carbon embodied in trade products is not accounted for (Ciais et al. 2021).

Friedlingstein et al. (2020) is taken as the reference point for our uncertainty assessment. The Global Carbon Budget provides a best-value judgement for the ±1σ absolute uncertainty range of CO_2-LULUCF emissions at ±2.6 $GtCO_2$ yr^{-1}, constant over the last decades. This constant, absolute uncertainty estimate corresponds roughly to a relative uncertainty of about ±50% over 1970–2019, which is much higher than for most fossil-fuel related emissions, but reflects the large model spread and large differences between the current estimate of H&N and its previous model versions (Houghton et al. 2012). This corresponds to a relative uncertainty of about ±80% for a 90% confidence interval (5th–95th percentile). However, here we opt for a slightly lower relative uncertainty estimate of about ±70% for a 90% confidence interval, given that the mean of the CO_2-LULUCF estimates has been increasing over the last few decades. This provides absolute uncertainty estimates that are consistent in magnitude with the constant value in Friedlingstein et al. (2020) over time – slightly lower for earlier years and slightly higher for the most recent years. Compared to AR5 this is larger than the ±50% uncertainty estimate applied in the assessment, but still in line with the upper end of the broader relative uncertainty range considered of ±50% to ±75% (Blanco et al. 2014). Finally note that much larger uncertainties in CO_2-LULUCF emissions have been identified across the literature, but were traced back to different definitions used in various modelling frameworks (Pongratz et al. 2014) as well as inventory data (Grassi et al. 2018).

Uncertainties can be much higher at a national level than at global level, since regional biases tend to cancel out. Land-use forcing has been identified as major driver of differences at regional and global level (Gasser et al. 2020; Hartung et al. 2021; Rosan et al. 2021), as have assumptions on carbon densities and the allocation of cleared or harvested material to slash or product pools of various lifetimes, for which accurate global data over long time periods is missing (Bastos et al. 2021). Although the bookkeeping models are conceptually similar, the bookkeeping estimates include country-specific information to different extents: for example, fire suppression (for the USA) is included in H&N (Houghton and Nassikas 2017), but not the other estimates. H&N includes peat drainage emissions only for Southeast Asia, while the FAO emissions estimates for organic soil drainage added to BLUE and OSCAR cover all countries (Friedlingstein et al. 2020). The effect of smoothing the FAO cropland and pasture information, which can be very variable in some countries, with a five-year running mean in H&N, while the annual data is used for the recent decades in History database of the Global Environment (HYDE) underlying BLUE and OSCAR, must also be expected to contribute to the spread in estimates on a country level. Overall, great care has to be taken when comparing estimates of individual countries across models so as not to over-interpret differences.

Finally, note that attempts to constrain the estimates of CO_2-LULUCF emissions from bookkeeping models and DGVMs by observed biomass densities have been undertaken, but were successful only in some non-tropical regions (Li et al. 2017). While providing valuable independent and observation-driven information, remote-sensing derived estimates of carbon stock changes have limited applicability for model evaluation for the total CO_2-LULUCF flux, since they usually only quantify vegetation biomass changes and exclude legacy emissions from the pre-satellite era. Further, with the exception of the (pan-tropical) estimates by Baccini et al. (2012) they either track committed instead of actual emissions (Tyukavina et al. 2015), combine a static carbon density map with forest cover changes, or include the natural land sink (e.g., Baccini et al. 2017) to infer fluxes directly from the carbon stock time series. None of these approaches therefore fully distinguishes natural from anthropogenic disturbances for actual emissions as the CO_2-LULUCF emissions estimate provided here do, based on bookkeeping models and DGVMs, such that a direct evaluation is hampered.

2.SM.2.3 Anthropogenic CH_4 Emissions

About 60% of total global methane emissions come from anthropogenic sources – that is, they are caused by direct human activities since pre-industrial times/pre-agricultural times (Saunois et al. 2020). Some studies suggest larger anthropogenic fossil emissions than currently estimated (e.g., Hmiel et al. 2020). Anthropogenic methane emissions cover a range of different sectors: livestock (enteric fermentation and manure management, rice cultivation, fossil fuel production, distribution and use, waste handling (solid and water waste) as well as biomass and biofuel burning. About 90% of biomass burning events are thought to be triggered by human action (Andreae 1991); as biomass burning contributes less than 5% to anthropogenic methane emissions, the misallocations of natural fires is likely lower than the overall uncertainty. Methane emissions can be derived either using bottom-up estimates that rely on anthropogenic inventories such as EDGAR (Janssens-Maenhout et al. 2019), land surface models that infer part of natural emissions (Wania et al. 2013) or flux observation-based estimates for some specific sources such as geological sources (Etiope et al. 2019). Alternatively, top-down approaches can be used, such as atmospheric transport models that assimilate methane atmospheric observations to estimate past methane emissions (Houweling et al. 2017). These techniques are applied to infer emissions for a specific facility, sector, region or other aggregation, based on in-situ or satellite-based observations. Satellite observations have greatly improved the coverage of available data to better constrain top-down approaches. Local or regional studies have proved important as independent estimate of inventories while being spared of the chemical sink uncertainty (Maasakkers et al. 2021). Some top-down systems aim to optimise certain emission sectors based on differences in their spatial and temporal distributions (Bergamaschi et al. 2013), while others only solve for net emissions at the surface. Then the partitioning of top-down posterior (output) fluxes between specific source sectors is carried out with various degrees of uncertainty, depending of the methods and the degree of refinement of sectors, but often rely on ratios from the prior knowledge of fluxes. Comprehensive assessments of methane sources and sinks have been provided by Saunois et al. (2016, 2020) and Kirschke et al. (2013).

EDGAR (Crippa et al. 2019, 2021; Janssens-Maenhout et al. 2019) is one of multiple global methane bottom-up inventories available. Other inventories – namely GAINS (Höglund-Isaksson 2012; Höglund-Isaksson et al. 2020), US-EPA (EPA 2011, 2021), CEDS (Hoesly et al. 2018; McDuffie et al. 2020; O'Rourke et al. 2020), PRIMAP-hist (Gütschow et al. 2016, 2021b) as well as FAOSTAT-CH_4 (Tubiello 2013, 2018, 2019; Federici et al. 2015) – can differ in terms of their country and sector coverage as well as detail. EDGAR, CEDS, US-EPA and GAINS cover all major source sectors (fossil fuels, agriculture and waste, biofuel) – except large-scale biomass burning – but this can be added from different databases such as FINN (Wiedinmyer et al. 2011), GFAS (Kaiser et al. 2012), GFED (Giglio et al. 2013) or QFED (Darmenov and da Silva 2013). Much like CO_2-FFI, these inventories of anthropogenic emissions are not completely independent as they either follow the same IPCC methodology to derive emissions, rely on similar data sources (e.g., FAOSTAT activity data for agriculture, reported fossil fuel production), or draw on reported country inventory data (Petrescu et al. 2020a). However, they may differ in the assumptions and data used for the calculation, and in the choice of IPCC Tier levels for the methodology (Box 2.SM.1). For example, while the US-EPA inventory uses the reported emissions by the countries

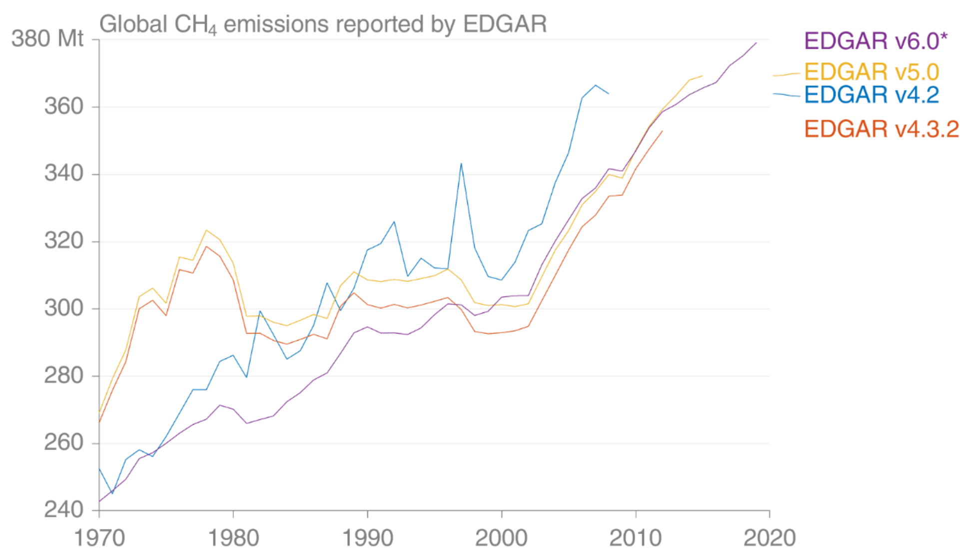

Figure 2.SM.4 | Comparison of estimates from different versions of the EDGAR database for anthropogenic CH_4 emissions.

to UNFCCC, other inventories produce their own estimates using a consistent approach for all countries, and country-specific activity data, emission factor and technological abatement when available. FAOSTAT and EDGAR mostly apply a Tier 1 approach to estimate CH_4 emissions while GAINS uses a Tier 2 approach (Box 2.SM.1). CEDS is based on pre-existing emission estimates from FAOSTAT and EDGAR, which are then scaled to match country-specific inventories, largely those reported to UNFCCC.

Global anthropogenic CH_4 emission estimates are compared in Figure 2.SM.4. EDGARv5.0 has revised total global CH_4 emissions by about 10 $MtCH_4\ yr^{-1}$ compared to the previous version due to a higher estimate for the waste sector (Figure 2.SM.1). Subsequent revisions of the estimation methodology in EDGARv6 in alignment with the IPCC guidelines refinement (IPCC 2019) lead to very substantial differences in total CH_4 emissions that are up to 50 $MtCH_4yr^{-1}$ lower before the 1990s compared to previous versions, but differences are smaller ranging from 1–13 $MtCH_4\ yr^{-1}$ since the 2000s (Figure 2.SM.1). The cause of these differences is a new procedure to separately estimate the venting component for gas and oil in the venting and flaring sector (1B2a/b2). Differences across different versions of the EDGAR dataset are shown in Figure 2.SM.4. US-EPA show the lowest estimates, probably due to missing estimates from a significant number of countries not reporting to UNFCCC (US-EPA 2020 includes estimates from only 195 countries) and incomplete sectoral coverage. EDGARv6 estimates of anthropogenic CH_4 emissions, as used here, are in the upper range of the different inventories across most anthropogenic sources. However, none of these inventories cover CH_4 emissions from forest and grassland burning, which amount to about 10–12 Mt yr^{-1} globally.

Saunois et al. (2020) provide estimates of CH_4 sources and sinks based on bottom-up and top-down approaches associated with an uncertainty range based on the minimum and maximum values of available studies (because for many individual source and sink estimates the number of studies is often relatively small). Thus, they do not consider the uncertainty of the individual estimates. As shown in Table 2.SM.5, uncertainties in total global CH_4 emissions across

Table 2.SM.5 | Uncertainties estimated for CH_4 sources at the global scale: based on ensembles of bottom-up (BU) and top-down (TD) estimates, national reports and specific uncertainty assessments of EDGAR. Note: this table is not intended to be exhaustive, but provides uncertainty estimates from some of the key literature based on different methodological approaches. Source: Minx et al. (2021).

	Estimated uncertainty in USA inventories[a]	Janssens-Maenhout et al. (2019) EDGARv4.3.2 uncertainty at 2σ	Solazzo et al. (2021) EDGARv5 uncertainty at 2σ	Global inventories uncertainty range[b]	Saunois et al. (2020) BU uncertainty range[c]	Saunois et al. (2020) TD uncertainty range[c]
Total global anthropogenic sources (incl. biomass burning)					±6%	±6%
Total global anthropogenic sources (excl. biomass burning)		±47%	–33% to +46%	±8%	±5%	
Agriculture and waste					**±8%**	**±8%**
Rice		±60%	31–38%	±22%	±20%	
Enteric fermentation	±10% to 20%			±5%	±8%	
Manure management	±20% and up to ±65%					
Landfill and waste	±10% but likely much larger	±91%	78–79%	±17%	±7%	
Fossil fuel production and use					**±20%**	**±25%**
Coal	–15% to +20%	±75%	65% 60–74%	±40%	±28%	
Oil and gas	–20% to +150%		93%	±19%	±15%	
Other		±100%	±100%	±64%	±130%*	
Biomass and biofuel burning					**±25%**	**±25%**
Biomass burning					±35%	
Biofuel burning		Included in 'Other'	147%	±24%	±17%	

Notes: [a] Based on NASEM (2018); [b] Uncertainty calculated as (min-max)/2)/mean*100 from the estimates of year 2017 of the six inventories plotted in Figure 2.SM.1. This does not consider uncertainty on each individual estimate; [c] Uncertainty calculated as (min-max)/2)/mean*100 from individual estimates for the 2008–2017 decade. This does not consider uncertainty on each individual estimate, which is probably larger than the range presented here. [d] Based on EDGARv432 for year 2010 (Janssens-Maenhout et al. 2019); [e] Based on Solazzo et al. (2021).

* Mainly due to difficulties in attributing emissions to small specific emission sector.

all anthropogenic and natural sources are comparatively small at ±6% – a range larger than errors in transport models only (Locatelli et al. 2015). However, this uncertainty on total emissions is probably underestimated as the uncertainty in the chemical sink was not fully considered in the top-down estimates in Saunois et al. (2020). About 90% of the chemical sink of methane is due to the oxidation by the hydroxyl radical (OH). Uncertainty on the global burden of OH is about ±5%, much lower than uncertainties derived from detailed analysis using EDGAR data by Janssens-Maenhout (2019) and Solazzo et al. (2021), reaching around ±45% at 2σ. Saunois et al. (2020) reported uncertainty of 10–15%, which translates to an uncertainty of about ±10% to ±30% depending on the category, with larger uncertainty in the fossil fuel sectors than in the agriculture and waste sector (Saunois et al. 2020). However, these uncertainties are also underestimated as they do not consider the uncertainty in each individual estimate, which includes potential uncertainties in activity data, emission factors, and equations used to estimate emissions.

Uncertainties in EDGAR CH_4 emissions using a Tier 1 approach are estimated at –33% to +46% at 2σ, but there is great variability across individual sectors ranging from ±30% (agriculture) to more than ±100% (fuel combustion), with high uncertainties in oil and gas sector (±93%) and coal fugitive emissions (±65%) (Solazzo et al. 2021). As an example of developed country with well-established emissions reporting, US methane emissions also report large uncertainties depending on the sector (NASEM 2018); although the activity data uncertainty may be lower than those for less-developed countries. For example, global inventories, such as EDGAR, estimate uncertainties in national anthropogenic emissions of about ± 32% for the 24 member countries of OECD, and up to ±57% for other countries, which have more uncertain activity data (Janssens-Maenhout et al. 2019).

The 2020 UN emissions gap report (UNEP 2020) gives an uncertainty range for global anthropogenic CH_4 emissions with one standard deviation of ±30% (i.e., ±60% for 2σ). On the other hand, IPCC AR5 provides a comparatively low estimate at ±20% for a 90% confidence interval. Overall, we apply a best value judgement of ±30% for global anthropogenic CH_4 emissions for a 90% confidence interval. This is justified by the larger uncertainties reported in studies on the EDGAR dataset (Janssens-Maenhout et al. 2019; Solazzo et al. 2021) as well as for FAO activity statistics by Tubiello et al. (2015).

2.SM.2.4 Anthropogenic N_2O Emissions

Anthropogenic nitrous oxide (N_2O) emissions occur in a number of sectors, namely agriculture, fossil fuel and industry, biomass burning, and waste. The emissions from the agriculture sector have four components: (i) direct and indirect emissions from soil and water bodies (inland, coastal, and oceanic waters); (ii) manure left on pasture; (iii) manure management; and (iv) aquaculture. Besides these main sectors, a final 'other' category represents the sum of the effects of climate, elevated atmospheric CO_2, and land cover change. This is a new sector that was developed as part of the global N_2O budget (Tian et al. 2020) – a recent assessment to quantify all sources and sinks of N_2O emissions updating previous work (Mosier et al. 1998; Kroeze et al. 1999; Mosier and Kroeze, 2000; Syakila and Kroeze, 2011). Estimates from the global N_2O budget are referred to as GCP-N_2O since the assessment was facilitated by the Global Carbon Project (GCP). Overall, anthropogenic sources contributed just over 40% to total global N_2O emissions (Tian et al. 2020).

There are a variety of approaches for estimating N_2O emissions. These include inventories (Tubiello et al. 2013; Tian et al. 2018; Janssens-Maenhout et al. 2019), statistical extrapolations of flux measurements (Wang et al. 2020a), and process-based land and ocean modelling (Tian et al. 2019; Yang et al. 2020). There are at least five relevant global N_2O emissions inventories available: EDGAR (Crippa et al. 2019, 2021; Janssens-Maenhout et al. 2019), GAINS

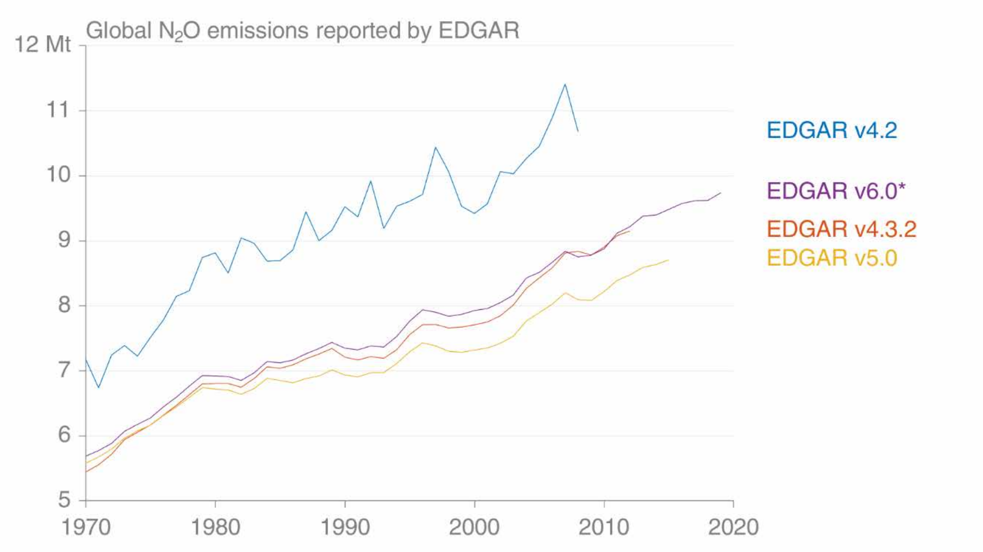

Figure 2.SM.5 | Comparison of estimates from different versions of the EDGAR database for anthropogenic N_2O emissions.

Table 2.SM.6 | Comparison of four global N_2O inventories: EDGAR (Crippa et al. 2019; Janssens-Maenhout et al. 2019); GCP (Tian et al. 2020); GAINS (Winiwarter et al. 2018; Höglund-Isaksson et al. 2020); FAOSTAT (Tubiello et al. 2013; Tubiello 2018). Source: Minx et al. (2021).

					Reported emissions in 2015 (in MtN_2O)					
Name	Time coverage	Geographical coverage	Activity split	IPCC Emissions factors	Agriculture	Fossil fuel and industry	Biomass burning	Waste and waste sector	Other	Total
EDGAR	1970–2018	Global, 226 countries	4 main sectors, 24 sub-sectors	Yes	6.2	2.3	0.05	0.4	–	8.9
GCP	1980–2016	Global, 10 regions	5 main sectors, 14 sub-sectors	No	8.4	1.6	1.1	0.6	0.3	11.9
GAINS	1990–2015 (every 5 years)	Global, 172 regions	3 main sectors, 16 sub-sectors	No	6.8	1.3	–	0.7	–	8.8
FAOSTAT	1961–2019	Global, 231 countries	2 main sectors, 9 sub-sectors	Yes	8.3	–	0.9	–	–	9.2

2SM

(Winiwarter et al. 2018), FAOSTAT-N_2O (Tubiello et al. 2013; Tubiello 2018), CEDS (Hoesly et al. 2018; McDuffie et al. 2020; O'Rourke et al. 2020), PRIMAP-hist (Gütschow et al. 2016, 2021b), and GFED (van der Werf et al. 2017). While EDGAR and GAINS cover all sectors except biomass burning, FAOSTAT-N_2O is focused on agriculture and biomass burning and GFED on biomass burning only. As shown in Figure 2.SM.1, EDGAR, GAINS, CEDS and FAOSTAT emissions are consistent in magnitude and trend. Recent revisions in estimating indirect N_2O emissions in EDGARv6 led to an average increase of 1.5% yr^{-1} in total N_2O emissions estimates between 1999 and 2018 compared to the two previous versions (differences before 1999 were negligible at less than 1% yr^{-1}). Differences across versions of the EDGAR dataset are shown in Figure 2.SM.5. The main discrepancies across different global inventories are in agriculture, where emissions estimates from the global N_2O budget and FAOSTAT are, on average, 1.5 MtN_2O yr^{-1} higher than those from GAINS and EDGAR during 1990–2016. This is due to higher estimates of direct emissions from fertilised soils and manure left on pasture. GCP-N_2O provides the largest estimate (Figure 2.SM.1), because it synthesised from the other three inventories and further informed by additional bottom-up modelling estimates – and is more comprehensive in scope due to the new sector discussed above. EDGAR estimates of anthropogenic N_2O emissions as used in this dataset should therefore be considered as lower bound estimates (see also Table 2.SM.6).

Anthropogenic N_2O emissions estimates are subject to considerable uncertainty – larger than those from FFI-CO_2 or CH_4 emissions. N_2O inventories suffer from high uncertainty on input data, including fertiliser use, livestock manure availability, storage and applications (Galloway et al. 2010; Steinfeld et al. 2010) as well as nutrient, crops and soils management (Ciais et al. 2014; Shcherbak et al. 2014). Emission factors are also uncertain (Crutzen et al. 2008; Hu et al. 2012; IPCC 2019; Yuan et al. 2019) and several sources are not yet well understood (e.g., peatland degradation, permafrost) (Elberling et al. 2010; Wagner-Riddle et al. 2017; Winiwarter et al. 2018). Model-based estimates face uncertainties associated with the specific model configuration as well as parametrisation (Buitenhuis et al. 2018; Tian et al. 2018, 2019). Total uncertainty is also large, because N_2O emissions are dominated by emissions from soils, where the level of process understanding is rapidly changing.

For EDGAR, uncertainties in N_2O emissions are estimated based on default values (IPCC 2006) at ±42% for 24 OECD90 countries and at ±93% for other countries for a 95% confidence interval (Janssens-Maenhout et al. 2019). However, Solazzo et al. (2021) arrive at substantially larger values allowing for correlation of uncertainties between sectors, countries and regions. At a sector level, uncertainties are larger for agriculture (263%) than for energy (113%), waste (181%), industrial processes and product use (14%) and other (112%). In the recent Emissions Gap Report (UNEP 2020) relative uncertainties for global anthropogenic N_2O emissions are estimated at ±50% for a 68% (1σ) confidence interval. This is larger than the ±60% uncertainties reported in IPCC AR5 for a 90% confidence interval (Blanco et al. 2014), but is comparable with the ranges for anthropogenic emissions in the global N_2O budget (Tian et al. 2020). Overall, we assess the relative uncertainty for global anthropogenic N_2O emissions at ±60% for a 90% confidence interval.

2.SM.2.5 Fluorinated Gases

Fluorinated gases comprise over a dozen different species that are primarily used as refrigerants, solvents and aerosols. Here we compare global emissions of F-gases estimated in EDGAR to top-down estimates from the 2018 World Meteorological Organization's (WMO) Scientific Assessment of Ozone Depletion (Engel and Rigby 2018; Montzka and Velders 2018). The top-down estimates were based on measurements by the Advanced Global Atmospheric Gases Experiment (AGAGE) (Prinn et al. 2018) and National Oceanic and Atmospheric Administration (NOAA) (Montzka et al. 2015), assimilated into a global box model – using the method described in Rigby et al. (2014) and Engel and Rigby, et al. (2018). Uncertainties in the top-down estimates are due to measurement and transport model uncertainty. As F-gas emissions are almost entirely anthropogenic in nature, top-down estimates of anthropogenic fluxes are much better known than CO_2, CH_4, N_2O, where large natural fluxes contribute to the observed trends. For substances with relatively short lifetimes (~50 years or less), uncertainties are typically dominated by uncertainties in the atmospheric lifetimes. Comparisons between the EDGAR and WMO 2018 estimates were available for HFCs 125, 134a, 143a, 152a, 227ea, 23, 236fa, 245fa, 32, 365mfc and 43-10-mee, PFCs CF_4, C_2F_6, C_3F_8 and c-C_4F_8, SF_6 and

NF_3 (EDGARv6 only). For the higher molecular weight PFCs (C_4F_{10}, C_5F_{12}, C_6F_{14}, C_7F_{16}), top-down estimates were not available in WMO (2018). Top-down estimates have previously been published for these compounds (Ivy et al. 2012), however, this comparison is not included here due to their very low emissions. For a small number of species, global top-down estimates are available for some years, based on an atmospheric model independent to that used in WMO (2018), although most of these inversions use similar measurement datasets: Fortems-Cheiney et al. (2015) for HFC-134a; Lunt et al. (2015) for

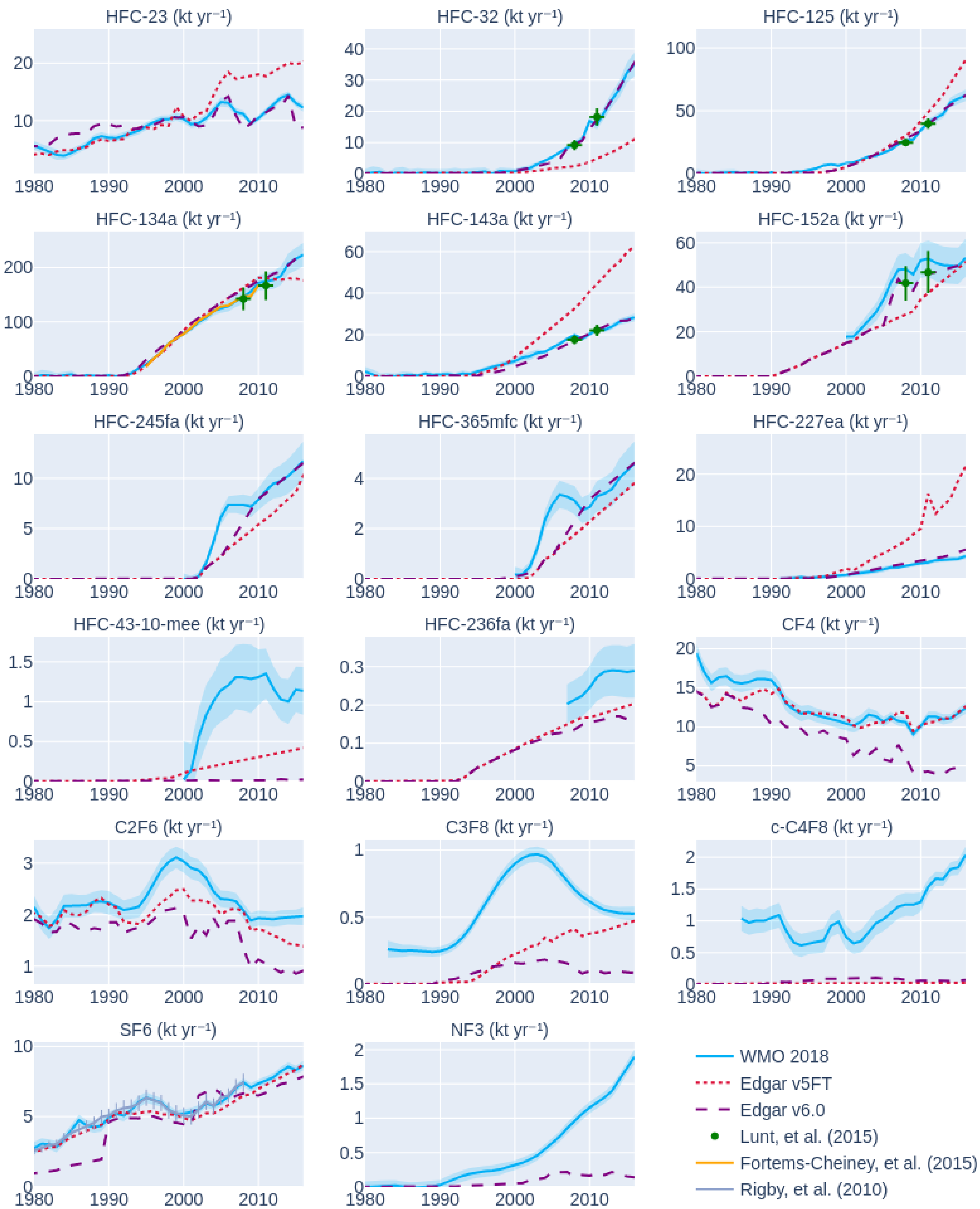

Figure 2.SM.6 | Comparison of top-down and bottom-up estimates for individual species of fluorinated gases in Olivier and Peters (2020) (EDGARv5FT) and EDGARv6 for 1980–2016. C_4F_{10}, C_5F_{12}, C_6F_{14} and C_7F_{16} are excluded. Top-down estimates from WMO 2018 (Engel and Rigby 2018; Montzka and Velders 2018) are shown as blue lines with blue shading indicating 1σ uncertainties. Bottom-up estimates from EDGARv5 and v6 (the emissions data used in Chapter 2) are shown in red dotted lines and purple dashed lines, respectively. Top-down estimates for some species are shown from Rigby et al. (2010), Fortems-Cheiney et al. (2015) and Lunt et al. (2015). Source: Minx et al. (2021).

HFC-134a; and –125, –152a, –143a and –32 and Rigby et al. (2010) for SF_6.

The comparison of global top-down and bottom-up emissions for EDGARv6 and Olivier and Peters (2020) (EDGARv5FT) F-gas species (excluding heavy PFCs) is shown in Figure 2.SM.6 for the years 1980–2016 (or a subset thereof, depending on the availability of the top-down estimates). Where available, the various top-down estimates agree with each other within uncertainties. The magnitude of the difference between the WMO (2018) and EDGAR estimates varies markedly between species, years and versions of EDGAR; for several HFCs, the top-down and bottom-up estimates often agree within uncertainties for EDGARv6 (but much less often in v5), whereas for c-C_4F_8, the top-down estimate is more than 100 times the EDGAR estimates. Some similarities and differences have been previously noted for earlier versions of EDGAR (Mühle et al. 2010, 2019; Rigby et al. 2010; Lunt et al. 2015). For SF_6, the relatively close agreement between EDGARv4.0 and a top-down estimate has been discussed in Rigby, et al. (2010). They estimated uncertainties in EDGARv4.0 of ±10% to ±15%, depending on the year, and top-down values were consistent within these uncertainties. However, the agreement is now poorer during the 1980s in EDGARv6. For some PFCs (e.g., CF_4, C_2F_6), it was previously noted that some assumptions within EDGARv4.0 had been validated against atmospheric observations, hence EDGAR might be considered a hybrid of top-down and bottom-up methodologies for these species (Mühle et al. 2010). However, it is unclear for which other species similar validation has taken place, or how these assumptions vary between versions of EDGAR.

When species are aggregated into F-gas total emissions, weighted by their current 100-year GWPs based on IPCC AR6 (Forster et al. 2021), we note that, in the left panel of Figure 2.SM.7, the Olivier and Peters (2020) (EDGARv5FT) estimates are around 10% lower than the WMO 2018 values in the 1980s. Subsequently, EDGARv5FT estimates grow more rapidly than the top-down values and are almost 30% higher than WMO 2018 by the 2010s. EDGARv6 emissions are around 10% lower than the WMO 2018 values throughout. Given that detailed uncertainty estimates are not available for all EDGAR F-gas species, we base our uncertainty estimate solely on this comparison with the top-down values (Figure 2.SM.7, left panel), and therefore suggest a conservative uncertainty in aggregated F-gas emissions of ±30% for a 90% confidence interval. For individual species, the magnitude of this discrepancy can be orders of magnitude larger.

The F-gases in EDGAR exclude species such as chlorofluorocarbons (CFCs) and hydrochlorofluorocarbons (HCFCs), which are groups of substances regulated under the Montreal Protocol. Historically, total CO_2-eq F-gas emissions have been dominated by the CFCs (Engel and Rigby 2018). In particular, during the 1980s, peak annual emissions due to CFCs reached 9.1 ± 0.4 $GtCO_2$-eq yr^{-1} (Figure 2.SM.7), comparable

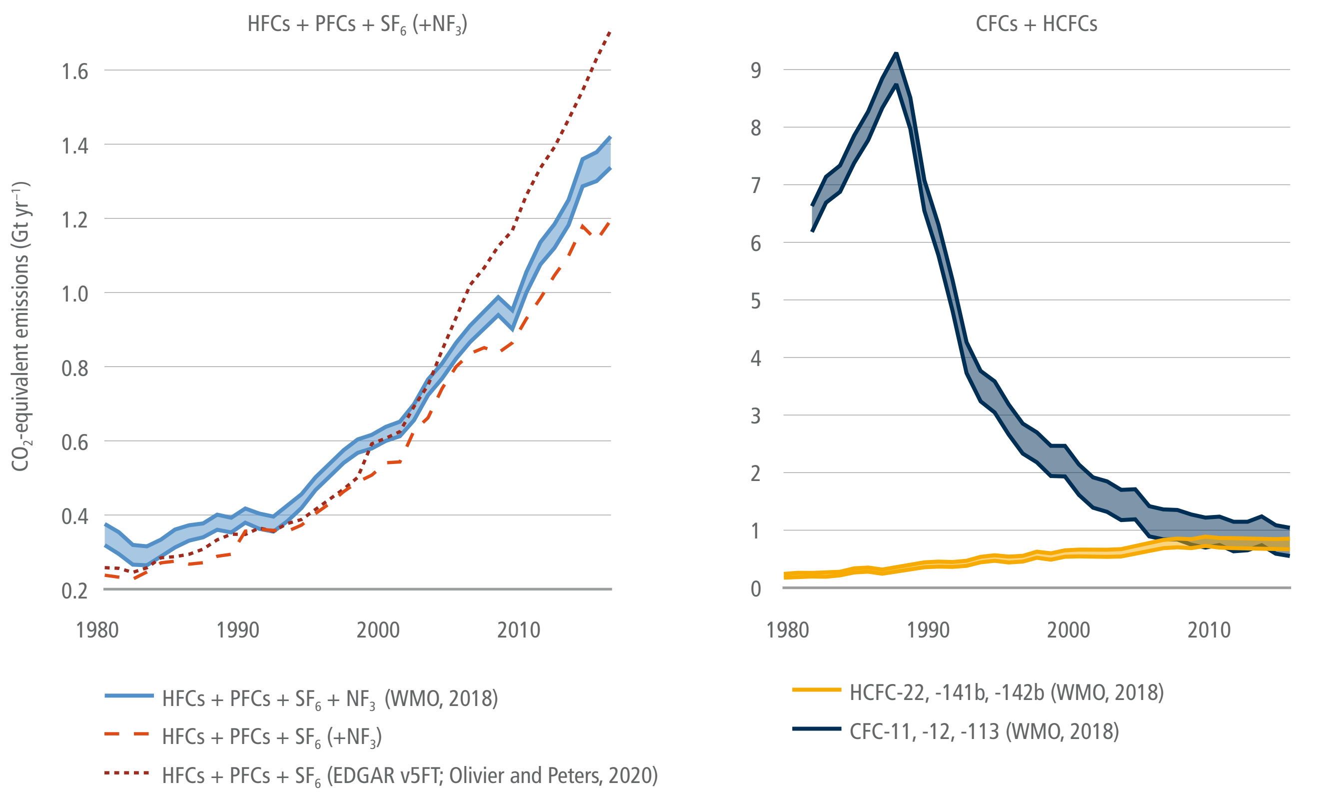

Figure 2.SM.7 | Comparison between top-down estimates and bottom-up EDGAR inventory data on GHG emissions for 1980–2016. Left panel: Total GWP100-weighted emissions based on IPCC AR6 (Forster et al. 2021) of F-gases in Olivier and Peters (2020) (EDGARv5FT) (red dashed line, excluding C_4F_{10}, C_5F_{12}, C_6F_{14} and C_7F_{16}) and EDGARv6 (purple dashed line) (Crippa et al. 2021) compared to top-down estimates based on AGAGE and NOAA data from WMO (2018) (blue lines; Engel and Rigby (2018); Montzka and Velders (2018)). **Right panel:** Top-down aggregated emissions for the three most abundant CFCs (–11, –12 and –113) and HCFCs (–22, –141b, –142b) not covered in bottom-up emissions inventories are shown in green and orange. For top-down estimates the shaded areas between two respective lines represent 1σ uncertainties. Source: Minx et al. (2021).

to that of CH_4, and substantially larger than the 2019 emissions of the gases included in EDGARv5FT and v6 (1.4 $GtCO_2$-eq). Subsequently, following the controls of the Montreal Protocol, emissions of CFCs declined substantially, while those of HCFCs and HFCs rose, such that CO_2-eq emissions of the HFCs, HCFCs and CFCs were approximately equal by 2016, with a smaller contribution from PFCs, SF_6, NF_3 and some more minor F-gases. Therefore, the GWP-weighted F-gas emissions in EDGAR, which are dominated by the HFCs, represent less than half of the overall CO_2-eq F-gas emissions in 2016.

2.SM.2.6 Aggregated GHG Emissions

Based on the assessment of relevant uncertainties above, constant, relative uncertainty estimates for GHGs are applied at a 90% confidence interval that range from relatively low for CO_2 FFI (±8%), to intermediate values for CH_4 and F-gases (±30%), to higher values for N_2O (±60%) and CO_2 from LULUCF (±70%). To aggregate these and estimate uncertainties for total GHGs in terms of CO_2-eq emissions, the square root of the squared sums of absolute uncertainties for individual (groups of) gases are taken, using 100-year global warming potentials (GWP100) with values from IPCC AR6 (Forster et al. 2021, Section 7.6 and Supplementary Material 7.SM.6) to weight emissions of non-CO_2 gases but excluding uncertainties in the metric itself. An estimate of this 'metric uncertainty' is provided in the next section. Overall, this uncertainty assessment is broadly in line with IPCC AR5 (Blanco et al. 2014), but provides important adjustments in the evaluation of uncertainties of individual gases (CH_4, F-gases, CO_2-LULUCF) as well as the approach in reporting total uncertainties across GHGs.

2.SM.2.7 Uncertainties of GHG Emission Metrics Used to Report Aggregated Emissions

GHG emission metrics are necessary if emissions of non-CO_2 gases and CO_2 are to be aggregated into CO_2-eq emissions (Section 2.3). GWP100 is the most common metric and has been adopted for emissions reporting under the transparency framework for the Paris Agreement (UNFCCC 2019), but many alternative metrics exist in the scientific literature. The most appropriate choice of metric depends on the climate policy objective and the specific use of the metric to support that objective (i.e., why do we want to aggregate or compare emissions of different gases? What specific actions do we wish to inform?).

Different metric choices and time horizons can result in very different weightings of the emissions of short-lived climate forcers (SLCFs), such as CH_4. For example, 1t CH_4 represents as much as 81 tCO_2-eq if a global warming potential (GWP) is used with a time horizon of 20 years, or as little as 5.4t CO_2-eq if the global temperature change potential (GTP) is used with a time horizon of 100 years (Forster et al. 2021a). More recent metric developments that compare emissions in new ways – e.g., the additional warming from sustained changes in SLCF emissions compared to pulse emissions of CO_2 – increase the range of metric values further and can even result in negative metric values for SLCFs, if their emissions are falling rapidly (Allen et al. 2018; Cain et al. 2019; Collins et al. 2019; Lynch et al. 2020).

The contribution of SLCF emissions to total GHG emissions expressed in CO_2-eq thus depends critically on the choice of GHG metric and its time horizon. However, even for a given choice, the metric value for each gas is also subject to uncertainties. For example, the GWP100 for biogenic CH_4 has changed from 21 based on the IPCC Second Assessment Report (SAR) in 1995 to 28 or 34 based on IPCC AR5 (excluding or including climate-carbon cycle feedbacks), and to 27 based on IPCC AR6. These changes and remaining uncertainties arise from parametric uncertainties, differences in methodological choices, and changes in metric values over time due to changing background conditions.

Parametric uncertainties arise from uncertainties in climate sensitivity, radiative efficacy and atmospheric lifetimes of CO_2 and non-CO_2 gases, etc. The WGI contribution to AR6 assessed the parametric uncertainty of GWP for CH_4 as ±32% and ±40% for time horizons of 20 and 100 years, ±43% and ±47% for N_2O, and ±26–31 and ±33–38% for various F-gases (Forster et al. 2021). The uncertainty of GTP100 for CH_4 was estimated at ±83%, which is larger than the uncertainty in a forcing-based metric due to uncertainties in climate responses to forcing (e.g., transient climate sensitivity).

Methodological choices introduce a different type of uncertainty, namely which indirect effects are included in the calculation of metric values and the strength of those feedbacks. For CH_4, indirect forcing caused by photochemical decay products (mainly tropospheric ozone and stratospheric water vapour) contributes almost 40% of the total forcing from CH_4 emissions. More than half of the changes in GWP100 values for CH_4 in successive IPCC assessments from 1995 to 2013 are due to re-evaluations of these indirect forcings. In addition, warming due to the emission of non-CO_2 gases extends the lifetime of CO_2 already in the atmosphere through climate-carbon cycle feedbacks (Friedlingstein et al. 2013). Including these feedbacks results in higher metric values for all non-CO_2 gases, but the magnitude of this effect is uncertain – for example, AR5 found the GWP100 value for CH_4 without climate-carbon cycle feedbacks to be 28, whereas including this feedback would raise the value to between 31 and 34 (Myhre et al. 2013; Gasser et al. 2016; Sterner and Johansson 2017). The AR6 includes climate-carbon cycle feedbacks (Forster et al. 2021). These parametric uncertainties associated with different feedbacks are incorporated into the above uncertainty estimates by WGI.

A third uncertainty arises from changes in metric values over time. Metric values depend on the radiative efficacy of CO_2 and non-CO_2 emissions, which in turn depend on the changing atmospheric background concentrations of those gases. Rising temperature can further affect the lifetime of some gases and hence their contribution to forcing over time for different emission scenarios (Reisinger et al. 2011). Successive IPCC assessments take changing starting-year background conditions into account, which explains part of the changes in GWP100 metric values in different reports. Applying a single metric value to a multi-decadal historical time series of emissions is therefore only an approximation of the correct metric value for any given emissions year – as, for example, the correct

GWP100 value for CH_4 emitted in the year 1970 will be different to the GWP100 value for an emission in the year 2018. However, the literature does not offer a complete set of GWP100 metric values for past concentrations and climate conditions covered in our time series.

Overall, we estimate the uncertainty in GWP100 metric values, if applied to an extended historical emission time series, as ±50% for CH_4 and other SLCFs, and ±40% for non-CO_2 gases with longer atmospheric lifetimes (specifically, those with lifetimes longer than 20 years). If uncertainties in GHG metrics are considered and assumed to be independent for each gas (which may lead to an underestimate), the overall uncertainty of total GHG emissions in 2019 increases from ±11% to ±13%. However, these GWP-related uncertainties are not included in the global, regional or sectoral emissions estimates in the remainder of the assessment.

The WGIII assessment uses GWP100 metric values from the WGI contribution to AR6 (Forster et al. 2021) as a default metric when presenting aggregated emissions and removals of different GHGs (Cross-Chapter Box 2, Supplementary Material Section 2.SM.3, and Annex II.8).

2.SM.3 GHG Emission Metrics

2.SM.3.1 Definition and Scope

GHG emission metrics are used to compare climate effects of different GHGs and to aggregate emissions and removals of different GHGs, such as for national inventory reporting and development of mitigation policies. GHG emission metrics provide simplified information about the effects that emissions of different gases GHGs have on global temperature or other aspects of climate, usually expressed relative to the effect of emitting CO_2.

The common glossary for the IPCC Sixth Assessment Report (AR6) defines GHG emission metrics as follows:

> A simplified relationship used to quantify the effect of emitting a unit mass of a given greenhouse gas (GHG) on a specified key measure of climate change. A relative GHG emission metric expresses the effect from one gas relative to the effect of emitting a unit mass of a reference GHG on the same measure of climate change. There are multiple emission metrics, and the most appropriate metric depends on the application. GHG emission metrics may differ with respect to: (i) the key measure of climate change they consider; (ii) whether they consider climate outcomes for a specified point in time or integrated over a specified time horizon; (iii) the time horizon over which the metric is applied; (iv) whether they apply to a single emission pulse, emissions sustained over a period of time, or a combination of both; and (v) whether they consider the climate effect from an emission compared to the absence of that emission or compared to a reference emissions level or climate state.
>
> Notes: most relative GHG emission metrics (such as the *g*lobal warming potential (GWP), global temperature change potential (GTP), global damage potential, and GWP*), use carbon dioxide (CO_2) as the reference gas. Emissions of non-CO_2 gases, when expressed using such metrics, are often referred to as 'carbon dioxide equivalent' emissions. A metric that establishes equivalence regarding one key measure of the climate system response to emissions does not imply equivalence regarding other key measures. The choice of a metric, including its time horizon, should reflect the policy objectives for which the metric is applied.

Emission metrics also exist for aerosols, but these are not commonly used in climate policy. This assessment focuses on GHG emission metrics only.

Parties to the Paris Agreement decided in the Paris Agreement Rulebook to report aggregated emissions based on the global warming potential with a time horizon of 100 years (GWP100) from AR5, or to use GWP100 values from a subsequent IPCC report as agreed upon by the CMA (UNFCCC 2019, 18/CMA.1), and to account for their second and subsequent Nationally Determined Contributions in accordance with this approach (UNFCCC 2019, 4/CMA.1). However, parties can report supplemental information about aggregate emissions and removals using other GHG emission metrics (e.g., global temperature change potential) expressed in CO_2-eq and assessed by the IPCC.

Apart from international reporting and accounting, countries or sectors might consider other GHG emission metrics to help achieve specific domestic policy objectives. A clear assessment of metrics can help decision-makers determine the consistency between policy goals and metrics and avoid potentially inadvertent consequences of alternative metric choices.

This Supplementary Material provides additional explanations, references and figures to the assessment of GHG emission metrics from a mitigation perspective in Cross-Chapter Box 2 on GHG emission metrics in Chapter 2. Both the Cross-Chapter Box and this Supplementary Material build on the physical science assessment of GHG emission metrics by WGI (Forster et al. 2021, Section 7.6).

2.SM.3.2 Key Characteristics of Pulse Emission Metrics GWP and GTP

The global warming potential (GWP) and the global temperature change potential (GTP) were the main metrics assessed in AR5 (Myhre et al. 2013; IPCC 2014; Kolstad et al. 2014). GWP with a time horizon of 100 years (GWP100) is the predominant metric used in literature assessed by WGIII.

These metrics compare the effect on climate of emitting a unit mass of a non-CO_2 gas over a chosen time horizon with the effect of emitting the same unit mass of CO_2. GWP compares CO_2 and non-CO_2 emissions based on the radiative forcing they would cause integrated over the entire time horizon, whereas GTP compares emissions based on the global mean surface temperature change they would cause only at the end point of the chosen time horizon.

Table 2.SM.7 | Illustrative metric values for CH_4 under a range of metrics and time horizons. GWP and GTP compare pulse emissions of non-CO_2 gases with a pulse emission of CO_2. Combined global temperature change potential (CGTP) compares a sustained step-change in non-CO_2 emissions with a pulse emission of CO_2. Values are based on Forster et al. (2021).

	GWP20	GWP100	GWP500	GTP20	GTP30	GTP50	GTP100	CGTP50 (years)	CGTP100 (years)
CH_4 (fossil)	82.5	29.8	10	54.4	30.6	13.2	7.5	2823	3531
CH_4 (biogenic)	80.8	27.0	7.3	51.7	27.9	10.3	4.7	2701	3254

The WGI contribution to AR6 includes updated values for these metrics based on updated scientific understanding of the response of the climate system to emissions of different gases, including changing background concentrations (Forster et al. 2021). It also assess new metrics published since AR5. Metric values in AR6 include climate-carbon cycle feedbacks by default; this provides an important update and clarification from AR5 which reported metric values both with and without such feedbacks (Table 2.SM.7).

By far the most commonly used, static time horizon for GWP, including in reporting under the UNFCCC and the Paris Agreement, is 100 years, but other time horizons (e.g., GWP20, GWP500) have also been applied (recent examples include Tanaka et al. 2019, 2021; and Skytt et al. 2020).

For GTP, both static and dynamic time horizons are used in the literature. A static GTP evaluates warming due to an emissions pulse at the end point of the stated time horizon (Shine et al. 2005). For example, the static GTP100 would evaluate emissions occurring in 2020 based on the warming they would cause in the year 2120, whereas emissions occurring in 2030 would be evaluated based on the warming they would cause in the year 2130. By contrast, the dynamic GTP (Shine et al. 2007) evaluates each emission based on its contribution to warming in a specified future target year. Depending on application, this can be the year in which global average temperature is expected to peak within a mitigation scenario, or any other time-bound temperature-related climate target. Policy-relevant time horizons and resulting metric values for the dynamic GTP therefore depend on the chosen temperature goal and implied target year.

The time horizon of a dynamic GTP shrinks for successive emissions as the target year is approached, which increases the weight given to emissions of short-lived climate forcers (SLCFs) such as CH_4 over time. For example, for a climate policy goal of limiting warming to 1.5°C with no or limited overshoot (scenario Category C1 in Chapter 3), global average surface temperature would peak by around 2055. To compare the importance of abating non-CO_2 and CO_2 emissions in any given year relative to that policy goal, emissions occurring in the year 2020 would be evaluated using GTP35, whereas emissions in 2030 would be evaluated using GTP25, and so on (see Table 2.SM.7 for illustrative values).

A key limitation of pulse emission metrics such as GWP and GTP, noted in AR5 and emphasised in more recent literature (Allen et al. 2018; Cain et al. 2019; Collins et al. 2019; Allen et al. 2021; see Forster et al. 2021 for the WGI assessment), is that metric values depend strongly on the selected time horizon, given that warming from a CH_4 emission pulse declines over time, whereas warming from a pulse of CO_2 is nearly constant over centuries. Universal use of a single metric and time horizon can thus result in mismatches between policy goals and actual climate outcomes. Moreover, 'CO_2 equivalence' of pulse emissions based on GWP or GTP does not imply equivalent climate outcomes from cumulative emissions, nor at all times even from a single emissions pulse.

This is illustrated in Figure 2.SM.8, which shows that the warming from CH_4 emissions sustained at a constant rate is greater than the warming from an 'equivalent' (based on GWP100) amount of sustained CO_2 emissions for the first 100 years, but the rate of warming from sustained CH_4 emissions declines over time and the total warming becomes less than that from sustained CO_2 emissions beyond the first century. The different cumulative behaviour of CO_2 and SLCF emissions is particularly relevant in mitigation scenarios: each tonne of additional CO_2 emissions causes further warming until emissions reach net zero (Canadell et al. 2021). By contrast, declining SLCF emissions can result in a declining SLCF contribution to global temperature since the warming from past emissions does not persist and declines over time. This behaviour is well known and can be readily replicated with simple climate models (Figure 2.SM.8) but cumulative SLCF emissions based on GWP100 do not capture this decline (Lynch et al. 2020).

A more detailed discussion of recently developed step-change metrics GWP* (Allen et al. 2018; Cain et al. 2019; Smith et al. 2021) and combined global temperature change potential (CGTP) (Collins et al. 2019) and their ability to reproduce temperature changes resulting from sustained changes in SLCF emissions is provided in Forster et al. (2021). These metrics indicate greater climate benefits from rapid and sustained CH_4 reductions compared to CO_2 over the next few decades than if such reductions are weighted by GWP100, while conversely, sustained methane increases have greater adverse climate impacts (Collins et al. 2019; Lynch et al. 2020; Brazzola et al. 2021). However, as indicated in Figure 2.SM.8, the warming from CH_4 (or conversely, the benefits of CH_4 reduction) do not continue to accumulate at the initial rate.

2.SM.3.3 Relationship of GWP and GTP to Cost-benefit and Cost-effectiveness Frameworks

The GWP with a static time horizon approximates the global damage potential – that is, the notion that the emission of a non-CO_2 forcer at any point in time should be weighted by the marginal economic damages from this emission, relative to the marginal damages from emitting a unit mass of CO_2 (Reilly and Richards 1993; Kandlikar 1996; Kolstad et al. 2014).

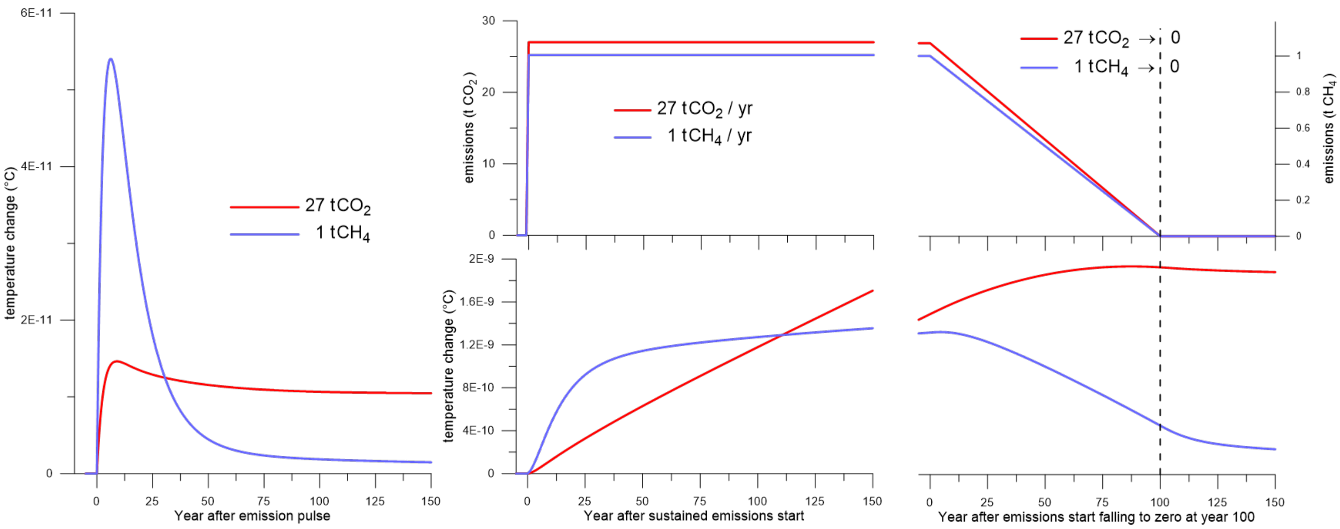

Figure 2.SM.8 | Temperature responses over time to emission pulses and sustained and declining emissions of CO_2 and CH_4. Left: Single emissions pulse of 1 tCH_4 and 27 tCO_2. **Middle panels:** Sustained annual emission (top) of 1 tCH_4 and 27 tCO_2, and temperature response (bottom). **Right:** Emissions linearly declining from 1 tCH_4 and 27 tCO_2 in year zero, to zero emissions of both gases in year 100 (top), and temperature outcome (bottom). The amount of 27 tCO_2 is chosen for illustrative purposes as it represents the 'CO_2-equivalent' emission of 1t CH_4 based on GWP100. Temperature responses are based on response functions from Forster et al. (2021).

The GWP time horizon can be linked to the social discount rate used in the global damage potential to calculate the net present value of economic damages over time from each emission. Recent studies (Sarofim and Giordano 2018; Mallapragada and Mignone 2019) confirm earlier work (Fuglestvedt et al. 2003; Boucher 2012) that, for methane, GWP100 is consistent with a discount rate of about 3%, with the specific value depending on the gas and other assumptions such as non-linearity of damages with warming. Detailed sensitivity analysis by Sarofim and Giordano (2018) gives an interquartile range of 2.7–4.1% for the implied discount rate for GWP100 in the case of CH_4, depending on a range of assumptions about climate scenarios, shape of damage functions, climate feedbacks and global economic growth. GWP20 would imply much higher discount rates of 11.1–14.6%, given the stronger weighting of near-term effects on climate. Use of a single discount rate based on pure time preference and future growth in wealth and its effects (known as the simple Ramsey rule) can be problematic (Drupp et al. 2018) but no studies so far have evaluated metrics with varying discount rates over time. In addition, the relationship between GWP time horizon and discount rate is not universal as it depends on the lifetime of the SLCF (Fuglestvedt et al. 2003).

Shindell et al. (2017) evaluated the social cost of methane emissions directly based on time-varying changes in climate and inferred economic damages, and found a wide range of possible values This reflects the range of judgements in determining social costs of pollutants including non-climate effects. However, their results are broadly consistent with a GWP100-based weighting of CH_4 relative to CO_2 when similar discount rates and consistent assumptions about climate-related damages and the temperature dependence of damage functions are chosen for both gases.

These studies indicate that, even though the GWP100 was not designed to meet any economic objectives and was not designed as a damage potential, the discount rate implied in GWP100 for CH_4 is broadly similar to social discount rates of 3–5% that are used in integrated assessment models (Chapter 3) and investments with multi-decadal lifetimes (Giglio et al. 2015; HM Treasury 2018).

In principle, GHG emission metrics focused on cost-effectiveness are better matched to the Paris Agreement's temperature goal than cost-benefit metrics, and are also supported by the UNFCCC principle that mitigation policies and measures should be cost-effective (Johansson, 2011; Tol et al. 2012; Tanaka et al. 2020). In cost-effectiveness metrics, values for SLCF emissions necessarily change over time since the closer SLCF emissions occur to the target year, the greater their contribution to climate change in that year (Aaheim and Mideksa 2017). The dynamic GTP (Shine et al. 2007) reflects such a cost-effectiveness approach by providing information on the marginal contribution of SLCF emissions in any given year to the expected peak warming at a future date (Tol et al. 2012; Mallapragada and Mignone 2017; Tanaka et al. 2020). However, the dynamic GTP does not fully match the optimal weighting of gases in least-cost mitigation pathways (also referred to as the global cost potential; e.g., Michaelis 1992; Manne and Richels 2001) because overall mitigation costs and hence the economically optimal amount and timing of SLCF abatement also depends on the discount rate as well as treatment of uncertainties, not only their contribution to warming in the target year (Johansson 2011; Ekholm 2014; Strefler et al. 2014; Tanaka et al. 2020).

The GTP with any static time horizon (e.g., GTP50 or GTP100) is not clearly matched to either a cost-benefit or a cost-effectiveness framework, as the year for which temperature outcomes are evaluated would shift forward each year and hence would not match the year when the global temperature limit is reached or the overall damages caused by each emission (Tol et al. 2012; Edwards and Trancik 2014; Strefler et al. 2014; Mallapragada and Mignone 2017). However, use of GTP with a static time horizon may be relevant where it is applied to emissions only in a given year or finite period, and if the time horizon matches a relevant climate policy goal (Fuglestvedt et al. 2010; Grewe and Dahlmann 2015; Balcombe et al. 2018).

2.SM.3.4 Global Cost-effectiveness of Physical-based Pulse Emission Metrics

A number of studies since AR5 have evaluated the impact of different pulse GHG emission metrics and time horizons on the global economic costs of limiting global average temperature change to a pre-determined level, including to *likely* below 2°C and to 1.5°C (Ekholm et al. 2013; Deuber et al. 2014; Strefler et al. 2014; Huntingford et al. 2015; Van Den Berg et al. 2015; Harmsen et al. 2016; Tanaka et al. 2020). These studies show consistently, with very few exceptions, that global costs to achieve the same temperature target below 2°C in 2100, or the same peak temperature before 2100, are higher if CH_4 emissions are weighted consistently less than indicated by GWP100 (e.g., if using GTP100 or GWP500). The increase in global mitigation costs ranges from a few percent to more than 30% in most studies, depending not only on the specific metric values used but also on the temperature limit, degree of overshoot, and abatement costs and potentials of different gases assumed in those studies. These studies also indicate, albeit less consistently and less significantly than for GTP100, that global mitigation costs would also increase if CH_4 emissions are valued consistently more highly than in GWP100 (e.g., using GWP20). Collectively, these studies indicate that, even though GWP100 does not represent the most cost-effective metric and time horizon choice possible (Tanaka et al. 2020), it is more cost-effective than any of the other static metrics and time horizons that have been tested in economic models and are used most commonly in the scientific literature.

Studies available for AR5 suggested that using a dynamic GTP or economic optimisation approaches, which defer high-cost CH_4 abatement until closer to the target year, could reduce global abatement costs compared to GWP100 by a few percent (Manne and Richels 2001; Shine et al. 2007; Johansson 2011; Reisinger et al. 2012). More recent studies confirm this theoretical cost saving in principle. However, these studies also demonstrate that the extent to which this cost saving would be realised depends on a range of assumptions, including the stringency of the target, degree of policy foresight, the speed with which CH_4 emissions can be reduced as metric values increase, allowance for any temporary temperature overshoot for end-of-century targets, the shape of marginal abatement cost curves, and the treatment of uncertainty (Ekholm et al. 2013; Strefler et al. 2014; Huntingford et al. 2015; Van Den Berg et al. 2015; Harmsen et al. 2016; Tanaka et al. 2020).

One reason why the literature shows only a limited, if any, reduction in global mitigation costs from using dynamic GTP or economic optimisation compared to GWP100 lies in the broad similarity of the metric values or exchange rates for CH_4 for temperature limits of *likely* below 2°C and lower. For such temperature limits, peak temperature would be reached between about 2050 and 2080 (Chapter 3). This means that emissions occurring in the year 2030 would be weighted by GTP20 to GTP50, but emissions in the year 2040 by GTP10 to GTP40, and so on. Across such time horizons, the numerical values of the dynamic GTP for CH_4 (as the main short-lived GHG) over the next few decades are broadly comparable on average to GWP100 (Table 2.SM.7). Since a large fraction of the total abatement potential for CH_4 is assumed to be available at relatively low costs (Harmsen et al. 2019) or co-abated with fossil CO_2 (Rogelj et al. 2014), abatement choices based on GWP100 differ little in such pathways from those based on the dynamic GTP or economic optimisation. For modelled mitigation pathways that *likely* limit warming to 2°C or below and with limited overshoot, GWP100 therefore results in overall abatement levels and costs at the global scale that are not very different from those based on dynamic GTP or economic optimisation, even though GWP100 reflects a cost-benefit rather than cost-effectiveness framework. However, differences can be more pronounced for individual sectors.

A common feature of virtually all GHG emission metrics studies to date is that they use a single emission metric (either static GWP or GTP, or dynamic GTP with predictably changing values) to inform abatement choices over the entire 21st century and beyond. This is not well matched to the new scenario logic proposed by Rogelj et al. (2019) for the Paris Agreement, which suggests that separate policy choices exist regarding the timing and magnitude of the temperature peak and the post-peak rate of temperature decline. This new scenario logic has not yet been used to evaluate GHG metrics, but Tanaka et al. (2021) show that global cost reductions could be obtained by using GWP100 as a starting metric and updating the GWP time horizon in discrete steps, depending on when and by how much the temperature goal might be exceeded based on actual emissions. This approach could reduce mitigation costs by a few percent, relative to GWP100 being used throughout the 21st century, in very high overshoot scenarios that reach the long-term temperature goal of 1.5°C or 2°C only in the 22nd century. For such scenarios, the most cost-effective weighting of SLCF emissions is generally less than GWP100 in the next few decades, but two to three times higher than GWP100 once temperature has peaked. These findings strengthen the conclusions by Fuglestvedt et al. (2018) and Tanaka and O'Neill (2018) that the choice of GHG metric is particularly important for the rate of temperature decline once net zero GHG emissions have been reached.

2.SM.3.5 Role of GHG Emission Metrics at the Sectoral Level Including Lifecycle Assessment

The AR5 noted that the choice of metric and time horizon could have significant implications for regions or sectors with high fractions of SLCF emissions (Brennan and Zaitchik 2013; Myhre et al. 2013; IPCC 2014; Strefler et al. 2014). The choice of GHG emission metric is therefore linked not only to cost-effectiveness but also to equity. Sectoral and national perspectives on mitigation pathways, including GHG emission metrics to inform such pathways, may therefore differ from a global least-cost perspective (Klinsky and Winkler 2018), but the literature has not provided a consistent framework for assessing GHG emission metrics based on a wider set of equity principles.

The shifting of costs between emitters due to different metrics has been demonstrated for the case of agriculture in New Zealand, which has a high fraction of enteric methane emissions. Even though global mitigation costs to limit warming to below 2°C would be lower under GWP100 than GTP100, costs to farmers would be greater under GWP100 than GTP100 if climate policy were to price all GHG emissions and place the cost burden on emitters (Dorner and Kerr 2017).

Various studies evaluated the extent to which cost-effective sectoral abatement strategies might change under different climate metrics. In some instances (e.g., for transport and fuel choices), the choice of metric can change abatement preferences and timing (Edwards and Trancik 2014; Edwards et al. 2016; Edwards et al. 2017). Similarly, the magnitude of the climate impact from aviation when expressed in CO_2-equivalents depends strongly on the choice of emission metric and time horizon, as SLCF emissions and contrails enhance warming significantly over days to decades, in addition to the warming from CO_2 that occurs over centuries to millennia (Fuglestvedt et al. 2010; Azar and Johansson 2012; Deuber et al. 2013; Lund et al. 2017; Lee et al. 2021). For the energy sector, Tanaka et al. (2019) show that switching from coal to gas (which has lower CO_2 but higher CH_4 emissions) for energy supply offers consistent climate benefits regardless of metric and time horizon unless CH_4 leakage rates are very high and a short-term metric (GWP20) is selected. Lynch and Pierrehumbert (2019) show that the climate impact of cultured meat (which they assume to have higher CO_2 but lower CH_4 emissions than cattle meat and a lower GHG footprint based on GWP100) increases over time, given the cumulative warming from CO_2 emissions. Substituting cattle meat with cultured meat would result in lower warming for at least the next several decades but could eventually result in higher warming than cattle meat, if this substitution is sustained over centuries and if the carbon intensity of energy supply for the manufacture of cultured meat does not decline.

For some sectors, mitigation strategies and the relative merit of specific technologies or practices compared to others (such as intensive vs extensive agricultural production and mitigation options, or choices to reduce air pollutants with a climate forcing effect) have been shown to be relatively robust against the choice of metric (Reisinger and Ledgard 2013; Ledgard and Reisinger 2014; Reisinger et al. 2017; Åström and Johansson 2019). Clark et al. (2020) show that current emissions trends in the global food system alone would be sufficient to exceed a 1.5°C temperature limit and associated global emission targets even if GWP* is used to calculate CO_2-equivalent emissions. This indicates that the importance of limiting food system emissions is not an artefact of using GWP100 as GHG emission metric, though it can change the quantification of CO_2-eq emissions over time. Even if the most effective mitigation option does not depend strongly on the choice of GHG emission metric, the cost to emitters (if emissions were priced based on their CO_2-equivalent values as part of national policies) can depend strongly on the GHG metric (Dorner and Kerr 2017).

The United Nations Environment Programme Society of Environmental Toxicology and Chemistry (UNEP-SETAC) task force on lifecycle assessment (LCA) recommended that at least two, but potentially even three, metrics with divergent weightings for SLCFs (GWP100 and GTP100 and potentially also GWP20) be used to better understand the extent to which GHG metric choices may implicitly or inadvertently affect reported carbon footprints (Cherubini et al. 2016; Levasseur et al. 2016; Jolliet et al. 2018). This matches recommendations by other researchers for the use of multiple metrics (Grewe and Dahlmann 2015; Ocko et al. 2017; Balcombe et al. 2018; Cooper et al. 2020; Allen et al. 2021) especially where there is no unambiguous policy goal for a sectoral or entity-level LCA. While there is a strong agreement in the literature that using multiple metrics provides a more nuanced understanding of the climate effects of emissions, there is no strong consensus specific pairs or sets of metrics to use (e.g., GWP20 and GWP100, or GWP100 and GTP100). GWP* has only had limited use in LCA so far, mainly to understand the impact of sustained changes in CH_4 emissions resulting from system changes or lifetime dietary choices, consistent with its focus on the effect of sustained emission changes (Clark et al. 2020; Barnsley et al. 2021).

Some studies use simple climate models or pulse-response functions to understand the climate impacts of emissions of different gases directly rather than relying on emission metrics (Berntsen and Fuglestvedt 2008; Reisinger and Clark 2017; Lynch and Pierrehumbert 2019; Mayfield et al. 2019; Cooper et al. 2020; Lee et al. 2021; Reisinger et al. 2021). Treating GHGs with different lifetimes separately supports the targeted treatment of different pollutants and avoids embedding value judgements about the climate outcome of concern, time horizons and reference levels into GHG emission metrics. This does not avoid the need for such value judgements to be made, but can allow them to be made more explicitly.

2.SM.3.6 Difference Between Marginal and Additional Warming and Relationship to Metrics

Cross-Chapter Box 2 in Chapter 2 notes that GWP* can calculate negative CO_2-eq emissions, while GWP or GTP calculate positive CO_2-eq emissions for the same CH_4 emissions path.

Rapidly declining CH_4 emissions can have a negative CO_2-warming-equivalent value based on GWP* because SLCF emissions that decline at a sufficient rate result in declining temperature, relative to the warming at a previous point in time caused by past SLCF emissions from that same source. The rate at which SLCF emissions have to decline to result in a roughly constant contribution to warming depends on the emissions history, changing background concentrations, and lifetime of the gas; for global CH_4 emissions, this has been estimated at about 0.3% per year (Forster et al. 2021).

GWP or GTP always assign a positive CO_2-equivalent value to SLCF emissions because every SLCF emission from any source results in increased future radiative forcing and higher global average temperature than would be the case without this emission, regardless of whether the rate of SLCF emissions is rising or declining

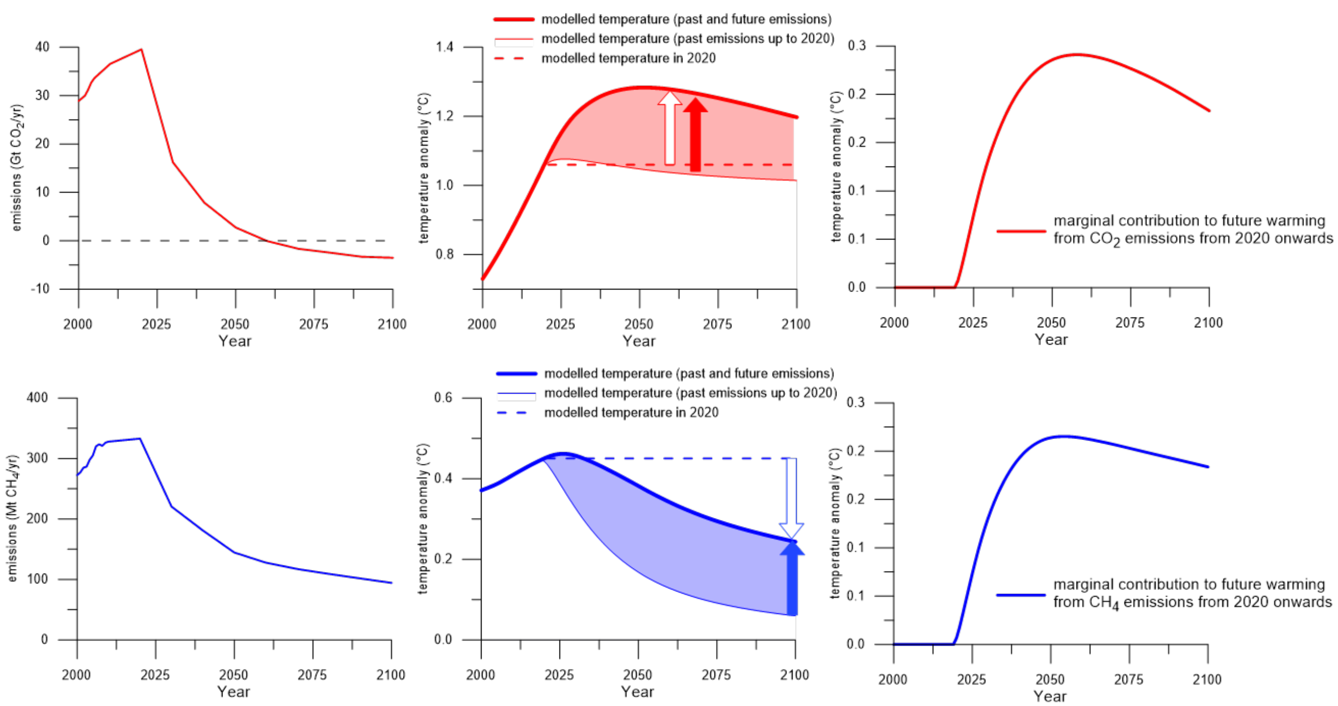

Figure 2.SM.9 | CO_2 (top) and CH_4 (bottom) emissions (left) and simulated temperature response (middle and right), for an Illustrative Mitigation Pathway (IMP-Ren15) that would limit likely warming to below 2°C. The middle panels show the modelled overall warming from the given CO_2 and CH_4 emissions trajectories (thick solid lines), the contribution to past and future warming from past emissions (up to 2020; thin solid lines), and the contribution to warming in the year 2020 from past emissions (dashed lines). The ***marginal*** warming from future CO_2 and CH_4 emissions (i.e., the difference between warming caused by emissions up to 2020, and warming caused by past and future emissions) are shown as shaded areas and solid arrows. The additional warming (i.e., the temperature change relative to the warming in 2020) is indicated by hollow arrows. The right panels show the marginal warming from CO_2 and CH_4 emissions from 2020 onwards (i.e., the increase in global average surface temperature that would occur with, compared to without, those emissions). Figure adapted from Reisinger et al. (2021); temperature responses are modelled using the pulse-response functions used in the assessment of GHG emission metrics by Forster et al. (2021).

over time. The amount of climate change (integrated radiative forcing, or temperature change at a given point in time) that occurs from these emissions, relative to the absence of these emissions (everything else being equal), has also been referred to as '*marginal* warming' (Reisinger et al. 2021), in alignment with the concepts of *marginal* damages and *marginal* costs that underpin the economics literature on multi-pollutant problems (Michaelis 1992, 1999; Reilly and Richards 1993; Kandlikar 1996; Manne and Richels 2001; Tol et al. 2012).

Figure 2.SM.9 illustrates these different perspectives: in an Illustrative Mitigation Pathway that limits warming to 1.5°C with no or limited overshoot (IMP-Ren15) (Chapter 3 and Annex III), the *marginal* warming from future CH_4 emissions is always positive and can be comparable to the *marginal* warming from future CO_2 emissions. That is, emissions of CH_4 and CO_2 from 2020 onwards (or any other specified reference year) both result in future global temperature being higher than it would be without those future emissions. Marginal warming is relevant for choices about the effort and costs that might be justified (from a damages, cost-benefit or cost-effectiveness perspective) to mitigate future emissions of either gas. The specific policy objective can then help determine what specific metric and time horizon would be optimal to use, provided that metrics are applied in a way that captures this marginal warming from future emissions. Information about marginal warming by definition does not include warming from past emissions that may continue into the future.

Warming relative to a given reference point provides a different perspective: the contribution from CH_4 emissions to global warming declines with declining emissions, whereas the contribution from CO_2 emissions to global warming continues to rise even when its emissions decline, and this contribution keeps rising until CO_2 emissions are reduced to net zero. CO_2 therefore remains and becomes the increasingly dominant driver of anthropogenic warming in virtually all emission scenarios (see also WGI Summary for Policymakers, Figure SPM.4). This information is relevant for policies and perspectives that are concerned with the changing contribution of individual gases and sectors to global warming over multiple decades, including their historical emissions (e.g., Lynch et al. 2021). Figure 2.SM.9 shows that, for CO_2, the marginal and additional warming from future emissions is virtually identical, whereas the marginal and additional warming from future CH_4 emissions point in opposite directions in a mitigation pathway. Marginal metrics such as GWP and GTP, and step/pulse metrics such as GWP* (as applied in the literature so far) can differ substantially in the CO_2 emissions they calculate as 'equivalent' to CH_4 emissions, because they focus on different aspects of climate change. The specific policy objective (e.g., a focus on cost-effective abatement, a cost-benefit approach, or a focus on additional warming compared to a reference level) is therefore crucial for choosing and applying a metric that matches a given objective.

2.SM.3.7 Influence of GHG Emission Metrics on the Timing of Reported Net Zero GHG Emissions

Cross-Chapter Box 2 in Chapter 2 notes that different metric choices can alter the reported quantity of CO_2-eq emissions and the time at which net zero GHG emissions are calculated to be reached, or whether net zero GHG emissions are reached at all. This is also an important conclusion from the assessment by WGI (Forster et al. 2021) building on Fuglestvedt et al. (2018) and Tanaka and O'Neill (2018), and highlighted by Schleussner et al. (2019) in relation to Article 4.1 of the Paris Agreement.

The degree to which reported CO_2-eq emissions would differ under alternative metrics, for the same actual emissions of different gases, is illustrated in Figure 2.SM.10. It shows calculated CO_2-eq emissions for four different IMPs from Chapter 3 (IMP-REN15, IMP-SP, IMP-REN2, and IMP-GS; see Chapter 3 for details on these pathways) for an illustrative range of metrics.

The following metrics and time horizons are used:

- GWP100 (using values from the Second Assessment Report (SAR); Fifth Assessment Report with and without climate-carbon cycle feedbacks (AR5-ccfb, and AR5-nofb); and the Sixth Assessment Report (AR6))
- GTP100 (using AR6 values)
- GWP20 (using AR6 values)
- GWP* (using the formula in Lynch et al. 2020, using AR6 values for GWP100).[1]

Overall, differences in the timing of net zero GHG (CO_2-eq) emissions are smaller for different versions of GWP100 than for fundamentally different choices of metric and/or time horizon (GWP20 or GTP100), and differ materially for GWP*.

Using GWP100 values from different IPCC assessment reports has a relatively minor effect on CO_2-eq emissions. It shifts the timing of net zero emissions by up to 10 years for those pathways that reach net zero before 2100. For pathways that reach net zero GHG emissions only very late in the 21st century, this could result in net zero not being reached at all before 2100 under some versions of GWP100. For example, IMP-GS reaches net zero GHG emissions in 2095 for GWP100 (SAR) but remains (just) above zero until after 2100 for GWP100 (AR5-ccfb) and for GWP100 (AR6).

Using GTP100 gives consistently lower weighting to SLCF emissions compared to GWP100. This brings the year of net zero GHG emissions forward by 12–18 years compared to GWP100 (AR6), since the remaining gross SLCF emissions would be aggregated into lower CO_2-eq emissions and hence would be compensated by a lower amount of net negative CO_2 emissions, which is reached earlier.

The difference in timing of net zero GHG emissions under GTP100 compared to GWP100 depends on the magnitude of SLCF (mostly CH_4) emissions at that point, as well as the slope of the emissions pathway when approaching net zero. IMP-SP has the largest reductions in CH_4 emissions and hence the difference between GTP100 and GWP100 is relatively smaller than for other pathways. Conversely, IMP-Ren2 relatively high residual CH_4 emissions. Therefore, expressing CO_2-equivalent emissions using GTP100 has a bigger impact on total CO_2-eq emissions compared to GWP100.

Using GWP20 gives consistently higher weighting to SLCF emissions compared to GWP100. This shifts the year of net zero emissions back by more than 20 years, as more net negative CO_2 emissions are needed to balance residual SLCF emissions; again the extent to which timing shifts depends on the amount of CH_4 emissions in the different pathways. Under GWP20, only IMP-REN2 reaches net zero in 2100 as it has the largest net-negative CO_2 emissions in 2100 of those four pathways; the three other pathways would remain at greater than net zero GHG emissions in 2100.

Using GWP* as a metric results in a significant change, not only in the timing of net zero emissions, but also the overall shape of the CO_2-eq emissions pathway. In the two pathways consistent with limiting warming to 1.5°C with no or limited overshoot (IMP-Ren15 and IMP-SP), CO_2-equivalent emissions using GWP* drop well below net zero before 2040 but then rebound again. IMP-Ren15 returns to net-positive GHG emissions before returning to net zero by 2100, while IMP-SP has emissions close to net zero for most of the second half of the 21st century.

CO_2-equivalent emissions using GWP* for IMP-GS follow a similar shape but have higher overall levels; net GHG emissions would briefly reach net zero in 2040 before returning to positive levels and dropping to net zero by 2080. For IMP-Ren2, CO_2-equivalent emissions based on GWP* look more similar to the emissions pathway based on other metrics but reach net zero GHG emissions about 20 years earlier than if using GWP100.

The reason for those different shapes of CO_2-equivalent emission trajectories under GWP* is that this metric translates rapid reductions of CH_4 emissions into negative CO_2-equivalent emissions. IMP-Ren2 pathway has less rapid reductions of CH_4 emissions in the near term than the three other pathways. The rapid reduction of methane in these three pathways results in a significantly faster and greater reduction of total CO_2-equivalent emissions under GWP*. As a result, net zero GHG emissions would be reached well before 2050, although (depending on further reductions) only temporarily in some pathways as the reduction of CH_4 emissions does not continue at the same rate.

Note that the different reported CO_2-equivalent emissions do not affect the climate outcome, as the actual emissions of individual gases in these pathways are unchanged. What Figure 2.SM.10 shows

[1] The GWP* formula was applied to the following gases: CH_4, HFC-134a, HFC-32, HFC-43-10-mee, HFC-152a, HFC-365-mfc. The parameters used in the calculation are based on the atmospheric lifetime of CH_4 and are not necessarily matched to other short-lived gases. Results should therefore be seen as indicative only; the existing literature provides parameters only for CH_4. Using further updated parameters from Smith et al. (2021) would not change the overall results substantially.

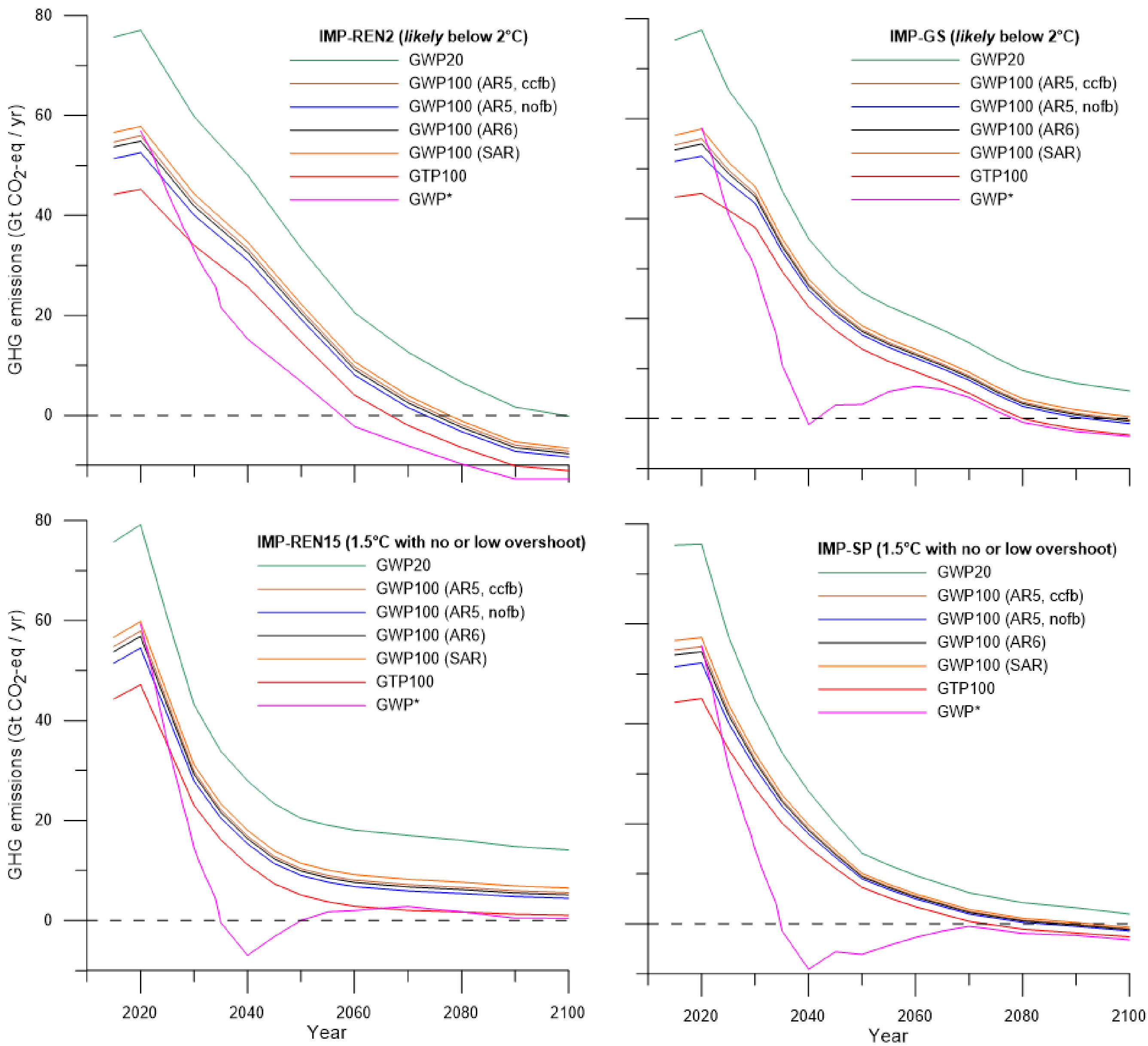

Figure 2.SM.10 | GHG emissions expressed in CO_2-eq, for four illustrative mitigation pathways (IMPs) from Chapter 3, using a range of GHG emission metrics assessed in AR6 (for details, see text). Illustrative Mitigation Pathways (IMPs) explore different ways of achieving long-term temperature goals. The four IMPs shown here are: higher Renewable Energy (IMP-Ren2 and IMP-Ren15); Gradual Strengthening of current policies (IMP-GS); and a Shifting Pathway (IMP-SP). Each of these pathways can be implemented with different levels of ambition. The IMP-Ren2 and IMP-GS (top panels) are consistent with limiting warming *likely* below 2°C, while IMP-Ren15 and IMP-SP (bottom panels) are consistent with limiting warming to 1.5°C with no or limited overshoot. (Box 3.1, 3.2.5, Annex III).

is only how the global aggregated emissions and removals would be reported for each pathway under different metrics.

The significant differences in the timing of net zero GHG emissions imply, however, that alternative emissions pathways that reach the same net zero GHG emissions target, but do so based on different GHG metrics, would necessarily result in different climate outcomes and would imply different levels of ambition to reach such an emissions target.

This is because depending on the GHG emission metric, a given amount of residual SLCF emissions in mitigation pathways would require different amounts of carbon dioxide removal (CDR) to achieve net zero GHG emissions. Emission metrics that give less weight to ongoing SLCF emissions imply a lesser rate of CO_2 removal and hence greater overall warming and/or lesser reduction in warming over time after net zero GHG emissions have been reached. Conversely, a given amount of CDR would permit different rates of SLCF emissions to achieve net zero GHG emissions under different metrics. This would result in different amounts of warming contributed by SLCF emissions in addition to the warming from CO_2.

For a given net zero target in a given year, using different metrics to monitor and verify achievement of that target therefore results in different levels of peak warming and different contributions of individual gases to this warming, and different rates of temperature change if net zero GHG emissions are sustained after the peak (Fuglestvedt et al. 2018; Tanaka and O'Neill 2018; Schleussner et al. 2019). This is before taking into account how the use of different GHG emission metrics might shape abatement choices leading up to an emission target.

2.SM.4 Trade as a Driver of Global GHG Emissions

This section assesses how trade openness and liberalisation may have changed the *global level* of GHG emissions, and complements Sections 2.3 and 2.4 in Chapter 2. It does not describe whether trade *has shifted* emissions between countries (transfer of embodied emissions) or has changed the level of emissions in individual countries (this is described in Chapter 2, Section 2.3). The effect of international emissions trading schemes, mechanisms, and policies are described in Chapter 2, Sections 2.8 and 14.5, respectively.

The question of whether international trade drives increases or decreases in global GHG emissions is difficult to answer since it not only depends on the emissions intensity of traded products, but also on the synergistic influence of trade on economic growth, income, consumption patterns, and the diffusion of low-carbon technologies or practices. All of these in turn are drivers of GHG emissions and the counterfactual question to answer is: What would happen without trade? (Jakob and Marschinski 2013). Trade also affects emissions through enhancing innovation and exchanging technologies between trading partners. These complex interactions are currently not fully understood (*limited evidence*, *low agreement*) (Cherniwchan et al. 2017). Consumption-based accounting alone (Chapter 2, Section 2.3) is therefore not suited to assess whether or not trade is driving global GHG emissions (Jakob and Marschinski 2013; Kander et al. 2015; Jiborn et al. 2018).

Only very few studies over the AR6 target time frame of 2010–2019 investigated the impacts of trade. Studies investigating global CO_2 emissions changes between 1995 and 2007/2008 found that the contribution of trade was moderately positive, whereas increases in overall and per capita consumption levels contributed much more strongly to the increase and improved technology had a significant decreasing effect (Arto and Dietzenbacher 2014; Hoekstra et al. 2016). A recent study modelled that international trade in 2015 increased global GDP by 10% and global total GHG emissions by 2% compared to a scenario where there was no trade (Wu et al. 2021).

Lin et al. (2019) investigated different scenarios on trade restrictions and found that a scenario with significant trade barriers based on additional 25% of tariffs would reduce global CO_2 emissions by 6.3% and GDP by 9.0%. On the other hand, the free trade scenario would increase global export volume by 5.4% and global CO_2 emissions by 1.2% for the base year of 2014 because of enhanced global production, especially in developing regions with high emissions intensities (Lin et al. 2019). It seems, however, that increased global GHG emissions only occur when the free trade agreements are between developed and developing countries (Nemati et al. 2019) because emissions reductions in the former group are counteracted by higher increases in the latter group of countries (Yao et al. 2019).

In contrast, one study suggests that international trade avoided 15 $GtCO_2$ emissions globally between 1995 and 2009, when compared to a hypothetical situation without trade (López et al. 2018). Zhu and Jiang (2019) found that the recent slowdown in globalisation from 2012 to 2016 did not lower but instead increased global CO_2 emissions by 202 Mt. This is because the consumption of domestic intermediate and final products increased in many countries, in particular in China and India, leading to increased domestic and therefore global CO_2 emissions (Mi et al. 2017; Guan et al. 2018; Khochiani and Nademi 2019; Liu et al. 2019; Wang and Jiang 2019; Zheng et al. 2019; Wang et al. 2020c). Partly, this is due to the fact that non-OECD countries have a higher emissions intensity than OECD economies at the aggregate level (Zhu and Jiang 2019; González-Torres et al. 2021). Scenario modelling of the USA-China trade war in 2018–2019 showed an increase in global CO_2 emissions, despite a decrease in global economic output (Lu et al. 2020). This was because the modelled change in trade patterns as a consequence of the trade war meant that increased emissions from land-use changes and higher production in some countries far exceeded the reductions through structural effects in other countries (Lu et al. 2020).

In summary, there is *low agreement* and *limited evidence* on how international trade influences global GHG emissions. Since the pricing of energy resources and GHG emissions is inconsistent across countries, the overall outcome of trade on global emissions is coincidental rather than by design. If shifts in production are accompanied by large-scale transfers of and investment in low-carbon technologies in carbon-intensive countries, the effects of trade on emissions can be mitigated (Jiang and Green 2017; Gozgor et al. 2020). While such investments and knowledge transfers are more likely to come from net importing nations leading in low-carbon technology, net exporters can help by targeting carbon-intensive export industries with additional mitigation measures (Ren et al. 2014; Liu et al. 2015b; Ji et al. 2017). Section 13.7 of this report deals with international interactions of national mitigation policies.

2.SM.5 Supporting Figures

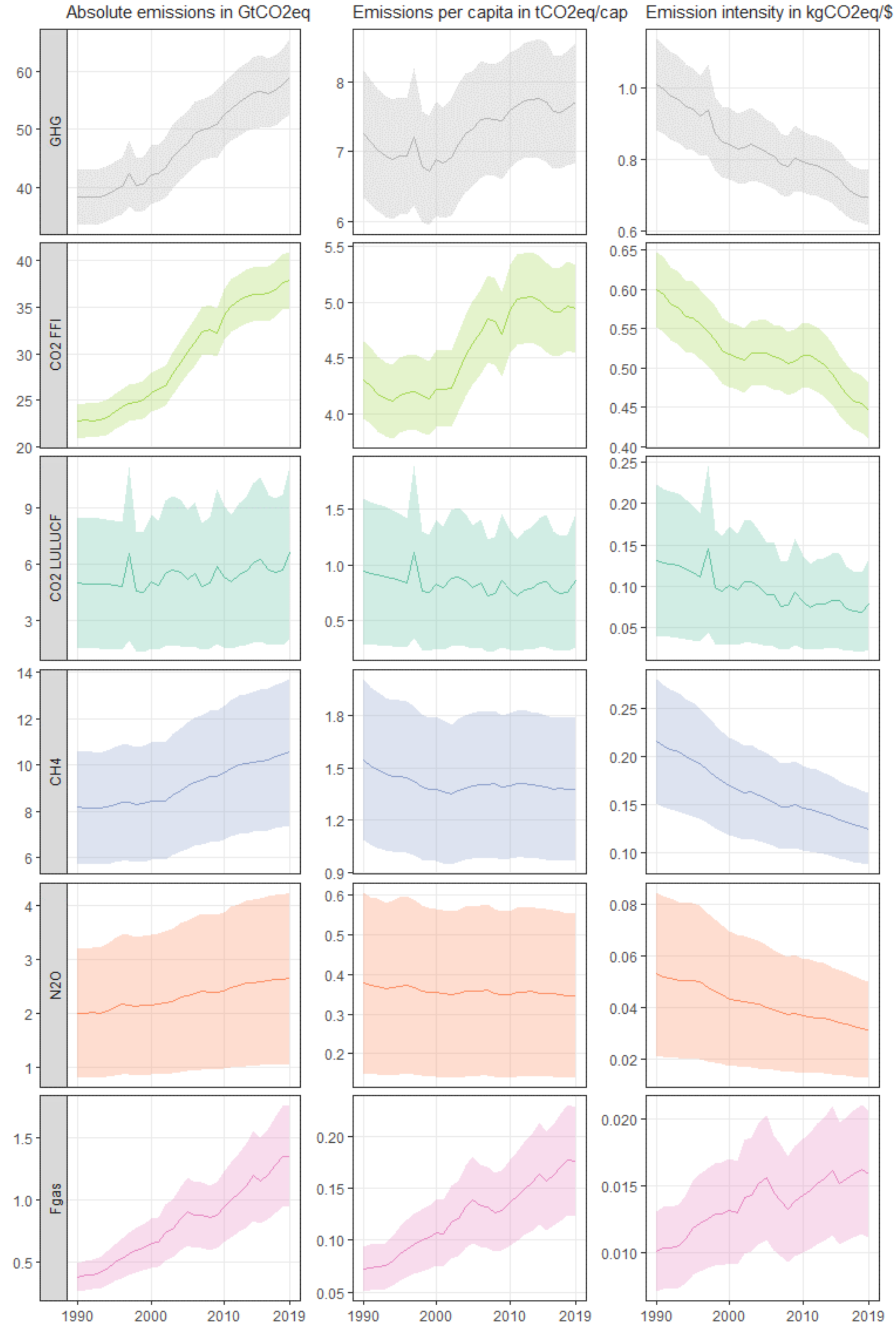

Figure 2.SM.11 | Global GHG emissions trends 1990–2019 by individual (groups of) gases and in aggregate: GHGs (black); CO_2-FFI (light green); CO_2-LULUCF (dark green); CH_4 (blue); N_2O (orange); fluorinated gases (pink). Aggregate GHG emissions trends by groups of gases reported in $GtCO_2$-eq converted based on global warming potential with a 100-year time horizon (GWP100) from IPCC AR5 (Myhre et al. 2013). Coloured shadings show the associated uncertainties at a 90% confidence interval without considering uncertainties in GDP and population data (see below). First column shows emissions trends in absolute levels ($GtCO_2$-eq). Second column shows per capita emissions trends (tCO_2-eq per capita) using UN population data for normalisation (World Bank 2021). Third column shows emissions trends per unit of GDP ($kgCO_2$-eq per USD) using GDP data in constant USD2010 from the World Bank for normalisation (World Bank 2021). Data: Minx et al. (2021).

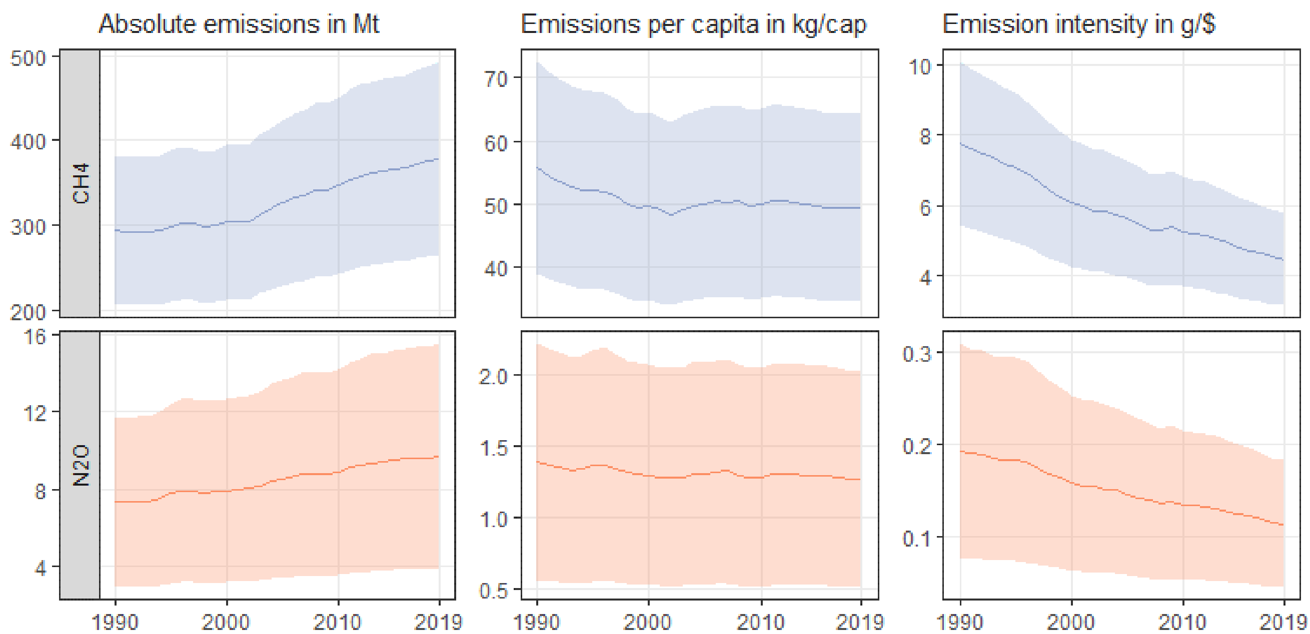

Figure 2.SM.12 | Global GHG emissions trends 1990–2019: CH_4 (blue); N_2O (orange). Aggregate GHG emissions trends by groups of gases reported in original mass units. Coloured shadings show the associated uncertainties at a 90% confidence interval without considering uncertainties in GDP and population data (see below). First column shows emissions trends in absolute levels ($MtCO_2$-eq). Second column shows per capita emissions trends (kg per capita) using UN population data for normalisation (World Bank 2021). Third column shows emissions trends per unit of GDP (g per USD) using GDP data in constant USD2010 from the World Bank for normalisation (World Bank 2021). Data: Minx et al. (2021).

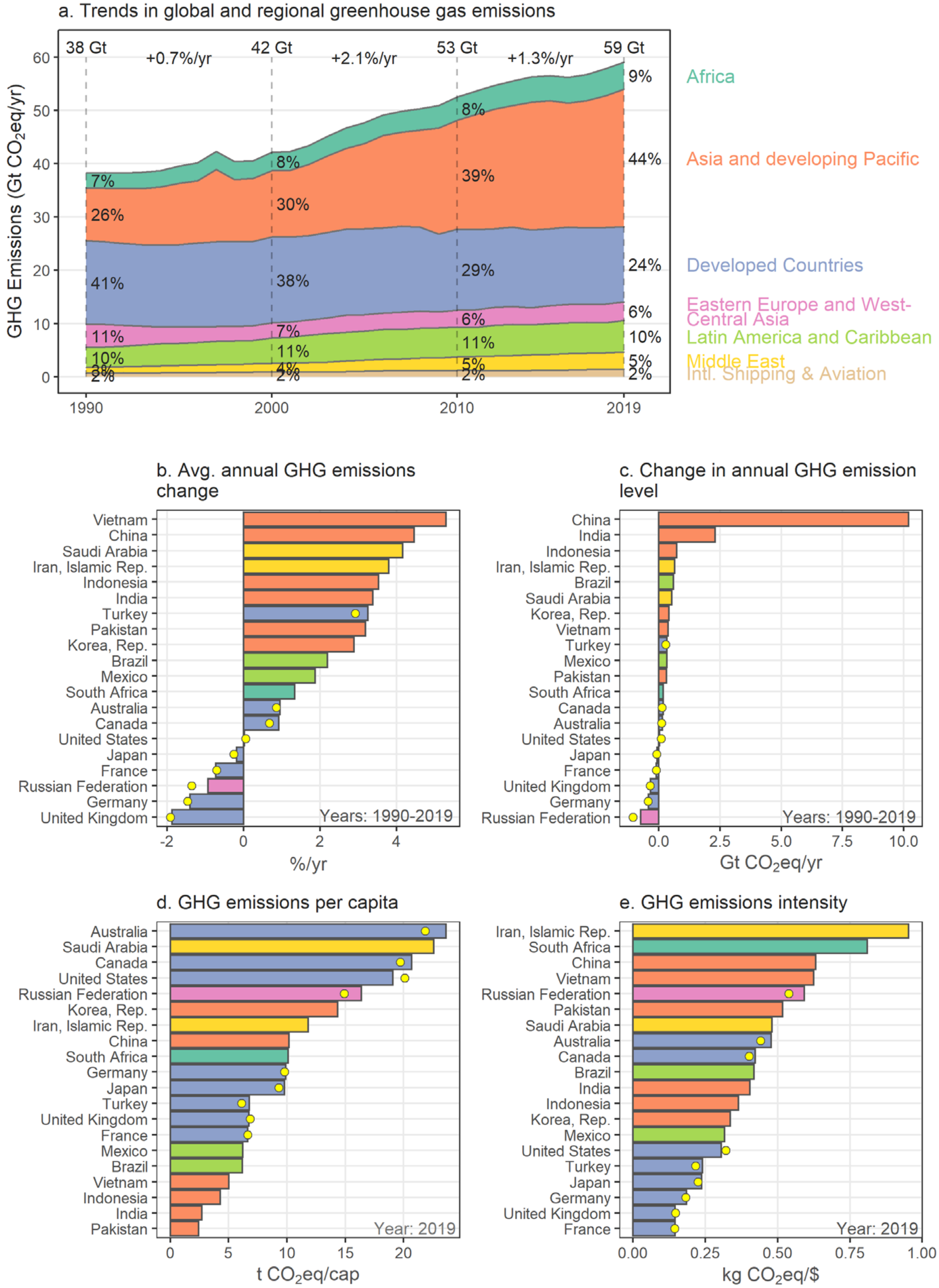

Figure 2.SM.13 | Change in regional GHGs from multiple perspectives and their underlying drivers. Panel (a): Regional GHG emissions trends (in $GtCO_2$-eq yr^{-1}) for 1990–2019. GHG emissions from international aviation and shipping are not assigned to individual countries and shown separately. **Panels (b) and (c):** Changes in GHG emissions for the 20 largest emitters (as of 2019) for 1990–2019 in relative (% annual change) and absolute terms ($GtCO_2$-eq). **Panels (d) and (e):** GHG emissions per capita and per unit of GDP in 2019 for the 20 largest emitters (as of 2019). GDP estimated using constant international purchasing power parity (USD2017). Emissions are converted into CO_2-equivalents based on global warming potential with a 100-year time horizon (GWP100) from IPCC's AR6 (Forster et al. 2021). The yellow dots represent the emissions data from UNFCCC-CRFs (2021) that were accessed through Gütschow et al. (2021a). Net LULUCF CO_2 emissions are included in panel (a), based on the average of three bookkeeping models (Chapter 2, Section 2.2), but are excluded in panels (b) to (e) due to a lack of country resolution.

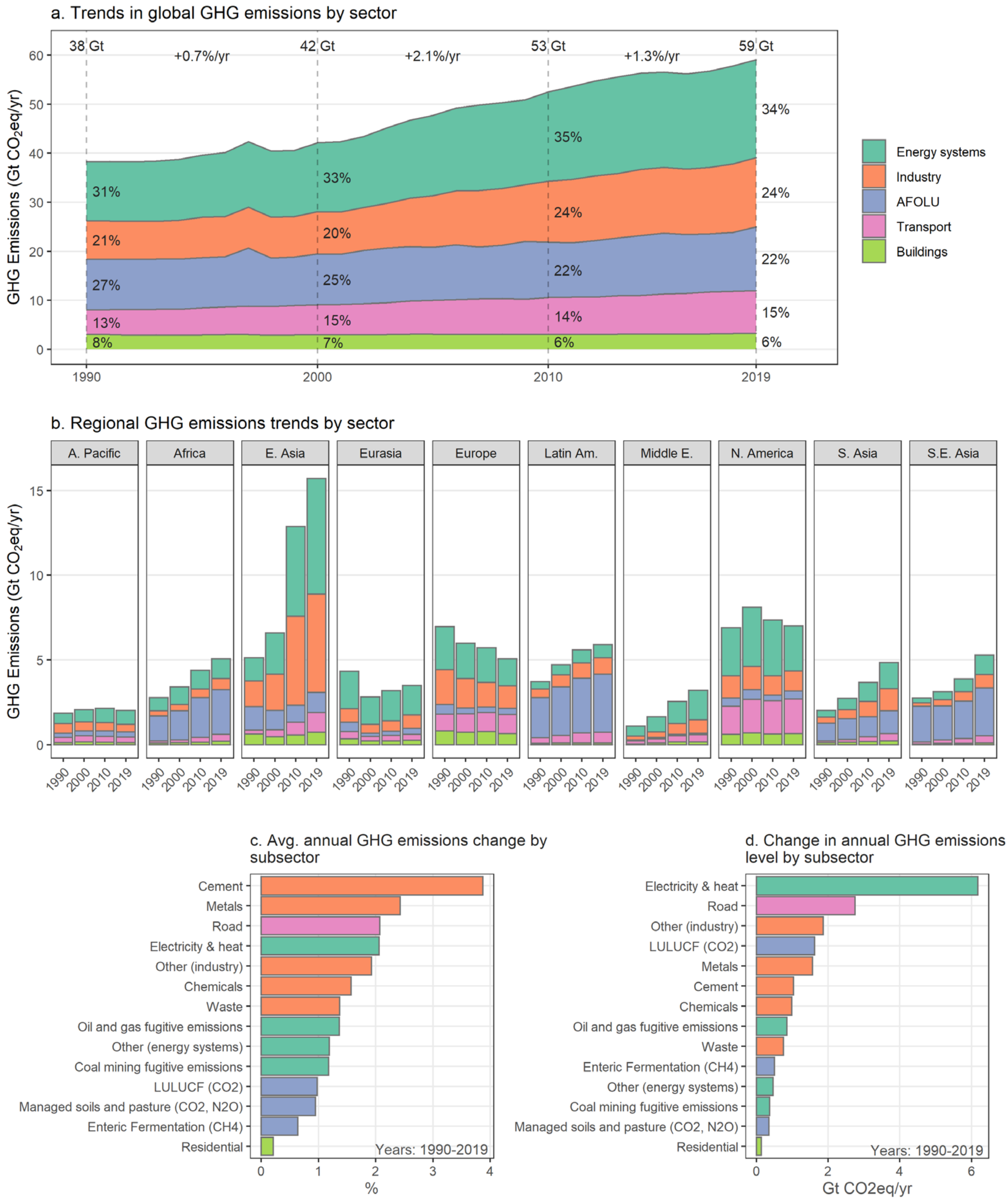

Figure 2.SM.14 | Total annual anthropogenic GHG emissions by major economic sector and their underlying trends by region. Panel (a): Trends in total annual anthropogenic GHG emissions (in $GtCO_2$-eq yr^{-1}) by major economic sector. **Panel (b):** Trends in total annual anthropogenic GHG emissions (in $GtCO_2$-eq yr^{-1}) by major economic sector and region. **Panels (c) and (d):** Largest sub-sectoral changes in GHG emissions for the reporting period 1990–2019 in relative (% annual change) and absolute terms ($GtCO_2$-eq). Emissions are converted into CO_2-equivalents based on global warming potential with a 100-year time horizon (GWP100) from IPCC's AR6. Based on Lamb et al. (2021); Data: Crippa et al. (2021); Minx et al. (2021).

References

Aaheim, A. and T. Mideksa, 2017: Requirements to metrics of greenhouse gas emissions, given a cap on temperature. *Ecol. Econ.*, **131**, 460–467, doi:10.1016/j.ecolecon.2016.09.026.

Allen, M. et al., 2021: Ensuring that offsets and other internationally transferred mitigation outcomes contribute effectively to limiting global warming. *Environ. Res. Lett.*, **16(7)**, 074009, doi:10.1088/1748-9326/abfcf9.

Allen, M.R. et al., 2018: A solution to the misrepresentations of CO_2-equivalent emissions of short-lived climate pollutants under ambitious mitigation. *Clim. Atmos. Sci.*, **1(1)**, 16, doi:10.1038/s41612-018-0026-8.

Andreae, M.O., 1991: Biomass burning: Its history, use, and distribution and its impact on environmental quality and global climate. In: *Global biomass burning – Atmospheric, climatic, and biospheric implications* [Levine, J.S., (ed.)]. MIT Press, Cambridge, MA, USA, pp. 1–21.

Andres, R.J. et al., 2012: A synthesis of carbon dioxide emissions from fossil-fuel combustion. *Biogeosciences*, **9(5)**, 1845–1871, doi:10.5194/bg-9-1845-2012.

Andres, R.J., T.A. Boden, and D. Higdon, 2014: A new evaluation of the uncertainty associated with CDIAC estimates of fossil fuel carbon dioxide emission. *Tellus B: Chem. Phys. Meteorol.*, **66(1)**, 23616, doi:10.3402/tellusb.v66.23616.

Andrew, R. and G. Peters, 2021: The Global Carbon Project's fossil CO_2 emissions dataset. doi:10.5281/zenodo.5569235.

Andrew, R.M., 2020: A comparison of estimates of global carbon dioxide emissions from fossil carbon sources. *Earth Syst. Sci. Data*, **12(2)**, 1437–1465, doi:10.5194/essd-12-1437-2020.

Arneth, A. et al., 2017: Historical carbon dioxide emissions caused by land-use changes are possibly larger than assumed. *Nat. Geosci.*, **10(2)**, 79–84, doi:10.1038/ngeo2882.

Arto, I. and E. Dietzenbacher, 2014: Drivers of the Growth in Global Greenhouse Gas Emissions. *Environ. Sci. Technol.*, **48(10)**, 5388–5394, doi:10.1021/es5005347.

Åström, S. and D.J.A. Johansson, 2019: The choice of climate metric is of limited importance when ranking options for abatement of near-term climate forcers. *Clim. Change*, **154(3–4)**, 401–416, doi:10.1007/s10584-019-02427-4.

Azar, C. and D.J.A. Johansson, 2012: Valuing the non-CO_2 climate impacts of aviation. *Clim. Change*, **111(3–4)**, 559–579, doi:10.1007/s10584-011-0168-8.

Baccini, A. et al., 2012: Estimated carbon dioxide emissions from tropical deforestation improved by carbon-density maps. *Nat. Clim. Change*, **2(3)**, 182–185, doi:10.1038/nclimate1354.

Baccini, A. et al., 2017: Tropical forests are a net carbon source based on aboveground measurements of gain and loss. *Science*, **358(6360)**, 230–234, doi:10.1126/science.aam5962.

Balcombe, P., J.F. Speirs, N.P. Brandon and A.D. Hawkes, 2018: Methane emissions: choosing the right climate metric and time horizon. *Environ. Sci. Process. Impacts*, **20(10)**, 1323–1339, doi:10.1039/C8EM00414E.

Ballantyne, A.P. et al., 2015: Audit of the global carbon budget: estimate errors and their impact on uptake uncertainty. *Biogeosciences*, **12(8)**, 2565–2584, doi:10.5194/bg-12-2565-2015.

Barnsley, J.E. et al., 2021: Lifetime Climate Impacts of Diet Transitions: A Novel Climate Change Accounting Perspective. *Sustainability*, **13(10)**, 5568, doi:10.3390/su13105568.

Bastos, A. et al., 2021: Comparison of uncertainties in land-use change fluxes from bookkeeping model parameterisation. *Earth Syst. Dyn.*, **12(2)**, 745–762, doi:10.5194/esd-12-745-2021.

Bergamaschi, P. et al., 2013: Atmospheric CH_4 in the first decade of the 21st century: Inverse modeling analysis using SCIAMACHY satellite retrievals and NOAA surface measurements. *J. Geophys. Res. Atmos.*, **118(13)**, 7350–7369, doi:10.1002/jgrd.50480.

Berntsen, T. and J. Fuglestvedt, 2008: Global temperature responses to current emissions from the transport sectors. *Proc. Natl. Acad. Sci.*, **105(49)**, 19154–19159, doi:10.1073/pnas.0804844105.

Blanco G., R. Gerlagh, S. Suh, J. Barrett, H.C. de Coninck, C.F. Diaz Morejon, R. Mathur, N. Nakicenovic, A. Ofosu Ahenkora, J. Pan, H. Pathak, J. Rice, R. Richels, S.J. Smith, D.I. Stern, F.L. Toth, and P. Zhou, 2014: Drivers, Trends and Mitigation. In: *Climate Change 2014: Mitigation of Climate Change. Contribution of Working Group III to the Fifth Assessment Report of the Intergovernmental Panel on Climate Change* [Edenhofer, O., R. Pichs-Madruga, Y. Sokona, E. Farahani, S. Kadner, K. Seyboth, A. Adler, I. Baum, S. Brunner, P. Eickemeier, B. Kriemann, J. Savolainen, S. Schlömer, C. von Stechow, T. Zwickel and J.C. Minx (eds.)]. Cambridge University Press, Cambridge, UK, and New York, NY, USA, 351–412.

Boucher, O., 2012: Comparison of physically- and economically-based CO_2-equivalences for methane. *Earth Syst. Dyn.*, **3(1)**, 49–61, doi:10.5194/esd-3-49-2012.

BP, 2020: *Statistical Review of World Energy, 2020*. 69th Edition. BP, London, UK, 66 pp.

Brazzola, N., J. Wohland, and A. Patt, 2021: Offsetting unabated agricultural emissions with CO_2 removal to achieve ambitious climate targets. *PLoS One*, **16(3)**, e0247887, doi:10.1371/journal.pone.0247887.

Brennan, M.E. and B.F. Zaitchik, 2013: On the potential for alternative greenhouse gas equivalence metrics to influence sectoral mitigation patterns. *Environ. Res. Lett.*, **8(1)**, 014033, doi:10.1088/1748-9326/8/1/014033.

Buitenhuis, E.T., P. Suntharalingam, and C. Le Quéré, 2018: Constraints on global oceanic emissions of N_2O from observations and models. *Biogeosciences*, **15(7)**, 2161–2175, doi:10.5194/bg-15-2161-2018.

Cain, M. et al., 2019: Improved calculation of warming-equivalent emissions for short-lived climate pollutants. *Clim. Atmos. Sci.*, **2(1)**, 29, doi:10.1038/s41612-019-0086-4.

Canadell, J.G., P.M.S. Monteiro, M.H. Costa, L. Cotrim da Cunha, P.M. Cox, A.V. Eliseev, S. Henson, M. Ishii, S. Jaccard, C. Koven, A. Lohila, P.K. Patra, S. Piao, J. Rogelj, S. Syampungani, S. Zaehle, K. Zickfeld, 2021: Global Carbon and other Biogeochemical Cycles and Feedbacks Supplementary Material. In: *Climate Change 2021: The Physical Science Basis. Contribution of Working Group I to the Sixth Assessment Report of the Intergovernmental Panel on Climate Change* [Masson-Delmotte, V., P. Zhai, A. Pirani, S.L. Connors, C. Péan, S. Berger, N. Caud, Y. Chen, L. Goldfarb, M.I. Gomis, M. Huang, K. Leitzell, E. Lonnoy, J.B.R. Matthews, T.K. Maycock, T. Waterfield, O. Yelekçi, R. Yu, and B. Zhou (eds.)] Cambridge University Press, Cambridge, United Kingdom and New York, NY, USA, pp. 673–816, doi:10.1017/9781009157896.007.

Cherniwchan, J., B.R. Copeland, and M.S. Taylor, 2017: Trade and the Environment: New Methods, Measurements, and Results. *Annu. Rev. Econom.*, **9(1)**, 59–85, doi:10.1146/annurev-economics-063016-103756.

Cherubini, F. et al., 2016: Bridging the gap between impact assessment methods and climate science. *Environ. Sci. Policy*, **64**, 129–140, doi:10.1016/j.envsci.2016.06.019.

Chini, L. et al., 2021: Land-use harmonization datasets for annual global carbon budgets. *Earth Syst. Sci. Data*, **13(8)**, 4175–4189, doi:10.5194/essd-13-4175-2021.

Ciais, P. et al., 2021: Empirical estimates of regional carbon budgets imply reduced global soil heterotrophic respiration. *Natl. Sci. Rev.*, **8(2)**, doi:10.1093/nsr/nwaa145.

Clark, M.A. et al., 2020: Global food system emissions could preclude achieving the 1.5° and 2°C climate change targets. *Science*, **370(6517)**, 705–708, doi:10.1126/science.aba7357.

2SM

Collins, W.J., D.J. Frame, J.S. Fuglestvedt, and K.P. Shine, 2019: Stable climate metrics for emissions of short and long-lived species – combining steps and pulses. *Environ. Res. Lett.*, **15(2)**, 024018, doi:10.1088/1748-9326/ab6039.

Conchedda, G. and F.N. Tubiello, 2020: Drainage of organic soils and GHG emissions: validation with country data. *Earth Syst. Sci. Data*, **12(4)**, 3113–3137, doi:10.5194/essd-12-3113-2020.

Cooper, S.J.G. et al., 2020: Exploring temporal aspects of climate-change effects due to bioenergy. *Biomass and Bioenergy*, **142**, 105778, doi:10.1016/j.biombioe.2020.105778.

Crippa, M. et al., 2019: *Fossil CO_2 and GHG emissions of all world countries: 2019 report.* Publications Office of the European Union, Luxembourg, 251 pp.

Crippa, M. et al., 2021: *GHG emissions of all world countries – 2021 Report*. European Commission Publications Office, Luxembourg, 263 pp.

Crutzen, P.J., A.R. Mosier, K.A. Smith, and W. Winiwarter, 2008: N_2O release from agro-biofuel production negates global warming reduction by replacing fossil fuels. *Atmos. Chem. Phys.*, **8(2)**, 389–395, doi:10.5194/acp-8-389-2008.

Darmenov, A. and A.M. da Silva, 2013: *The Quick Fire Emissions Dataset (QFED) – Documentation of versions 2.1, 2.2 and 2.4.* NASA, Maryland, 212 pp.

Deng, Z. et al., 2021: Comparing national greenhouse gas budgets reported in UNFCCC inventories against atmospheric inversions. *Earth Syst. Sci. Data* **14(4)**:1639–1675, 1–59, doi:10.5194/essd-2021-235.

Deuber, O., M. Sigrun, S. Robert, P. Michael, and L. Ling, 2013: A physical metric-based framework for evaluating the climate trade-off between CO_2 and contrails – The case of lowering aircraft flight trajectories. *Environ. Sci. Policy*, **25**, 176–185, doi:10.1016/j.envsci.2012.10.004.

Deuber, O., G. Luderer, and R. Sausen, 2014: CO_2 equivalences for short-lived climate forcers. *Clim. Change*, **122(4)**, 651–664, doi:10.1007/s10584-013-1014-y.

Dorner, Z. and S. Kerr, 2017: Implications of global emission policy scenarios for domestic agriculture: a New Zealand case study. *Clim. Policy*, **17(8)**, 998–1013, doi:10.1080/14693062.2016.1215285.

Drupp, M.A., M.C. Freeman, B. Groom, and F. Nesje, 2018: Discounting Disentangled. *Am. Econ. J. Econ. Policy*, **10(4)**, 109–134, doi:10.1257/pol.20160240.

Edwards, M.R. and J.E. Trancik, 2014: Climate impacts of energy technologies depend on emissions timing. *Nat. Clim. Change*, **4(5)**, 347–352, doi:10.1038/nclimate2204.

Edwards, M.R., J. McNerney, and J.E. Trancik, 2016: Testing emissions equivalency metrics against climate policy goals. *Environ. Sci. Policy*, **66**, 191–198, doi:10.1016/j.envsci.2016.08.013.

Edwards, M.R. et al., 2017: Vehicle emissions of short-lived and long-lived climate forcers: trends and tradeoffs. *Faraday Discuss.*, **200(0)**, 453–474, doi:10.1039/C7FD00063D.

EIA, 2021: International Energy Statistics. https://www.eia.gov/beta/international/data/browser/ (Accessed July 8, 2019).

Ekholm, T., 2014: Hedging the climate sensitivity risks of a temperature target. *Clim. Change*, **127(2)**, 153–167, doi:10.1007/s10584-014-1243-8.

Ekholm, T., T.J. Lindroos, and I. Savolainen, 2013: Robustness of climate metrics under climate policy ambiguity. *Environ. Sci. Policy*, **31**, 44–52, doi:10.1016/j.envsci.2013.03.006.

Elberling, B., H.H. Christiansen, and B.U. Hansen, 2010: High nitrous oxide production from thawing permafrost. *Nat. Geosci.*, **3(5)**, 332–335, doi:10.1038/ngeo803.

Engel, A. et al., 2018: Chapter 1: Update on Ozone Depleting Substances (ODSs) and Other Gases of Interest to the Montreal Protocol. In: *Scientific Assessment of Ozone Depletion: 2018*, World Meterological Organization, Geneva, Switzerland, 91 pp.

EPA, 2011: *Global Anthropogenic Non-CO_2 Greenhouse Gas Emissions: 1990–2030*. US EPA, Washington DC, USA, 188 pp.

EPA, 2021: *Global Non-CO_2 Greenhouse Gas Emission Projections & Mitigation: 2015–2050*. US EPA, Washington DC, USA, 84 pp.

Etiope, G., G. Ciotoli, S. Schwietzke, and M. Schoell, 2019: Gridded maps of geological methane emissions and their isotopic signature. *Earth Syst. Sci. Data*, **11(1)**, 1–22, doi:10.5194/essd-11-1-2019.

FAO, 2015: *Global Forest Resources Assessment 2015*. Food and Agriculture Organization of the United Nations, Rome, Italy, 54 pp.

FAOSTAT, 2021: Emissions Totals. http://www.fao.org/faostat/en/#data/GT/visualize (Accessed September 30, 2021).

Federici, S., F.N. Tubiello, M. Salvatore, H. Jacobs, and J. Schmidhuber, 2015: New estimates of CO_2 forest emissions and removals: 1990–2015. *For. Ecol. Manage.*, **352**, 89–98, doi:10.1016/j.foreco.2015.04.022.

Forster, P., T. Storelvmo, K. Armour, W. Collins, J.L. Dufresne, D. Frame, D.J. Lunt, T. Mauritsen, M.D. Palmer, M. Watanabe, M. Wild, and H. Zhang, 2021, The Earth's Energy Budget, Climate Feedbacks, and Climate Sensitivity. In: *Climate Change 2021: The Physical Science Basis. Contribution of Working Group I to the Sixth Assessment Report of the Intergovernmental Panel on Climate Change* [Masson-Delmotte, V., P. Zhai, A. Pirani, S.L. Connors, C. Péan, S. Berger, N. Caud, Y. Chen, L. Goldfarb, M.I. Gomis, M. Huang, K. Leitzell, E. Lonnoy, J.B.R. Matthews, T.K. Maycock, T. Waterfield, O. Yelekçi, R. Yu and B. Zhou (eds.)]. Cambridge University Press, Cambridge, UK (in press).

Fortems-Cheiney, A. et al., 2015: Increase in HFC-134a emissions in response to the success of the Montreal Protocol. *J. Geophys. Res. Atmos.*, **120(22)**, 11,728-11,742, doi:10.1002/2015JD023741.

Friedlingstein, P. et al., 2014: Uncertainties in CMIP5 Climate Projections due to Carbon Cycle Feedbacks. *J. Clim.*, **27(2)**, 511–526, doi:10.1175/JCLI-D-12-00579.1.

Friedlingstein, P. et al., 2019: Global Carbon Budget 2019. *Earth Syst. Sci. Data*, **11(4)**, 1783–1838, doi:10.5194/essd-11-1783-2019.

Friedlingstein, P. et al., 2020: Global Carbon Budget 2020. *Earth Syst. Sci. Data*, **12(4)**, 3269–3340, doi:10.5194/essd-12-3269-2020.

Fuglestvedt, J. et al., 2018: Implications of possible interpretations of 'greenhouse gas balance' in the Paris Agreement. *Philos. Trans. R. Soc. A Math. Phys. Eng. Sci.*, **376(2119)**, 20160445, doi:10.1098/rsta.2016.0445.

Fuglestvedt, J.S. et al., 2003: Metrics of climate change: Assessing radiative forcing and emission indices. *Clim. Change*, **58**, 267–331, doi:10.1023/A:1023905326842.

Fuglestvedt, J.S. et al., 2010: Transport impacts on atmosphere and climate: Metrics. *Atmos. Environ.*, **44(37)**, 4648–4677, doi:10.1016/j.atmosenv.2009.04.044.

Galloway, J. et al., 2010: The impact of animal production systems on the nitrogen cycle. In: *Livestock in a Changing Landscape. Drivers, Consequences and Responses* [H. Steinfield, H.A. Mooney, F. Schneider, and L.E. Neville, (eds.)], Island Press, Washington DC, USA, pp. 83–95.

Gasser, T. et al., 2016: Accounting for the climate-carbon feedback in emission metrics. *Earth Syst. Dynam. Discuss.*, **2016**, 1–29, doi:10.5194/esd-2016-55.

Gasser, T. et al., 2020: Historical CO_2 emissions from land use and land cover change and their uncertainty. *Biogeosciences*, **17(15)**, 4075–4101, doi:10.5194/bg-17-4075-2020.

Giglio, L., J.T. Randerson, and G.R. van der Werf, 2013: Analysis of daily, monthly, and annual burned area using the fourth-generation global fire emissions database (GFED4). *J. Geophys. Res. Biogeosciences*, **118(1)**, 317–328, doi:10.1002/jgrg.20042.

Giglio, S., M. Maggiori, and J. Stroebel, 2015: Very Long-Run Discount Rates. *Q. J. Econ.*, **130(1)**, 1–53, doi:10.1093/qje/qju036.

Gilfillan, D., G. Marland, T. Boden, and R. Andres, 2020: Global, Regional, and National Fossil-Fuel CO_2 Emissions: 1751–2017. Zenodo, doi:10.5281/ZENODO.4281271.

Goldewijk, K.K., A. Beusen, J. Doelman, and E. Stehfest, 2017: Anthropogenic land use estimates for the Holocene – HYDE 3.2. *Earth Syst. Sci. Data*, **9(2)**, 927–953, doi:10.5194/essd-9-927-2017.

González-Torres, M., L. Pérez-Lombard, J.F. Coronel, and I.R. Maestre, 2021: Revisiting Kaya Identity to define an Emissions Indicators Pyramid. *J. Clean. Prod.*, **317**, 128328, doi:10.1016/j.jclepro.2021.128328.

Gozgor, G., M.K. Mahalik, E. Demir, and H. Padhan, 2020: The impact of economic globalization on renewable energy in the OECD countries. *Energy Policy*, **139**, 111365, doi:10.1016/j.enpol.2020.111365.

Grassi, G. et al., 2018: Reconciling global-model estimates and country reporting of anthropogenic forest CO_2 sinks. *Nat. Clim. Change*, **8(10)**, 914–920, doi:10.1038/s41558-018-0283-x.

Grassi, G. et al., 2021: Critical adjustment of land mitigation pathways for assessing countries' climate progress. *Nat. Clim. Change*, **11(5)**, 425–434, doi:10.1038/s41558-021-01033-6.

Gregg, J.S., R.J. Andres, and G. Marland, 2008: China: Emissions pattern of the world leader in CO_2 emissions from fossil fuel consumption and cement production. *Geophys. Res. Lett.*, **35(8)**, L08806, doi:10.1029/2007GL032887.

Grewe, V. and K. Dahlmann, 2015: How ambiguous are climate metrics? And are we prepared to assess and compare the climate impact of new air traffic technologies? *Atmos. Environ.*, **106**, 373–374, doi:10.1016/j.atmosenv.2015.02.039.

Guan, D., Z. Liu, Y. Geng, S. Lindner, and K. Hubacek, 2012: The gigatonne gap in China's carbon dioxide inventories. *Nat. Clim. Change*, **2(9)**, 672–675, doi:10.1038/nclimate1560.

Guan, D. et al., 2018: Structural decline in China's CO_2 emissions through transitions in industry and energy systems. *Nat. Geosci.*, **11(8)**, 551–555, doi:10.1038/s41561-018-0161-1.

Guo, R. et al., 2021: Global CO_2 uptake by cement from 1930 to 2019. *Earth Syst. Sci. Data*, **13(4)**, 1791–1805, doi:10.5194/essd-13-1791-2021.

Gütschow, J. et al., 2016: The PRIMAP-hist national historical emissions time series. *Earth Syst. Sci. Data*, **8(2)**, 571–603, doi:10.5194/essd-8-571-2016.

Gütschow, J., A. Günther, and M. Pflüger, 2021a: The PRIMAP-hist national historical emissions time series **(1750–2019)** v2.3., doi:10.5281/ZENODO.5175154.

Gütschow, J., M.L. Jeffery, and A. Günther, 2021b: PRIMAP-crf: UNFCCC CRF data in IPCC categories (PRIMAP-crf-2021-v1). **10**, 1427–1438, doi:10.5281/ZENODO.4723476.

Hansen, M.C. et al., 2013: High-Resolution Global Maps of 21st-Century Forest Cover Change. *Science*, **342(6160)**, 850–853, doi:10.1126/science.1244693.

Hansis, E., S.J. Davis, and J. Pongratz, 2015: Relevance of methodological choices for accounting of land use change carbon fluxes. *Global Biogeochem. Cycles*, **29(8)**, 1230–1246, doi:10.1002/2014GB004997.

Harmsen, J.H.M. et al., 2019: Long-term marginal abatement cost curves of non-CO_2 greenhouse gases. *Environ. Sci. Policy*, **99**(March), 136–149, doi:10.1016/j.envsci.2019.05.013.

Harmsen, M.J.H.M. et al., 2016: How climate metrics affect global mitigation strategies and costs: a multi-model study. *Clim. Change*, **136(2)**, 203–216, doi:10.1007/s10584-016-1603-7.

Hartung, K. et al., 2021: Bookkeeping estimates of the net land-use change flux – a sensitivity study with the CMIP6 land-use dataset. *Earth Syst. Dyn.*, **12(2)**, 763–782, doi:10.5194/esd-12-763-2021.

Hmiel, B. et al., 2020: Preindustrial 14CH4 indicates greater anthropogenic fossil CH_4 emissions. *Nature*, **578(7795)**, 409–412, doi:10.1038/s41586-020-1991-8.

HM Treasury, 2018: *The Green Book: Central Government Guidance on Appraisal and Evaluation*. HM Treasury, London, UK, 132 pp.

Hoekstra, R., B. Michel, and S. Suh, 2016: The emission cost of international sourcing: using structural decomposition analysis to calculate the contribution of international sourcing to CO_2 emission growth. *Econ. Syst. Res.*, **28(2)**, 151–167, doi:10.1080/09535314.2016.1166099.

Hoesly, R.M. and S.J. Smith, 2018: Informing energy consumption uncertainty: an analysis of energy data revisions. *Environ. Res. Lett.*, **13(12)**, 124023, doi:10.1088/1748-9326/aaebc3.

Hoesly, R.M. et al., 2018: Historical **(1750–2014)** anthropogenic emissions of reactive gases and aerosols from the Community Emissions Data System (CEDS). *Geosci. Model Dev.*, **11(1)**, 369–408, doi:10.5194/gmd-11-369-2018.

Höglund-Isaksson, L., 2012: Global anthropogenic methane emissions 2005–2030: technical mitigation potentials and costs. *Atmos. Chem. Phys.*, **12(19)**, 9079–9096, doi:10.5194/acp-12-9079-2012.

Höglund-Isaksson, L., A. Gómez-Sanabria, Z. Klimont, P. Rafaj, and W. Schöpp, 2020: Technical potentials and costs for reducing global anthropogenic methane emissions in the 2050 timeframe –results from the GAINS model. *Environ. Res. Commun.*, **2(2)**, 025004, doi:10.1088/2515-7620/ab7457.

Hooijer, A. et al., 2010: Current and future CO_2 emissions from drained peatlands in Southeast Asia. *Biogeosciences*, **7(5)**, 1505–1514, doi:10.5194/bg-7-1505-2010.

Houghton, R.A., 2003: Revised estimates of the annual net flux of carbon to the atmosphere from changes in land use and land management 1850–2000. *Tellus B*, **55(2)**, 378–390, doi:10.1034/j.1600-0889.2003.01450.x.

Houghton, R.A. and A.A. Nassikas, 2017: Global and regional fluxes of carbon from land use and land cover change 1850-2015. *Global Biogeochem. Cycles*, **31(3)**, 456–472, doi:10.1002/2016GB005546.

Houghton, R.A. et al., 2012: Carbon emissions from land use and land-cover change. *Biogeosciences*, **9(12)**, 5125–5142, doi:10.5194/bg-9-5125-2012.

Houweling, S. et al., 2017: Global inverse modeling of CH_4 sources and sinks: An overview of methods. *Atmos. Chem. Phys.*, doi:10.5194/acp-17-235-2017.

Hu, Z., J.W. Lee, K. Chandran, S. Kim, and S.K. Khanal, 2012: Nitrous Oxide (N_2O) Emission from Aquaculture: A Review. *Environ. Sci. Technol.*, **46(12)**, 6470–6480, doi:10.1021/es300110x.

Huntingford, C. et al., 2015: The implications of carbon dioxide and methane exchange for the heavy mitigation RCP2.6 scenario under two metrics. *Environ. Sci. Policy*, **51**, 77–87, doi:10.1016/j.envsci.2015.03.013.

Hurtt, G.C. et al., 2020: Harmonization of global land use change and management for the period 850–2100 (LUH2) for CMIP6. *Geosci. Model Dev.*, **13(11)**, 5425–5464, doi:10.5194/gmd-13-5425-2020.

IEA, 2021b: *Global Energy Review 2021*. International Energy Agency (IEA), Paris, France, 1–36 pp.

IEA, 2021a: *CO_2 emissions from fossil fuel combustion 2020*. International Energy Agency (IEA), Paris, France.

IPCC 2006, 2006 IPCC Guidelines for National Greenhouse Gas Inventories, *Agriculture, Forestry and other land use*. Prepared by the National Greenhouse Gas Inventories Programme, Eggleston, H.S., Buendia, L., Miwa, K., Ngara, T. and Tanabe, K. (eds). Published: IGES, Japan.

IPCC, 2014: *Climate Change 2014: Synthesis Report*. Contribution of Working Groups I, II and III to the Fifth Assessment Report of the Intergovernmental Panel on Climate Change [Core Writing Team, R.K. Pachauri and L.A. Meyer (eds.)]. IPCC, Geneva, Switzerland, 151 pp.

IPCC, 2019: 2019 Refinement to the 2006 IPCC Guidelines for National Greenhouse Gas Inventories, [Calvo Buendia, E., Tanabe, K., Kranjc, A., Baasansuren, J., Fukuda, M., Ngarize, S., Osako, A., Pyrozhenko, Y., Shermanau, P. and Federici, S. (eds)]. IPCC, Geneva, Switzerland.

Ivy, D.J., M. Rigby, M. Baasandorj, J.B. Burkholder, and R.G. Prinn, 2012: Global emission estimates and radiative impact of C4F10, C5F12, C6F14, C7F16 and C8F18. *Atmos. Chem. Phys.*, **12(16)**, 7635–7645, doi:10.5194/acp-12-7635-2012.

Jakob, M. and R. Marschinski, 2013: Interpreting trade-related CO_2 emission transfers. *Nat. Clim. Change*, **3(1)**, 19–23, doi:10.1038/nclimate1630.

Janssens-Maenhout, G. et al., 2019: EDGAR v4.3.2 Global Atlas of the three major greenhouse gas emissions for the period 1970–2012. *Earth Syst. Sci. Data*, **11(3)**, 959–1002, doi:10.5194/essd-11-959-2019.

Ji, J., C. Zhang, and X. Ma, 2017: Factors Driving Embodied Carbon Emissions from China-US Trade for 1992-2012: A Structural Decomposition Analysis. *Proceedings of the 2017 2nd International Conference on Civil,* *Transportation and Environmental Engineering (ICCTE 2017)*, Atlantis Press, Paris, France, 674–678.

Jiang, X. and C. Green, 2017: The Impact on Global Greenhouse Gas Emissions of Geographic Shifts in Global Supply Chains. *Ecol. Econ.*, **139**, 102–114, doi:10.1016/j.ecolecon.2017.04.027.

Jiborn, M., A. Kander, V. Kulionis, H. Nielsen, and D.D. Moran, 2018: Decoupling or delusion? Measuring emissions displacement in foreign trade. *Glob. Environ. Change*, **49**, 27–34, doi:10.1016/j.gloenvcha.2017.12.006.

Johansson, D.J.A., 2012: Economics- and physical-based metrics for comparing greenhouse gases. *Clim. Change*, **110(1–2)**, 123–141, doi:10.1007/s10584-011-0072-2.

Jolliet, O. et al., 2018: Global guidance on environmental life cycle impact assessment indicators: impacts of climate change, fine particulate matter formation, water consumption and land use. *Int. J. Life Cycle Assess.*, **23(11)**, 2189–2207, doi:10.1007/s11367-018-1443-y.

Kaiser, J.W. et al., 2012: Biomass burning emissions estimated with a global fire assimilation system based on observed fire radiative power. *Biogeosciences*, **9(1)**, 527–554, doi:10.5194/bg-9-527-2012.

Kander, A., M. Jiborn, D.D. Moran, and T.O. Wiedmann, 2015: National greenhouse-gas accounting for effective climate policy on international trade. *Nat. Clim. Change*, **5(5)**, 431–435, doi:10.1038/nclimate2555.

Kandlikar, M., 1996: Indices for comparing greenhouse gas emissions: integrating science and economics. *Energy Econ.*, **18(4)**, 265–281, doi:10.1016/S0140-9883**(96)**00021-7.

Khochiani, R. and Y. Nademi, 2019: Energy consumption, CO_2 emissions, and economic growth in the United States, China, and India: A wavelet coherence approach. *Energy Environ.*, 0958305X19881750-0958305X19881750, doi:10.1177/0958305X19881750.

Kirschke, S. et al., 2013: Three decades of global methane sources and sinks. *Nat. Geosci.*, **6(10)**, 813–823, doi:10.1038/ngeo1955.

Klinsky, S. and W. Harald, 2018: Building equity in: strategies for integrating equity into modelling for a 1.5°C world. *Philos. Trans. R. Soc. A Math. Phys. Eng. Sci.*, **376(2119)**, 20160461, doi:10.1098/rsta.2016.0461.

Kolstad C., K. Urama, J. Broome, A. Bruvoll, M. Cariño Olvera, D. Fullerton, C. Gollier, W.M. Hanemann, R. Hassan, F. Jotzo, M.R. Khan, L. Meyer, and L. Mundaca, 2014: Social, Economic and Ethical Concepts and Methods. In: *Climate Change 2014: Mitigation of Climate Change. Contribution of Working Group III to the Fifth Assessment Report of the Intergovernmental Panel on Climate Change* [Edenhofer, O., R. Pichs-Madruga, Y. Sokona, E. Farahani, S. Kadner, K. Seyboth, A. Adler, I. Baum, S. Brunner, P. Eickemeier, B. Kriemann, J. Savolainen, S. Schlömer, C. von Stechow, T. Zwickel and J.C. Minx (eds.)]. Cambridge University Press, Cambridge, UK, and New York, NY, USA, 207–282.

Korsbakken, J.I., G.P. Peters, and R.M. Andrew, 2016: Uncertainties around reductions in China's coal use and CO_2 emissions. *Nat. Clim. Change*, **6(7)**, 687–690, doi:10.1038/nclimate2963.

Kroeze, C., A. Mosier, and L. Bouwman, 1999: Closing the global N_2O budget: A retrospective analysis 1500-1994. *Global Biogeochem. Cycles*, **13(1)**, 1–8, doi:10.1029/1998GB900020.

Lamb, W.F. et al., 2021: A review of trends and drivers of greenhouse gas emissions by sector from 1990 to 2018. *Environ. Res. Lett.*, **16(7)**, 073005, doi:10.1088/1748-9326/abee4e.

Le Quéré, C. et al., 2018: Global Carbon Budget 2017. *Earth Syst. Sci. Data*, **10(1)**, 405–448, doi:10.5194/essd-10-405-2018.

Ledgard, S. and A. Reisinger, 2014: Implications of alternative greenhouse gas metrics for life cycle assessments of livestock food products. *Proc. 9th Int. Conf. Life Cycle Assess. Agri-Food Sect. (LCA Food 2014), San Fr. California, USA, 8-10 October, 2014*.

Lee, D.S. et al., 2021: The contribution of global aviation to anthropogenic climate forcing for 2000 to 2018. *Atmos. Environ.*, **244**, 117834, doi:10.1016/j.atmosenv.2020.117834.

Levasseur, A. et al., 2016: Enhancing life cycle impact assessment from climate science: Review of recent findings and recommendations for application to LCA. *Ecol. Indic.*, **71**, 163–174, doi:10.1016/j.ecolind.2016.06.049.

Li, J. et al., 2020: Reduction of carbon emissions from China's coal-fired power industry: Insights from the province-level data. *J. Clean. Prod.*, **242**, 118518, doi:10.1016/j.jclepro.2019.118518.

Li, W. et al., 2017: Land-use and land-cover change carbon emissions between 1901 and 2012 constrained by biomass observations. *Biogeosciences*, **14(22)**, 5053–5067, doi:10.5194/bg-14-5053-2017.

Li, W. et al., 2018: Gross and net land cover changes in the main plant functional types derived from the annual ESA CCI land cover maps **(1992–2015)**. *Earth Syst. Sci. Data*, **10(1)**, 219–234, doi:10.5194/essd-10-219-2018.

Lin, J. et al., 2019: Carbon and health implications of trade restrictions. *Nat. Commun.*, **10(1)**, 4947, doi:10.1038/s41467-019-12890-3.

Liu, D., X. Guo, and B. Xiao, 2019: What causes growth of global greenhouse gas emissions? Evidence from 40 countries. *Sci. Total Environ.*, **661**, 750–766, doi:10.1016/j.scitotenv.2019.01.197.

Liu, Z. et al., 2016: Targeted opportunities to address the climate–trade dilemma in China. *Nat. Clim. Change*, **6(2)**, 201–206, doi:10.1038/nclimate2800.

Liu, Z. et al., 2020: Near-real-time monitoring of global CO_2 emissions reveals the effects of the COVID-19 pandemic. *Nat. Commun.*, **11(1)**, 5172, doi:10.1038/s41467-020-18922-7.

Locatelli, R., P. Bousquet, M. Saunois, F. Chevallier, and C. Cressot, 2015: Sensitivity of the recent methane budget to LMDz sub-grid-scale physical parameterizations. *Atmos. Chem. Phys.*, **15(17)**, 9765–9780, doi:10.5194/acp-15-9765-2015.

López, L.A., G. Arce, T. Kronenberg, and J.F.D. Rodrigues, 2018: Trade from resource-rich countries avoids the existence of a global pollution haven hypothesis. *J. Clean. Prod.*, **175**, 599–611, doi:10.1016/j.jclepro.2017.12.056.

Lu, J., X. Mao, M. Wang, Z. Liu, and P. Song, 2020: Global and National Environmental Impacts of the US–China Trade War. *Environ. Sci. Technol.*, **54(24)**, 16108–16118, doi:10.1021/acs.est.0c03863.

Lund, M.T. et al., 2017: Emission metrics for quantifying regional climate impacts of aviation. *Earth Syst. Dyn.*, **8(3)**, 547–563, doi:10.5194/esd-8-547-2017.

Lunt, M.F. et al., 2015: Reconciling reported and unreported HFC emissions with atmospheric observations. *Proc. Natl. Acad. Sci.*, **112(19)**, 5927–5931, doi:10.1073/pnas.1420247112.

Lynch, J. and R. Pierrehumbert, 2019: Climate Impacts of Cultured Meat and Beef Cattle. *Front. Sustain. Food Syst.*, **3**, doi:10.3389/fsufs.2019.00005.

Lynch, J., M. Cain, R. Pierrehumbert, and M. Allen, 2020: Demonstrating GWP: a means of reporting warming-equivalent emissions that captures the contrasting impacts of short- and long-lived climate pollutants. *Environ. Res. Lett.*, **15(4)**, 044023, doi:10.1088/1748-9326/ab6d7e.

Lynch, J., M. Cain, D. Frame, and R. Pierrehumbert, 2021: Agriculture's Contribution to Climate Change and Role in Mitigation Is Distinct From Predominantly Fossil CO_2-Emitting Sectors. *Front. Sustain. Food Syst.*, **4**, 1–9, doi:10.3389/fsufs.2020.518039.

Maasakkers, J.D. et al., 2021: 2010–2015 North American methane emissions, sectoral contributions, and trends: a high-resolution inversion of GOSAT observations of atmospheric methane. *Atmos. Chem. Phys.*, **21(6)**, 4339–4356, doi:10.5194/acp-21-4339-2021.

Macknick, J., 2011: Energy and CO_2 emission data uncertainties. *Carbon Manag.*, **2(2)**, 189–205, doi:10.4155/cmt.11.10.

Mallapragada, D.S. and B.K. Mignone, 2017: A consistent conceptual framework for applying climate metrics in technology life cycle assessment. *Environ. Res. Lett.*, **12(7)**, 074022, doi:10.1088/1748-9326/aa7397.

Mallapragada, D.S. and B.K. Mignone, 2020: A theoretical basis for the equivalence between physical and economic climate metrics and implications for the choice of Global Warming Potential time horizon. *Clim. Change*, **158(2)**, 107–124, doi:10.1007/s10584-019-02486-7.

Manne, A.S. and R.G. Richels, 2001: An alternative approach to establishing trade-offs among greenhouse gases. *Nature*, **410(6829)**, 675–677, doi:10.1038/35070541.

Marland, G., 2008: Uncertainties in Accounting for CO_2 From Fossil Fuels. *J. Ind. Ecol.*, **12(2)**, 136–139, doi:10.1111/j.1530-9290.2008.00014.x.

Marland, G., K. Hamal, and M. Jonas, 2009: How Uncertain Are Estimates of CO_2 Emissions? *J. Ind. Ecol.*, **13(1)**, 4–7, doi:10.1111/j.1530-9290.2009.00108.x.

Matricardi, E.A.T. et al., 2020: Long-term forest degradation surpasses deforestation in the Brazilian Amazon. *Science*, **369(6509)**, 1378–1382, doi:10.1126/science.abb3021.

Mayfield, E.N., J.L. Cohon, N.Z. Muller, I.M.L. Azevedo, and A.L. Robinson, 2019: Cumulative environmental and employment impacts of the shale gas boom. *Nat. Sustain.*, **2(12)**, 1122–1131, doi:10.1038/s41893-019-0420-1.

McDuffie, E.E. et al., 2020: A global anthropogenic emission inventory of atmospheric pollutants from sector- and fuel-specific sources **(1970–2017)**: an application of the Community Emissions Data System (CEDS). *Earth Syst. Sci. Data*, **12(4)**, 3413–3442, doi:10.5194/essd-12-3413-2020.

Mi, Z. et al., 2017: Pattern changes in determinants of Chinese emissions. *Environ. Res. Lett.*, **12(7)**, 074003, doi:10.1088/1748-9326/aa69cf.

Michaelis, P., 1992: Global warming: Efficient policies in the case of multiple pollutants. *Environ. Resour. Econ.*, **2(1)**, 61–77, doi:10.1007/BF00324689.

Michaelis, P., 1999: Sustainable greenhouse policies: the role of non-CO_2 gases. *Struct. Change Econ. Dyn.*, **10**, 239–260.

Minx, J.C. et al., 2021: A comprehensive and synthetic dataset for global, regional, and national greenhouse gas emissions by sector 1970–2018 with an extension to 2019. *Earth Syst. Sci. Data*, **13(11)**, 5213–5252, doi:10.5194/essd-13-5213-2021.

Monni, S., P. Perälä, and K. Regina, 2007: Uncertainty in Agricultural CH_4 and N_2O Emissions from Finland – Possibilities to Increase Accuracy in Emission Estimates. *Mitig. Adapt. Strateg. Glob. Change*, **12(4)**, 545–571, doi:10.1007/s11027-006-4584-4.

Montzka, S.A. and G.J.M. Velders, 2018: Chapter 2: Hydrofluorocarbons (HFCs). In: *Scientific Assessment of Ozone Depletion: 2018*, World Meterological Organization, Geneva, Switzerland.

Montzka, S.A. et al., 2015: Recent Trends in Global Emissions of Hydrochlorofluorocarbons and Hydrofluorocarbons: Reflecting on the 2007 Adjustments to the Montreal Protocol. *J. Phys. Chem. A*, **119(19)**, 4439–4449, doi:10.1021/jp5097376.

Mosier, A. and C. Kroeze, 2000: Potential impact on the global atmospheric N_2O budget of the increased nitrogen input required to meet future global food demands. *Chemosph. - Glob. Change Sci.*, **2(3–4)**, 465–473, doi:10.1016/S1465-9972**(00)**00039-8.

Mosier, A., C. Kroeze, C. Nevison, O. Oenema, and S. Seitzinger, 1998: Closing the global N_2O budget: nitrous oxide emissions through the agricultural nitrogen cycle inventory methodology. *Nutr. Cycl. Agroecosystems*.

Mühle, J. et al., 2010: Perfluorocarbons in the global atmosphere: tetrafluoromethane, hexafluoroethane, and octafluoropropane. *Atmos. Chem. Phys.*, **10(11)**, 5145–5164, doi:10.5194/acp-10-5145-2010.

Mühle, J. et al., 2019: Perfluorocyclobutane (PFC-318, C4F) in the global atmosphere. *Atmos. Chem. Phys.*, **19(15)**, 10335–10359, doi:10.5194/acp-19-10335-2019.

Myhre, G., D. Shindell, F.-M. Bréon, W. Collins, J. Fuglestvedt, J. Huang, D. Koch, J.-F. Lamarque, D. Lee, B. Mendoza, T. Nakajima, A. Robock, G. Stephens, T. Takemura and H. Zhang, 2013: Anthropogenic and Natural Radiative Forcing. In: *Climate Change 2013: The Physical Science Basis. Contribution of Working Group I to the Fifth Assessment Report of the Intergovernmental Panel on Climate Change* [Stocker, T.F., D. Qin, G.-K. Plattner, M. Tignor, S.K. Allen, J. Boschung, A. Nauels, Y. Xia, V. Bex and P.M. Midgley (eds.)]. Cambridge University Press, Cambridge, UK and New York, NY, USA.

NASEM, 2018: *Improving Measurement, Monitoring, Presentation of Results, and Development of Inventories. Improving Characterization of Anthropogenic Methane Emissions in the United States*., Washington DC, USA.

Nemati, M., W. Hu, and M. Reed, 2019: Are free trade agreements good for the environment? A panel data analysis. *Rev. Dev. Econ.*, **23(1)**, 435–453, doi:10.1111/rode.12554.

O'Rourke, P.R. and S.J. Smith et al., 2021: CEDS v_2021_04_21 Release Emission Data, doi:10.5281/ZENODO.4741285.

O'Rourke, P.R. et al., 2020: CEDS v-2020-09-11 Pre-Release Emission Data 1975-2019, doi:10.5281/zenodo.4025316.

Obermeier, W.A. et al., 2021: Modelled land use and land cover change emissions – a spatio-temporal comparison of different approaches. *Earth Syst. Dyn.*, **12(2)**, 635–670, doi:10.5194/esd-12-635-2021.

Ocko, I.B. et al., 2017: Unmask temporal trade-offs in climate policy debates. *Science*, doi:10.1126/science.aaj2350.

Olivier, J.G.J. and J.A.H.W. Peters, 2018: *Trends in global CO_2 and total greenhouse gas emissions – 2018 report*. PBL Netherlands Environmental Assessment Agency, The Hague, Netherlands, 53 pp.

Olivier, J.G.J. and J.A.H.W. Peters, 2020: *Trends in CO_2 and total greenhouse gas emissions: 2019 Report*. PBL Netherlands Environmental Assessment Agency, The Hague, Netherlands, 70 pp.

Oreggioni, G.D. et al., 2021: Climate change in a changing world: Socio-economic and technological transitions, regulatory frameworks and trends on global greenhouse gas emissions from EDGAR v.5.0. *Glob. Environ. Change*, **70**, 102350, doi:10.1016/j.gloenvcha.2021.102350.

Petrescu, A.M.R. et al., 2020: European anthropogenic AFOLU greenhouse gas emissions: a review and benchmark data. *Earth Syst. Sci. Data*, **12(2)**, 961–1001, doi:10.5194/essd-12-961-2020.

Petrescu, A.M.R. et al., 2021a: The consolidated European synthesis of CH_4 and N_2O emissions for the European Union and United Kingdom: 1990–2017. *Earth Syst. Sci. Data*, **13(5)**, 2307–2362, doi:10.5194/essd-13-2307-2021.

Petrescu, A.M.R. et al., 2021b: The consolidated European synthesis of CO_2 emissions and removals for the European Union and United Kingdom: 1990–2018. *Earth Syst. Sci. Data*, **13(5)**, 2363–2406, doi:10.5194/essd-13-2363-2021.

Pongratz, J., C.H. Reick, R.A. Houghton, and J.I. House, 2014: Terminology as a key uncertainty in net land use and land cover change carbon flux estimates. *Earth Syst. Dyn.*, **5(1)**, 177–195, doi:10.5194/esd-5-177-2014.

Prinn, R.G. et al., 2018: History of chemically and radiatively important atmospheric gases from the Advanced Global Atmospheric Gases Experiment (AGAGE). *Earth Syst. Sci. Data*, **10(2)**, 985–1018, doi:10.5194/essd-10-985-2018.

Prosperi, P. et al., 2020: New estimates of greenhouse gas emissions from biomass burning and peat fires using MODIS Collection 6 burned areas. *Clim. Change*, **161(3)**, 415–432, doi:10.1007/s10584-020-02654-0.

Ramankutty, N. et al., 2007: Challenges to estimating carbon emissions from tropical deforestation. *Glob. Change Biol.*, **13(1)**, 51–66, doi:10.1111/j.1365-2486.2006.01272.x.

Reilly, J.M. and K.R. Richards, 1993: Climate change damage and the trace gas index issue. *Environ. Resour. Econ.*, **3(1)**, 41–61, doi:10.1007/BF00338319.

Reisinger, A. and S. Ledgard, 2013: Impact of greenhouse gas metrics on the quantification of agricultural emissions and farm-scale mitigation strategies: A New Zealand case study. *Environ. Res. Lett.*, doi:10.1088/1748-9326/8/2/025019.

Reisinger, A. and H. Clark, 2018: How much do direct livestock emissions actually contribute to global warming? *Glob. Change Biol.*, **24(4)**, 1749–1761, doi:10.1111/gcb.13975.

Reisinger, A. et al., 2013: Implications of alternative metrics for global mitigation costs and greenhouse gas emissions from agriculture. *Clim. Change*, **117(4)**, 677–690, doi:10.1007/s10584-012-0593-3.

Reisinger, A. et al., 2021: How necessary and feasible are reductions of methane emissions from livestock to support stringent temperature goals? *Philos. Trans. R. Soc. A Math. Phys. Eng. Sci.*, **379(2210)**, 20200452, doi:10.1098/rsta.2020.0452.

Reisinger, A., M. Meinshausen, and M. Manning, 2011: Future changes in global warming potentials under representative concentration pathways. *Environ. Res. Lett.*, **6(2)**, 024020, doi:10.1088/1748-9326/6/2/024020.

Reisinger, A., S.F. Ledgard, and S.J. Falconer, 2017: Sensitivity of the carbon footprint of New Zealand milk to greenhouse gas metrics. *Ecol. Indic.*, **81**, 74–82, doi:10.1016/j.ecolind.2017.04.026.

Ren, S., B. Yuan, X. Ma, and X. Chen, 2014: The impact of international trade on China's industrial carbon emissions since its entry into WTO. *Energy Policy*, **69**, 624–634, doi:10.1016/j.enpol.2014.02.032.

Rigby, M. et al., 2010: History of atmospheric SF6 from 1973 to 2008. *Atmos. Chem. Phys.*, **10(21)**, 10305–10320, doi:10.5194/acp-10-10305-2010.

Rigby, M. et al., 2014: Recent and future trends in synthetic greenhouse gas radiative forcing. *Geophys. Res. Lett.*, **41(7)**, 2623–2630, doi:10.1002/2013GL059099.

Rogelj, J. et al., 2014: Disentangling the effects of CO_2 and short-lived climate forcer mitigation. *Proc. Natl. Acad. Sci.*, **111(46)**, 16325–16330, doi:10.1073/pnas.1415631111.

Rogelj, J. et al., 2019: A new scenario logic for the Paris Agreement long-term temperature goal. *Nature*, **573(7774)**, 357–363, doi:10.1038/s41586-019-1541-4.

Rosan, T.M. et al., 2021: A multi-data assessment of land use and land cover emissions from Brazil during 2000–2019. *Environ. Res. Lett.*, **16(7)**, 074004, doi:10.1088/1748-9326/ac08c3.

Sanjuán, M.Á., C. Andrade, P. Mora, and A. Zaragoza, 2020: Carbon Dioxide Uptake by Cement-Based Materials: A Spanish Case Study. *Appl. Sci.*, **10(1)**, 339, doi:10.3390/app10010339.

Sarofim, M.C. and M.R. Giordano, 2018: A quantitative approach to evaluating the GWP timescale through implicit discount rates. *Earth Syst. Dyn.*, **9(3)**, 1013–1024, doi:10.5194/esd-9-1013-2018.

Saunois, M. et al., 2016: The global methane budget 2000–2012. *Earth Syst. Sci. Data*, **8(2)**, 697–751, doi:10.5194/essd-8-697-2016.

Saunois, M. et al., 2020: The Global Methane Budget 2000–2017. *Earth Syst. Sci. Data*, **12(3)**, 1561–1623, doi:10.5194/essd-12-1561-2020.

Schleussner, C.-F., A. Nauels, M. Schaeffer, W. Hare, and J. Rogelj, 2019: Inconsistencies when applying novel metrics for emissions accounting to the Paris agreement. *Environ. Res. Lett.*, **14(12)**, 124055, doi:10.1088/1748-9326/ab56e7.

Shcherbak, I., N. Millar, and G.P. Robertson, 2014: Global metaanalysis of the nonlinear response of soil nitrous oxide (N_2O) emissions to fertilizer nitrogen. *Proc. Natl. Acad. Sci.*, **111(25)**, 9199–9204, doi:10.1073/pnas.1322434111.

Shindell, D.T., J.S. Fuglestvedt, and W.J. Collins, 2017: The social cost of methane: theory and applications. *Faraday Discuss.*, **200**, 429–451, doi:10.1039/C7FD00009J.

Shine, K.P., J.S. Fuglestvedt, K. Hailemariam, and N. Stuber, 2005: Alternatives to the Global Warming Potential for Comparing Climate Impacts of Emissions of Greenhouse Gases. *Clim. Change*, **68(3)**, 281–302, doi:10.1007/s10584-005-1146-9.

Shine, K.P., T.K. Berntsen, J.S. Fuglestvedt, R.B. Skeie, and N. Stuber, 2007: Comparing the climate effect of emissions of short- and long-lived climate agents. *Philos. Trans. R. Soc. A Math. Phys. Eng. Sci.*, **365(1856)**, 1903–1914, doi:10.1098/rsta.2007.2050.

Skytt, T., S.N. Nielsen, and B.-G. Jonsson, 2020: Global warming potential and absolute global temperature change potential from carbon dioxide and methane fluxes as indicators of regional sustainability – A case study of Jämtland, Sweden. *Ecol. Indic.*, **110**, 105831, doi:10.1016/j.ecolind.2019.105831.

Smith, M.A., M. Cain, and M.R. Allen, 2021: Further improvement of warming-equivalent emissions calculation. *Clim. Atmos. Sci.*, **4(1)**, 19, doi:10.1038/s41612-021-00169-8.

Solazzo, E. et al., 2021: Uncertainties in the Emissions Database for Global Atmospheric Research (EDGAR) emission inventory of greenhouse gases. *Atmos. Chem. Phys.*, **21(7)**, 5655–5683, doi:10.5194/acp-21-5655-2021.

Steinfeld, H., H. Mooney, F. Schneider, and L. Neville, 2010: *Livestock in a Changing Landscape, Volume 1: Drivers, Consequences, and Responses*. Island Press, Washington DC, USA, 416 pp.

Sterner, E.O. and D.J.A. Johansson, 2017: The effect of climate–carbon cycle feedbacks on emission metrics. *Environ. Res. Lett.*, **12(3)**, 034019, doi:10.1088/1748-9326/aa61dc.

Strefler, J., G. Luderer, T. Aboumahboub, and E. Kriegler, 2014: Economic impacts of alternative greenhouse gas emission metrics: a model-based assessment. *Clim. Change*, **125(3–4)**, 319–331, doi:10.1007/s10584-014-1188-y.

Syakila, A. and C. Kroeze, 2011: The global nitrous oxide budget revisited. *Greenh. Gas Meas. Manag.*, **1(1)**, 17–26, doi:10.3763/ghgmm.2010.0007.

Tanaka, K. and B.C. O'Neill, 2018: The Paris Agreement zero-emissions goal is not always consistent with the 1.5°C and 2°C temperature targets. *Nat. Clim. Change*, **8(4)**, 319–324, doi:10.1038/s41558-018-0097-x.

Tanaka, K., O. Boucher, P. Ciais, and D.J.A. Johansson, 2020: Cost-effective implementation of the Paris Agreement using flexible greenhouse gas metrics. *Nat. Commun.* In press.

Tanaka, K., O. Cavalett, W.J. Collins, and F. Cherubini, 2019: Asserting the climate benefits of the coal-to-gas shift across temporal and spatial scales. *Nat. Clim. Change*, **9(5)**, 389–396, doi:10.1038/s41558-019-0457-1.

Tian, H. et al., 2018: The Global N_2O Model Intercomparison Project. *Bull. Am. Meteorol. Soc.*, **99(6)**, 1231–1251, doi:10.1175/BAMS-D-17-0212.1.

Tian, H. et al., 2019: Global soil nitrous oxide emissions since the preindustrial era estimated by an ensemble of terrestrial biosphere models: Magnitude, attribution, and uncertainty. *Glob. Change Biol.*, **25(2)**, 640–659, doi:10.1111/gcb.14514.

Tian, H. et al., 2020: A comprehensive quantification of global nitrous oxide sources and sinks. *Nature*, **586(7828)**, 248–256, doi:10.1038/s41586-020-2780-0.

Tol, R.S.J., T.K. Berntsen, B.C. O'Neill, J.S. Fuglestvedt, and K.P. Shine, 2012: A unifying framework for metrics for aggregating the climate effect of different emissions. *Environ. Res. Lett.*, **7(4)**, 044006, doi:10.1088/1748-9326/7/4/044006.

Tubiello, F.N., 2019: Greenhouse Gas Emissions Due to Agriculture. In: *Encyclopedia of Food Security and Sustainability* [Ferranti, P., E. Berry, and A. Jock, (eds.)], Elsevier, New York, NY, USA, pp. 196–205.

Tubiello, F.N. et al., 2013: The FAOSTAT database of greenhouse gas emissions from agriculture. *Environ. Res. Lett.*, **8(1)**, 015009, doi:10.1088/1748-9326/8/1/015009.

Tubiello, F.N. et al., 2015: The Contribution of Agriculture, Forestry and other Land Use activities to Global Warming, 1990-2012. *Glob. Change Biol.*, **21(7)**, 2655–2660, doi:10.1111/gcb.12865.

Tubiello, F.N. et al., 2021: Carbon emissions and removals from forests: new estimates, 1990–2020. *Earth Syst. Sci. Data*, **13(4)**, 1681–1691, doi:10.5194/essd-13-1681-2021.

Tyukavina, A. et al., 2015: Aboveground carbon loss in natural and managed tropical forests from 2000 to 2012. *Environ. Res. Lett.*, **10(7)**, 074002, doi:10.1088/1748-9326/10/7/074002.

UNEP, 2020: *The Emissions Gap Report 2020 – A UN Environment Synthesis Report*. United Nations Environment Programme, Nairobi, Kenya, 128 pp.

UNFCCC, 2019: *Report of the Conference of the Parties Serving as the Meeting of the Parties to the Paris Agreement on the Third Part of Its First Session, Held in Katowice from 2 to 15 December 2018. Addendum, Part 2:*

Action Taken by the Conference of the. UNFCCC, Bonn, Germany, Decision 4/CMA.1. pp.

UNFCCC, 2021: National Inventory Submissions 2021. https://unfccc.int/ghg-inventories-annex-i-parties/2021 (Accessed September 30, 2021).

US-EPA, 2019: *Global Non-CO_2 Greenhouse Gas Emission Projections & Mitigation*. Washington DC, USA, https://www.epa.gov/global-mitigation-non-co2-greenhouse-gases.

van den Berg, M., A.F. Hof, J. van Vliet, and D.P. van Vuuren, 2015: Impact of the choice of emission metric on greenhouse gas abatement and costs. *Environ. Res. Lett.*, **10(2)**, 024001, doi:10.1088/1748-9326/10/2/024001.

van der Werf, G.R. et al., 2017: Global fire emissions estimates during 1997–2016. *Earth Syst. Sci. Data*, **9(2)**, 697–720, doi:10.5194/essd-9-697-2017.

Wagner-Riddle, C. et al., 2017: Globally important nitrous oxide emissions from croplands induced by freeze–thaw cycles. *Nat. Geosci.*, **10(4)**, 279–283, doi:10.1038/ngeo2907.

Wang, Q. and R. Jiang, 2019: Is China's economic growth decoupled from carbon emissions? *J. Clean. Prod.*, **225**, 1194–1208, doi:10.1016/j.jclepro.2019.03.301.

Wang, Q. and Y. Zhou, 2020: Evolution and drivers of production-based carbon emissions in China and India: Differences and similarities. *J. Clean. Prod.*, **277**, 123958, doi:10.1016/j.jclepro.2020.123958.

Wang, Q. et al., 2020a: Data-driven estimates of global nitrous oxide emissions from croplands. *Natl. Sci. Rev.*, **7(2)**, 441–452, doi:10.1093/nsr/nwz087.

Wang, Z., J. Meng, and D. Guan, 2020b: Dynamic Driving Forces of India's Emissions From Production and Consumption Perspectives. *Earth's Futur.*, **8(8)**, e2020EF001485, doi:10.1029/2020EF001485.

Wania, R. et al., 2013: Present state of global wetland extent and wetland methane modelling: methodology of a model inter-comparison project (WETCHIMP). *Geosci. Model Dev.*, **6(3)**, 617–641, doi:10.5194/gmd-6-617-2013.

Wiedinmyer, C. et al., 2011: The Fire INventory from NCAR (FINN): a high resolution global model to estimate the emissions from open burning. *Geosci. Model Dev.*, **4(3)**, 625–641, doi:10.5194/gmd-4-625-2011.

Winiwarter, W., L. Höglund-Isaksson, Z. Klimont, W. Schöpp, and M. Amann, 2018: Technical opportunities to reduce global anthropogenic emissions of nitrous oxide. *Environ. Res. Lett.*, **13(1)**, 014011, doi:10.1088/1748-9326/aa9ec9.

WMO, 2018: *Scientific Assessment of Ozone Depletion: 2018*. Global Ozo. World Meterological Organization, Geneva, Switzerland.

World Bank, 2021: World Development Indicators. https://datatopics.worldbank.org/world-development-indicators/ (Accessed June 30, 2021).

Wu, Z., L. Yang, Q. Chen, and Q. Ye, 2021: The impacts of international trade on global greenhouse gas emissions: A thought experiment based on a novel no-trade analysis. *J. Environ. Manage.*, **300**, 113836, doi:10.1016/j.jenvman.2021.113836.

Xi, F. et al., 2016: Substantial global carbon uptake by cement carbonation. *Nat. Geosci.*, **9(12)**, 880–883, doi:10.1038/ngeo2840.

Yang, S. et al., 2020: Global reconstruction reduces the uncertainty of oceanic nitrous oxide emissions and reveals a vigorous seasonal cycle. *Proc. Natl. Acad. Sci.*, **117(22)**, 11954–11960, doi:10.1073/pnas.1921914117.

Yao, X., R. Yasmeen, Y. Li, M. Hafeez, and I. Padda, 2019: Free Trade Agreements and Environment for Sustainable Development: A Gravity Model Analysis. *Sustainability*, **11(3)**, 597, doi:10.3390/su11030597.

Yuan, J. et al., 2019: Rapid growth in greenhouse gas emissions from the adoption of industrial-scale aquaculture. *Nat. Clim. Change*, **9(4)**, 318–322, doi:10.1038/s41558-019-0425-9.

Zheng, J. et al., 2019: The Slowdown in China's Carbon Emissions Growth in the New Phase of Economic Development. *One Earth*, **1(2)**, 240–253, doi:10.1016/j.oneear.2019.10.007.

Zhu, K. and X. Jiang, 2019: Slowing down of globalization and global CO_2 emissions – A causal or casual association? *Energy Econ.*, **84**, 104483, doi:10.1016/j.eneco.2019.104483.